CHAPTER 4

Stratospheric Ozone Changes and Climate

Lead Authors:
J.M. Arblaster
N.P. Gillett

Coauthors:
N. Calvo
P.M. Forster
L.M. Polvani
S.-W. Son
D.W. Waugh
P.J. Young

Contributors:
E.A. Barnes
I. Cionni
C.I. Garfinkel
E.P. Gerber
S.C. Hardiman
D.F. Hurst
J.-F. Lamarque
E.-P. Lim
M.P. Meredith
J. Perlwitz
R.W. Portmann
M. Previdi
M. Sigmond
N.C. Swart
J.-P. Vernier
Y. Wu

Chapter Editors:
L.J. Gray
D.W.J. Thompson

[Formatted for double-sided printing.]

From:
WMO (World Meteorological Organization), *Scientific Assessment of Ozone Depletion: 2014*, Global Ozone Research and Monitoring Project – Report No. 55, 416 pp., Geneva, Switzerland, 2014.

This chapter should be cited as:
Arblaster, J.M., and N.P Gillett (Lead Authors), N. Calvo, P.M. Forster, L.M. Polvani, S.-W. Son, D.W. Waugh, and P.J. Young, Stratospheric ozone changes and climate, Chapter 4 in *Scientific Assessment of Ozone Depletion: 2014*, Global Ozone Research and Monitoring Project – Report No. 55, World Meteorological Organization, Geneva, Switzerland, 2014.

CHAPTER 4

STRATOSPHERIC OZONE CHANGES AND CLIMATE

Contents

SCIENTIFIC SUMMARY

Since the last Assessment, new research has better quantified the impact of stratospheric ozone changes on climate. Additional model and observational analyses are assessed which examine the influence of stratospheric ozone changes on stratospheric temperatures and circulation, Southern Hemisphere tropospheric circulation and composition, surface climate, oceans, and sea ice.

- **Stratospheric ozone changes are the dominant driver of observed globally averaged long-term temperature changes in the lower stratosphere.** Between 1979 and 1995 global mean lower stratospheric temperature decreased by about 1 K but has since remained approximately constant.
  - Models broadly reproduce the evolution of global mean lower stratospheric temperature change. Stratospheric ozone changes are the dominant driver of these changes, with volcanic aerosol driving episodic warming, and greenhouse gas increases having only a minor contribution.
  - Observed mid- and upper-stratospheric temperatures decreased from 1979 to 2005, but the magnitude of the cooling is uncertain. A newly reprocessed data set of satellite measurements exhibits substantially different cooling trends compared to the existing data set. Models indicate that increasing greenhouse gases, as well as ozone changes, both made comparable contributions to observed cooling in the mid and upper stratosphere.
  - There was little overall change in global lower stratospheric water vapor concentration between 2000 and 2012, based on satellite measurements, which show a decrease between 2000 and 2004 followed by an increase to 2012.
  - The observed cooling of the Antarctic lower stratosphere since 1979 during austral spring is consistent with the average simulated cooling in models forced with observed ozone depletion. There is a large range in the magnitude of the simulated cooling, with models that underestimate the ozone depletion also underestimating the temperature trends.

- **Climate models consistently predict a long-term increase in the strength of the Brewer-Dobson circulation due to greenhouse gas increases, with important impacts on stratospheric and tropospheric composition.**
  - The predicted increase in the strength of the Brewer-Dobson circulation extends throughout the depth of the stratosphere.
  - Observations of changes in temperature, ozone, and trace gases over the past three to five decades are suggestive of increased upwelling in the tropical lower stratosphere, consistent with a strengthening of the shallow branch of the Brewer-Dobson circulation predicted by models. There is large uncertainty in changes in the deep branch of the Brewer-Dobson circulation inferred from observations in the mid and upper stratosphere.
  - Stratospheric ozone recovery and an acceleration of the Brewer-Dobson circulation in the future would both tend to increase the global tropospheric ozone burden. The projected net changes in tropospheric ozone and other compounds vary regionally and are scenario and model dependent.

- **Stratospheric temperature changes due to Antarctic ozone depletion are very likely the dominant driver of the observed changes in Southern Hemisphere tropospheric circulation in summer over recent decades, with associated surface climate and ocean impacts.**
  - The contribution of Antarctic ozone depletion to the observed increase in the Southern Annular Mode index in austral summer is substantially larger in most models than the contribution from greenhouse gas increases over the past three to five decades. An increase in this index corresponds to a decrease in atmospheric pressure at high latitudes, an increase at midlatitudes, and a poleward shift of the midlatitude jet. The role of ozone depletion is largest in summer. Observations and models suggest smaller Southern Annular Mode trends in other seasons.
  - Stratospheric ozone depletion has likely contributed to the observed expansion of the Southern Hemisphere Hadley Cell in austral summer.

- Climate models simulate a poleward shift of the Southern Hemisphere midlatitude maximum in precipitation and a moistening of the subtropics in response to stratospheric ozone depletion in austral summer. There is some evidence of a consistent pattern of trends in observations.
- Observational and modeling studies present a broadly consistent picture of the ocean's response to surface wind stress changes, which have likely been substantially caused by stratospheric ozone changes, with intensification of the subtropical ocean gyres and the meridional overturning circulations, and a subsurface warming. The impact of these wind stress changes on oceanic carbon uptake remains uncertain. The role of ocean eddies, which modify the ocean circulation and temperature response to wind stress changes, is better understood than at the time of the last Ozone Assessment, but remains a source of uncertainty.
- The influence of stratospheric ozone depletion on Antarctic sea ice increases reported in the last Ozone Assessment is not supported by a number of new coupled modeling studies. These suggest that ozone depletion drives a decrease in Southern Hemisphere sea ice extent and thus did not lead to the small observed increase. However, there is low confidence in this model result because of large uncertainties in the simulation of Antarctic sea ice.
- No robust link between stratospheric ozone changes and Northern Hemisphere tropospheric climate has been found, consistent with the conclusions of the previous Ozone Assessment.

- **There is further evidence that in austral summer over the next 50 years, Antarctic stratospheric ozone recovery and increases in greenhouse gases will have opposite effects on the Southern Hemisphere tropospheric circulation, with associated surface climate and ocean impacts.**
  - Ozone recovery is expected to drive a weakening and equatorward shift of the midlatitude jet, while increases in greenhouse gases are expected to drive a strengthening and poleward shift of the jet. Under a low greenhouse gas emissions scenario, ozone recovery is expected to dominate the effect of greenhouse gas increases on Southern Hemisphere tropospheric circulation in austral summer to give a weakening and equatorward shift of the midlatitude jet over the next 50 years, whereas in a high emissions scenario the jet is projected to continue to strengthen and shift poleward.
  - An equatorward shift in the Southern Hemisphere Hadley Cell boundary and extratropical rainfall in summer is simulated in response to ozone recovery. These changes offset a scenario-dependent fraction of projected greenhouse-gas induced changes in these variables.
  - Simulations from multiple models indicate that if the concentrations of ozone-depleting substances (ODSs) had continued to increase in the absence of the Montreal Protocol, the enhanced ozone depletion from uncontrolled ODSs would be expected to have led to substantial additional cooling in the Antarctic polar stratosphere, with associated changes in Southern Hemisphere circulation and rainfall patterns.

- **New estimates of global mean ozone radiative forcing due to emissions of ozone-depleting substances, which account for stratospheric ozone change and its indirect effect on tropospheric ozone, indicate a stronger surface cooling effect than that due to stratospheric ozone changes alone.**
  - The overall global mean ozone radiative forcing from the effects of ODS emissions on both tropospheric and stratospheric ozone is assessed to be −0.15 (−0.3 to 0) watts per square meter (W m^{-2}) in 2011. Approximately three quarters of this results from ozone changes in the stratosphere.
  - Models indicate that ODS-induced stratospheric ozone depletion has acted to decrease tropospheric ozone. This ODS-driven decrease in tropospheric ozone contributes to the overall negative ozone radiative forcing, although the magnitude is uncertain.
  - The radiative forcing due to observed decreases in stratospheric ozone concentration alone is estimated to be −0.05 W m^{-2} (−0.15 to 0.05) W m^{-2} in 2011. A rapid adjustment to radiative forcing may also arise from cloud changes, resulting from the circulation changes driven by ODS-induced ozone depletion. The radiative effect of this cloud adjustment may be of a larger magnitude than the non-adjusted forcing.
  - Uncertainty in future lower stratospheric ozone trends in the tropics precludes a confident assessment of the sign of future stratospheric ozone radiative forcing. Current models give a range of stratospheric ozone radiative forcing of −0.05 to +0.25 W m^{-2} in 2100 under a high greenhouse gas emissions scenario, which is generally suggestive of a slight warming contribution relative to present.

4.1 INTRODUCTION AND SCOPE

4.1.1 Summary of the Previous Ozone Assessment

Chapter 4 of the 2010 Ozone Assessment (Forster and Thompson et al., 2011) assessed stratospheric changes and their influence on climate. The chapter considered the tropospheric response to stratospheric change induced by greenhouse gases (GHGs), solar variability, and volcanic eruptions, as well as ozone. New data sets and improved simulations allowed an improved characterization of lower stratospheric temperature trends, and the influence of both natural and human factors was identified. The evolution of lower stratospheric temperature was described, with progressive cooling from 1960 to the late 1990s followed by a period with approximately constant temperature. Based on updated data sets the observed cooling was found to have occurred in the tropics as well as the extratropics and to have been similar at all latitudes in the annual mean. Ozone decreases were assessed to be the dominant driver of the observed long-term lower stratospheric cooling, with volcanic eruptions causing episodic warming. Temperature trends in the mid and upper stratosphere were assessed to be relatively uncertain, due to the existence of only a single reconstruction of satellite observed mid- and upper-stratospheric temperature available at the time.

The 2010 Ozone Assessment described an upward trend in stratospheric water vapor from 1980 to around 2000, followed by an abrupt decrease that was assessed to be sustained through to 2009 based on measurements available at the time. An increase of stratospheric aerosol concentrations of 4–7% yr^{-1} between the late 1990s and 2009 was reported, though the causes of the trend were not clear, with both volcanic sources and increased coal burning cited as possible contributors.

The radiative impact of stratospheric ozone on climate was concluded to be smaller than had previously been thought. The chapter concluded that much of the observed southward shift of the Southern Hemisphere tropospheric midlatitude jet in summer was due to Antarctic ozone depletion, which in turn had driven trends in surface winds and temperature over Antarctica. It was concluded with somewhat less confidence that Antarctic ozone depletion had contributed to the observed increase in Antarctic sea ice extent, a southward shift of the Southern Hemisphere storm track and associated precipitation, a warming of the subsurface Southern Ocean, and decreases of carbon uptake over the Southern Ocean. No link between Arctic ozone depletion and tropospheric circulation had been established.

Projected changes in stratospheric temperature were discussed, with GHGs driving a cooling, moderated by ozone increases driven by this cooling itself and by decreasing concentrations of ozone-depleting substances (ODSs). The opposing effects of ozone recovery and GHG increases on the latitude of the Southern Hemisphere midlatitude jet in summer were discussed, and the net effect of these forcings was assessed to be uncertain. The chapter reported that climate models simulate an increase in the Brewer-Dobson circulation (BDC) in response to GHG increases, consistent with earlier assessments. It was concluded that stratospheric ozone recovery would increase the transport of ozone into the troposphere.

4.1.2 Scope of the Chapter

The previous chapters of this report have described and assessed past and projected future changes in stratospheric ozone. This chapter assesses new research since the 2010 Ozone Assessment on the impact of those changes on climate. To facilitate easy comparison with the 2010 Ozone Assessment, this chapter will follow a similar structure to Chapter 4 of that Assessment (Forster and Thompson et al., 2011). Stratospheric ozone changes, together with changes in other stratospheric constituents, directly affect the radiative budget of the stratosphere, causing changes in stratospheric temperature and

circulation, which in turn influence tropospheric climate. Therefore after assessing observed variations in stratospheric constituents that relate to climate (Section 4.2), the chapter will continue to assess simulated and observed variations in stratospheric temperature and circulation, with a focus on attribution of observed changes to variations in ozone and other drivers (Section 4.3). The chapter will then assess the influence of stratospheric ozone changes on the troposphere, surface, and ocean, as requested by the Parties to the Montreal Protocol. In 1987 when the Montreal Protocol was signed, the impacts of stratospheric ozone depletion on tropospheric climate were not generally known, but over the past fifteen years an increasingly mature body of research on these impacts has developed. While the 2010 Ozone Assessment also considered the tropospheric response to other stratospheric changes, including changes in stratospheric water vapor, stratospheric aerosol, and solar irradiance variations, these topics were comprehensively assessed in the recently published Fifth Assessment Report of the Intergovernmental Panel on Climate Change (IPCC, 2013). For this reason this chapter will focus on the influence of stratospheric ozone change, with the influence of other stratospheric changes on climate discussed only briefly for context. Sections on the influence of stratospheric ozone on the troposphere in the past (Section 4.4) and future (Section 4.5) will start by considering ozone-induced effects on tropospheric circulation and resulting climate impacts, followed by sections considering radiative effects and chemical effects in turn.

4.2 OBSERVED CHANGES IN STRATOSPHERIC CONSTITUENTS THAT RELATE TO CLIMATE

The stratospheric constituents considered in this section impact climate directly through radiative effects and indirectly through their influence on stratospheric ozone. We review and assess observed variations in these constituents to inform our understanding and attribution of changes in stratospheric temperature and circulation.

4.2.1 Long-Lived Greenhouse Gases and Ozone-Depleting Substances

Carbon dioxide (CO_2), methane (CH_4), nitrous oxide (N_2O), and ODSs are all gases of tropospheric origin that impact climate both directly by absorbing and emitting long-wave radiation and indirectly by impacting stratospheric ozone. ODSs, N_2O, and CH_4 are source gases for compounds that deplete stratospheric ozone, whereas changes in CO_2 impact ozone through changes in stratospheric temperature and circulation.

Recent measurements and growth rates for ODSs and N_2O are covered in Chapter 1 of this report, with a summary of recent growth rates shown in Tables 1-1 and 1-12. The measurements and growth rates for CO_2 and CH_4 are covered in detail in the IPCC Fifth Assessment Report (Hartmann et al., 2013) and are briefly summarized here. The tropospheric abundance of CO_2 was around 390.5 parts per million (ppm) in 2011, which is around 40% greater than in 1750, and the average annual increase in globally averaged CO_2 concentration from 1980 to 2011 was 1.7 ppm yr^{-1} (2.0 ppm yr^{-1} since 2001) (Hartmann et al., 2013). There are large year-to-year variations (from an annual increase of around 0.7 ppm in 1992 to 2.9 ppm in 1998) that are primarily due to small changes in the balance between carbon fluxes from photosynthesis and respiration on land. Tropospheric CH_4 abundance was around 1803 ppb in 2011, which is 150% greater than before 1750. There have been substantial changes in the growth rate of CH_4 since 1980: there was an increase in the global-average annual abundance from 1980 to 1998, little change from 1999 to 2006, and an increase in atmospheric burden since 2007 (Ciais et al., 2013).

4.2.2 Stratospheric Water Vapor

Stratospheric water vapor is important for Earth's radiative balance (influencing stratospheric and tropospheric temperatures) and for stratospheric chemistry. Changes in stratospheric water vapor can alter

stratospheric ozone chemistry in several different ways: Water vapor is the main source of reactive hydrogen oxide molecules (HO_x) that destroy ozone, and changes in water vapor alter stratospheric temperatures (and hence rates of chemical reactions) and the formation of polar stratospheric clouds. Changes in stratospheric water vapor can also impact the stratospheric circulation, as well as the tropospheric midlatitude jets (Maycock et al., 2013).

As discussed in the previous Ozone Assessment (Forster and Thompson et al., 2011), satellite measurements of lower stratospheric H_2O from the early 1990s to the present show substantial variability, with a large (~ 0.6 ppmv) step-like decrease after 2001 followed by roughly constant values. In more recent years these measurements show an increase in both tropical and midlatitude lower stratospheric water vapor, and there is only a small net change between 2000 and 2012 both in the midlatitudes and in the tropics (Randel and Jensen 2013; Fueglistaler et al., 2013). These changes are observed in both balloon-borne and satellite measurements. Figure 4-1 compares balloon-borne measurements at Boulder, Colorado, with corresponding zonal mean satellite observations (Hurst et al., 2011). There are unresolved discrepancies between the balloon and satellite measurements over the period 1992–1996. An updated trend analysis of the full (1980–2010) Boulder record shows sensitivity to the time period considered for the trends (due to the large decadal variability, Figure 4-1) and to the altitude (Hurst et al., 2011). For the full 30-year period there is a net increase of 1.0 ± 0.2 ppm between 16–26 kilometers (which corresponds to around 0.75% yr^{-1}).

The principal sources of water vapor in the bulk of the stratosphere are entry through the tropical tropopause and CH_4 oxidation. There is a small additional source from oxidation of molecular hydrogen (H_2). In the extratropical lowermost stratosphere, an additional source of water vapor is quasi-horizontal (isentropic) transport across the subtropical tropopause and deep convection, while dehydration in the polar lower stratosphere is a sink. Long-term H_2O trends are due to trends in the flux of water vapor entering the stratosphere and increased production of H_2O from CH_4 oxidation (for example, around 30% of the 1980–2010 increase in water vapor over Boulder can be attributed to increases in CH_4; Fujiwara et al., 2010; Hurst et al., 2011). Many of the year-to-year and longer variations in the observational H_2O record can be linked to observed changes in tropical tropopause temperatures but some discrepancies still exist (e.g., Schoeberl et al., 2012; Fueglistaler et al., 2013; Randel and Jensen, 2013). For example, the long-term trends cannot be reproduced with trajectory-based models based on observed changes in tropical

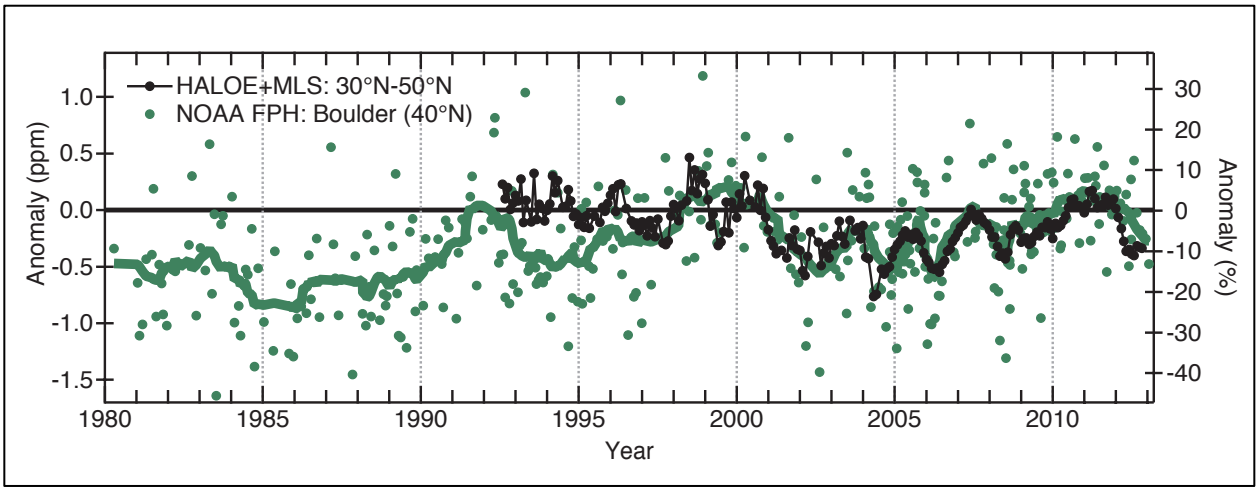

Figure 4-1. Water vapor anomalies in the Northern Hemisphere lower stratosphere (~16–19 km) from satellite sensors and in situ measurements normalized to 2000–2011. Approximately monthly balloon-borne measurements (FPH = frost point hygrometer) of stratospheric water vapor from Boulder, Colorado, at 40°N (green dots; green curve is 15-point running mean) averaged over 16–18 km and monthly means at 83 hPa for 30°N–50°N (black) determined from Halogen Occultation Experiment (HALOE) and Microwave Limb Sounder (MLS) satellite sensors. Updated from Figure 2.5 of Hartmann et al. (2013), which is updated from Solomon et al. (2011).

tropopause temperatures. It is still unclear whether the inability to model the observed trends is due to the large uncertainties in the observed stratospheric water vapor and tropical tropopause temperatures (e.g., Wang et al., 2012), uncertainties in the models, or whether the models have missing mechanisms.

4.2.3 Stratospheric Aerosols

Stratospheric aerosols influence climate in many ways, including shortwave radiative forcing (with surface cooling following an increase in stratospheric aerosols), changes in circulation caused by differential (vertical or horizontal) heating, and by changing stratospheric ozone with its associated radiative and circulation impacts. Observed changes in stratospheric aerosols are discussed in Section 2.3.4 of Chapter 2 of this Assessment. Briefly, the eruption of Mt. Pinatubo in 1991 was the last major volcanic eruption and the current stratospheric aerosol concentrations are much lower than in the years immediately following this eruption**.** However, as reported in the previous Ozone Assessment (Forster and Thompson et al., 2011), there has been an increase in stratospheric aerosol optical depth since the late 1990s, with an average increase of 4–10% per year from 2000–2010 (see Figure 2-18 of Chapter 2).

4.2.4 Ozone

As discussed in detail in this chapter, changes in stratospheric ozone influence climate both by direct radiative effects and by affecting stratospheric and tropospheric circulation. Past changes in global and polar stratospheric ozone are reviewed in Chapters 2 and 3, respectively, and only the key points are briefly summarized here.

There is substantial year-to-year variability in extratropical column ozone, but there have been only weak trends since 2000, especially compared to the large decreases observed from 1980 to the mid-1990s. The differences between total column ozone in the recent past (circa 2008–2012) and pre-1980 values are similar to those quoted for 2006–2008 in the previous Ozone Assessment (Forster and Thompson et al., 2011), i.e., near-global (60°N–60°S) column ozone is approximately 2% lower than pre-1980 values. The Antarctic ozone hole has continued to form each year, with springtime Antarctic (October, 60–90°S) column ozone values substantially lower than pre-1980 values. There has, however, been large year-to-year variability in the ozone amount in the last few years, due to variability in stratospheric temperatures and dynamical processes. Large year-to-year variability is also evident in tropical lower stratospheric ozone concentrations, complicating the detection of long-term trends there.

4.3 OBSERVED AND SIMULATED CHANGES IN STRATOSPHERIC CLIMATE

The previous section summarized the observed changes in long-lived GHGs and ODSs, as well as stratospheric water vapor, aerosols, and ozone (see also Chapters 1–3 of this Assessment). Changes in these constituents have a direct impact on stratospheric temperatures through their radiative effects, which in turn can affect the stratospheric circulation. In this section, we assess observed changes in stratospheric temperature and circulation and simulated changes in the past and future, as well as current understanding of the causes of these changes. In addition to influencing tropospheric climate, stratospheric temperature and circulation are also important drivers of stratospheric ozone change (Box 3-2 of Chapter 3).

4.3.1 Stratospheric Temperature

4.3.1.1 OBSERVATIONS

Identifying robust long-term trends in stratospheric temperature requires records of at least a few decades and global coverage. Observations of stratospheric temperatures are mainly derived from

balloon-borne radiosondes and satellite retrievals. Radiosondes provide measurements since 1957 over an irregular network with quasi-global coverage, although certain regions such as the oceans and the Antarctic are poorly sampled. Radiosondes have very good vertical resolution in the lower stratosphere, but coverage does not extend to the middle and upper stratosphere. Microwave Sounding Unit (MSU) and Stratospheric Sounding Unit (SSU) satellite instruments provided global coverage measurements from late 1978 to 2005. However, their vertical resolution is coarse as they measure over broad altitude ranges corresponding to the instrument weighting functions. The highest MSU channel (MSU channel 4) peaks in the lower stratosphere near 20 km, while SSU channels peak in the middle and upper stratosphere, at 25–35 km (SSU channel 1), 35–45 km (SSU channel 2), and 40–50 km (SSU channel 3). SSU channels 1, 2, and 3 are also referred in the literature as channels 25, 26, and 27, respectively. MSU and SSU instruments have now been replaced by the Advanced Microwave Sounding Unit (AMSU; in service since 1998), which has channels covering the domains of both the MSU and SSU instruments.

New trend estimates in the lower stratosphere, published since the last Ozone Assessment and based on longer records of several radiosonde and satellite temperature data sets, agree with previous estimates of temperature trends in this region. The global mean temperature in the lower stratosphere decreased by around 1 K from 1979 to 2012, as shown in Figure 4-2 in MSU channel 4 data processed by three different institutions (RSS, UAH, and NOAA; see also Hartmann et al., 2013). Short-term warming periods appear after the volcanic eruptions of El Chichón (1982) and Mt. Pinatubo (1991), and a lack of any statistically significant trend in globally averaged lower stratospheric temperatures since the mid-1990s continues to 2012 (Thompson et al., 2012; Seidel et al., 2011). Estimates of lower stratospheric temperature trends from radiosondes and the MSU instrument up to 2012 are listed in Table 2.8 from the IPCC AR5 (Hartmann et al., 2013).

Interest in temperature trends in the middle and upper stratosphere has grown recently. While the tropospheric climate response may be most sensitive to changes in stratospheric composition and temperature in the lower stratosphere (e.g., Forster and Shine, 1997), trends in the middle and upper stratosphere are potentially useful for understanding stratospheric circulation changes. The number of temperature data sets available in the middle and upper stratosphere is much smaller than in the lower stratosphere and as discussed below, the trend uncertainties are larger. SSU data from a series of instruments are available from 1979, SSU and AMSU data are available from 1998 to 2005, and only AMSU data are available after 2005. Like most satellite data, SSU data require several corrections before they can be used for climatic studies. These corrections are related to 1) the cell of CO_2 that is used to calibrate the long-wave emissions, which leaks over time, changing the altitudes measured, and whose CO_2 content also varies among SSU instruments (Kobayashi et al., 2009); 2) interactions between the large amplitudes of the diurnal and semidiurnal thermal tides in the middle and upper stratosphere and satellite orbital drift (Nash and Forrester, 1986), and 3) the long-term increase in CO_2 in the atmosphere, which can change the weighting function of the instruments and thus the altitudes measured (Shine et al., 2008). In addition, there is no overlap period between several pairs of consecutive satellites and thus, merging data from different satellites may produce inaccurate results. Comparison with radiosonde observations is also not possible since radiosonde data are not generally available at these altitudes.

Only two independent analyses of SSU data are available. Originally, SSU data were processed by scientists at the U.K. Met Office in the 1980s (Nash and Forrester, 1986; Nash, 1988) and this data set was subsequently updated by Shine et al. (2008) and Randel et al. (2009). Recently, an additional alternative analysis of SSU data has been generated by Wang et al. (2012), taking advantage of improvements in radiative transfer modeling. Figure 4-2 (left panels) shows the global mean stratospheric temperature anomalies since 1979 in the three SSU channels as produced by Wang et al. (NOAA STAR, red line) and Shine et al. (Met Office, blue line). Comparison of these data sets (Thompson et al., 2012) shows that global mean trends are similar in the upper stratosphere (SSU channel 3). However, in the middle stratosphere, the two data sets exhibit differences in SSU channels 1 and 2 of as large as 0.5 K decade^{-1}, with the NOAA STAR data set showing a global mean cooling almost twice as large as the Met Office data set (Wang et al., 2012; Thompson et al., 2012). The full reasons for these discrepancies remain unknown (e.g., Nash and Saunders, 2013), but planned updates to the data sets may resolve the discrepancies in part.

Thus, the agreement between satellite measurements and radiosonde observations over the longer record since the 2010 Ozone Assessment increases confidence in the robustness of the temperature trends in the lower stratosphere. Observed changes in global-mean temperature in the middle and upper stratosphere are considerably more uncertain. All data sets exhibit a cooling trend from 1979 to 2005 (to 2012 for the lower stratosphere), which is stronger in the upper stratosphere than at lower levels, consistent with physical understanding.

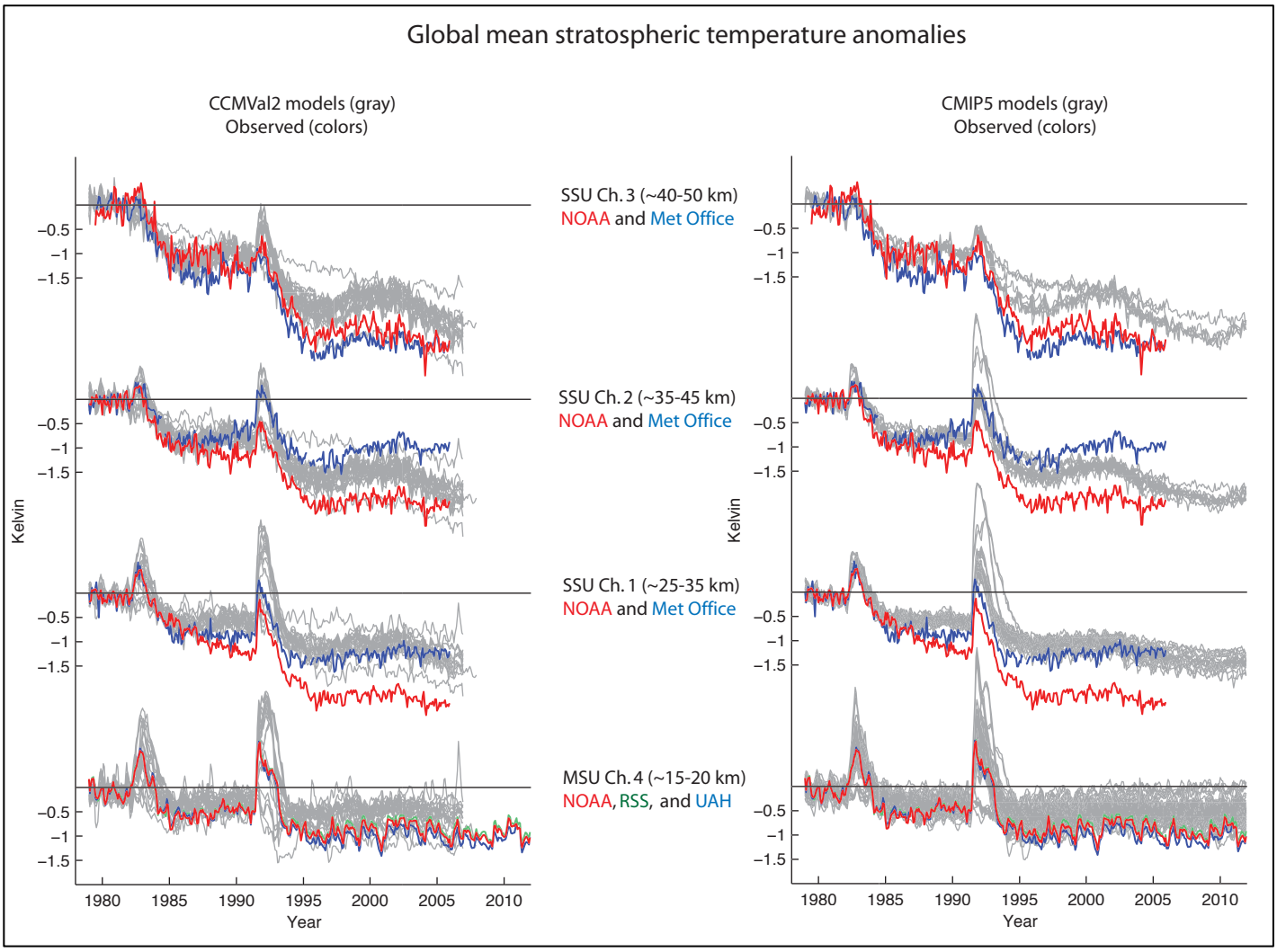

Figure 4-2. Time series of global mean stratospheric temperature anomalies from 1979 to 2012 for SSU channels 1-3 (*top three rows*) and MSU channel 4 (*bottom row*) for the altitude ranges, data sets, and model output indicated. Colored lines indicate results based on observations processed by different research groups: the Met Office (blue in top three panels), Remote Sensing Systems (green), the University of Alabama-Huntsville (blue in bottom panel) and the National Oceanic Atmospheric Administration Center for Satellite Applications and Research (red). Gray lines indicate results from the Chemistry-Climate Model Validation-2 (CCMVal2) and Coupled Model Intercomparison Project Phase 5 (CMIP5) models weighted by the appropriate satellite weighting function for easy comparison with observations. Time series are plotted so that their 1979–1982 mean anomalies are zero. Adapted from Thompson et al. (2012).

Seasonal and spatial structure of trends

Changes in the seasonal and spatial patterns of stratospheric temperature trends can arise from the radiative response to homogeneous changes in long-lived GHGs (Fels et al., 1980; Forster and Shine, 1999), constituents with a strong spatial and seasonal structure (such as ozone), as well as changes in the stratospheric mean meridional circulation (as will be discussed in Section 4.3.2). The pattern of zonal mean lower stratospheric temperature trends as a function of month over the period 1979–2012 (Figure 4-3a, b) is similar to that shown over the period 1979–2007 in the previous Ozone Assessment (Forster and Thompson et al., 2011). The largest trends in lower stratospheric temperatures occur over the Antarctic in November and December in satellite data (Figure 4-3a) and October–November in HadAT (Hadley Centre Atmospheric Temperature) radiosonde data (Figure 4-3b) following the maximum in ozone depletion in October. However, this feature is somewhat sensitive to the period over which the trend is calculated due partly to the

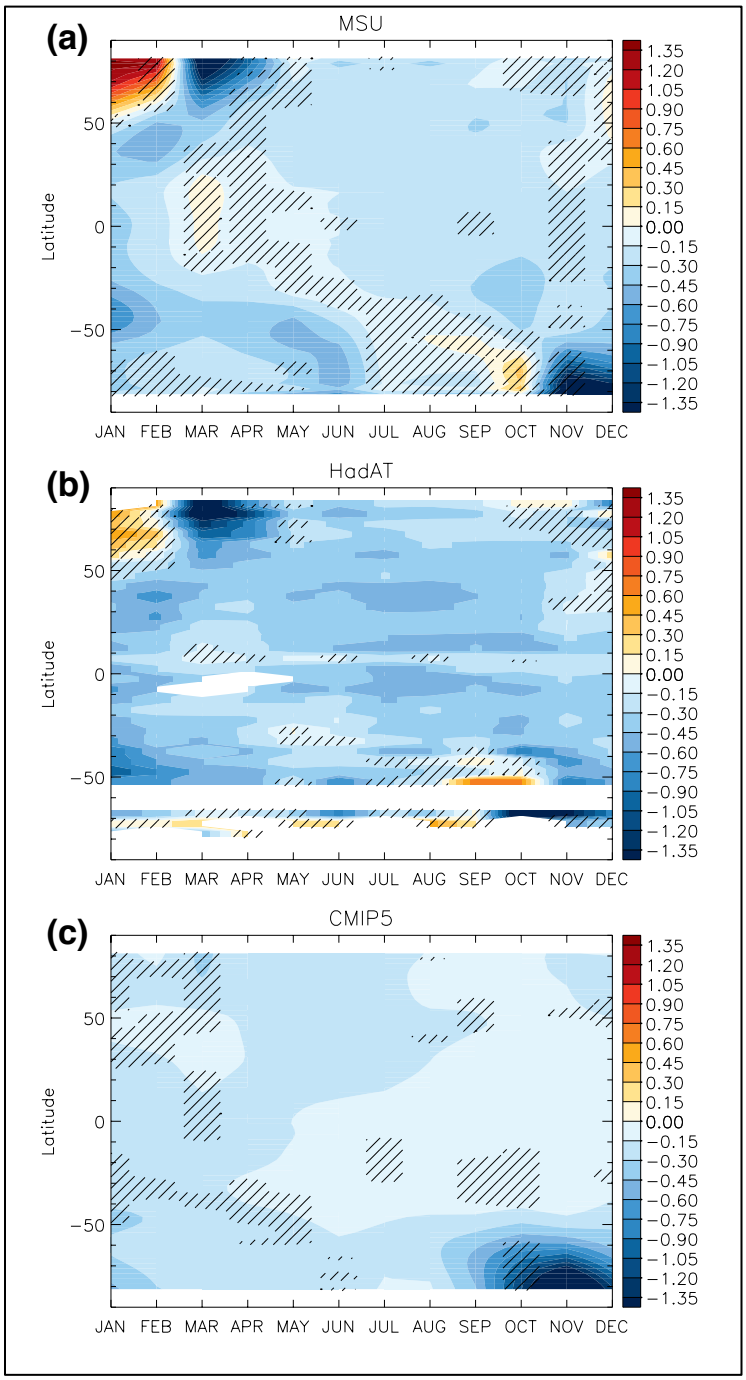

Figure 4-3. Lower stratospheric temperature trends over the period 1979–2012 in K per decade as a function of latitude and month from (a) satellite MSU RSS v3.3 (channel 4); (b) HadAT radiosonde (averaged with the MSU channel 4 weighting function), and (c) synthetic MSU channel 4 temperatures from merged CMIP5 historical and RCP8.5 (Representative Concentration Pathway) simulations covering 1979–2012 taken from Santer et al. (2013). The following volcano years are treated as missing data (1982, 1983, 1991, 1992, 1993) and trends are calculated where at least 50% of monthly anomalies are present over the 1979–2012 period. The hatching in a) and b) shows where the observed trend is within the 5–95% range of simulated internal variability and thus not significant, where internal variability is assessed from the spread of trends in the CMIP5 historical simulations. Hatching in c) shows where the observed MSU trend in (a) lies outside the 5–95% range of trends simulated in the 33 individual CMIP5 simulations, thus showing thus showing areas where the simulated and observed trends are inconsistent.

large internal variability in this region (Figure 4-4). Anomalously warm conditions over Antarctica in 2002–2006 were followed by anomalously low temperatures in the period 2007–2010. In the Arctic, both satellite and radiosonde observations agree on a large warming trend in January and February and large cooling trend in March and April (Figure 4-3a and b) although some of these trends are not statistically robust, likely because of the large interannual variability at high latitudes, particularly in the Northern Hemisphere, and decadal variability possibly associated with changes in the seasonal distribution of Sudden Stratospheric Warmings (Gómez-Escolar et al., 2012). In the tropics, the seasonal cycle is amplified through the significant cooling from June to October and December to February observed in satellite data (Figure 4-3a) as pointed out in the last Ozone Assessment (Forster and Thompson et al., 2011) and confirmed in radiosonde observations (Figure 4-3b and Free et al., 2011). However, it is not clear whether the changes in the seasonal patterns in the tropical lowermost stratosphere represent a long-term trend or are related to decadal-scale variability (Free, 2011).

In the middle and upper stratosphere, there are large differences between the latitudinal structure of the trends in the NOAA STAR (Wang et al., 2012) and Met Office (Shine et al., 2008) SSU data sets (not shown; see Thompson et al., 2012). Large meridional variations are present in the NOAA STAR data set, with the largest cooling trend in the tropics, and decreasing trends toward the high latitudes, with smaller trends in the Antarctic than in the Arctic. In contrast, the Met Office data set shows a relatively uniform cooling at all latitudes in the middle stratosphere (channels 1 and 2). Near the stratopause (channel 3), the high-latitude differences between the data sets reverse and the Met Office data set exhibits a larger cooling than the NOAA STAR data set (Thompson et al., 2012).

In summary, in the lower stratosphere, there is high confidence in the observations of the global mean trends and good agreement across different data sets. This is not the case in the mid and upper stratosphere, where only satellite data are available and different satellite reconstructions exhibit different trends. Changes in mid- and upper-stratospheric temperature are relevant to the climate change signal detection problem and as explained in Section 4.3.2, they are used to characterize changes in the BDC, which in turn can affect the amount of ozone entering the troposphere. Uncertainties in the seasonal and spatial patterns of stratospheric temperature trends are larger than those in the global mean especially in the dynamically active season in each hemisphere, boreal winter and austral spring.

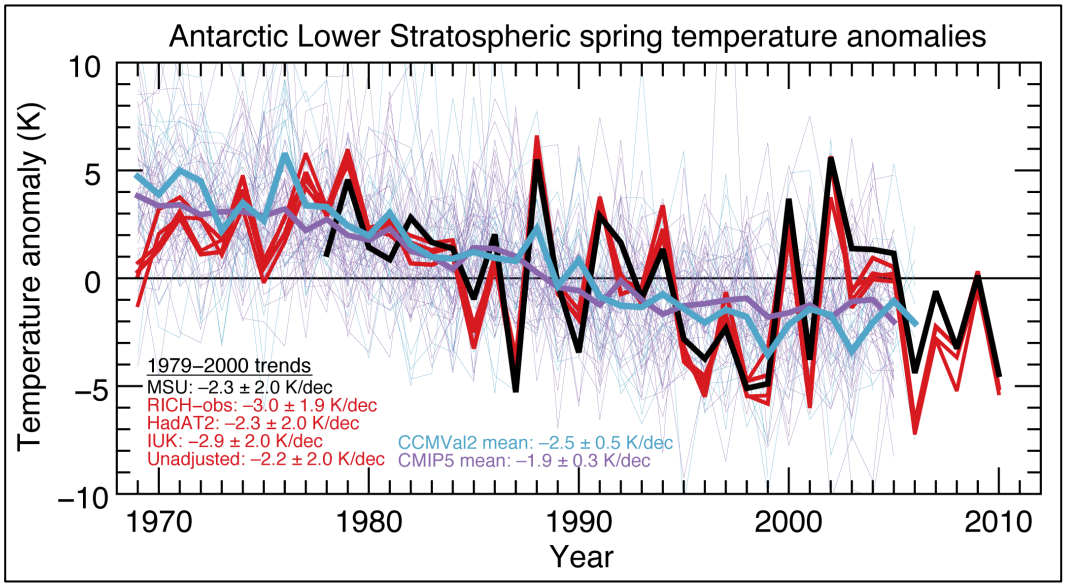

Figure 4-4. Time series of MSU channel 4-weighted temperature anomalies for the October to January average for four different radiosonde data sets and the unadjusted radiosondes at the Antarctic locations examined by Thompson and Solomon (2002) (red), MSU channel 4 data (black), the CMIP5 ensemble mean (purple), and the CCMVal-2 models and ensemble mean (blue). Individual model results are shown with the thin blue and purple lines. Adapted from Young et al. (2013b).

4.3.1.2 SIMULATED PAST AND FUTURE CHANGES

Temperature changes in the stratosphere can have a natural or anthropogenic origin, and attribution of the past or projected changes to a given driver relies on using climate model simulations. Since the last Ozone Assessment, two types of models have been widely analyzed for climate purposes in the stratosphere: Chemistry-Climate Models (CCMs) and atmosphere-ocean general circulation models (AOGCMs). They are described in Box 2-2, along with details of the model intercomparison projects in which such models are compared. While the last Ozone Assessment (Forster and Thompson et al., 2011) relied principally on CCM simulations, this Assessment makes use of results from a more comprehensive set of CCM and AOGCM simulations.

Figure 4-2 shows time series of global mean stratospheric temperatures simulated by CCMs (from the Chemistry-Climate Model Validation-2 (CCMVal-2) experiment) and AOGCMs (from the Coupled Model Intercomparison Project Phase 5 (CMIP5) experiment) together with the time evolution of satellite observations from different channels, corresponding to the different altitude ranges already discussed above. Model data have been weighted by the satellite weighting functions. The model simulations were forced with changes in well-mixed GHGs, anthropogenic aerosols, and stratospheric ozone or ODSs, as well as with changes in solar irradiance, volcanic aerosols, and in the case of most CMIP5 simulations, land use change. It is clear that both sets of models exhibit a global mean cooling trend at all levels, which is larger in the upper stratosphere in general agreement with the observations. Nevertheless, there are discrepancies in the magnitude of the long-term cooling.

For the lower stratosphere, both sets of models underestimate the global mean cooling seen in the MSU channel 4 measurements (Thompson et al., 2012; Santer et al., 2013; Charlton-Perez et al., 2013). The cause (or causes) of the model-observation discrepancy remains unexplained at this time, but could relate to forcing errors related to ozone trends or prescribed stratospheric aerosol loadings (Free and Lanzante, 2009; Solomon et al., 2011; Santer et al., 2013), as well as errors in the evolution of the modeled stratospheric water vapor (Gettelman et al., 2010; Maycock et al., 2014), or even errors in the model radiation code (Forster et al., 2011). For example, the prescribed ozone data set used by most of the CMIP5 models without interactive chemistry (Cionni et al., 2011) has been shown to underestimate Antarctic ozone depletion relative to the 1979–2007 observations (Cionni et al., 2011; Hassler et al., 2013), although only a subset of models in Figure 4-2 used this data set and the discrepancy shown here is for the global mean temperature. Stratospheric water vapor changes (Section 4.2.2) are estimated to have cooled the lower stratosphere by up to ~0.2 K decade^{-1} in the global and annual mean from 1980–2010, a substantial portion of the total trend (Maycock et al., 2014). However, stratospheric water vapor changes in this region are likely dominated by indirect climate feedbacks due to global warming (Dessler et al., 2013), rather than forced by increases in methane.

In the middle stratosphere at around 30 km (SSU channel 1), both the CCMVal2 and CMIP5 models exhibit cooling trends more in agreement with the Nash and Forrester (1986) Met Office SSU data set than the Wang et al. (2012) NOAA SSU data set. At altitudes centered around 40 km (SSU channel 2) the models lie in between both observational data sets. In the upper stratosphere, where the agreement between the two SSU data sets is better, the models show a smaller cooling than observed. Some of the model-observation differences were already highlighted in the previous Ozone Assessment based on the CCMVal2 models (Forster and Thompson et al., 2011). The fact that the differences remain in the CMIP5 AOGCMs (Thompson et al., 2012; Santer et al., 2013) suggests that they are not related to coupling to the ocean. The reasons for these model-observation differences or the discrepancy between SSU data sets remain unknown.

When comparing the latitudinal and seasonal distribution of lower stratospheric zonal mean temperature trends (Figure 4-3) there is a tendency for models to overestimate the seasonal extent of the Southern Hemisphere polar cooling and underestimate the tropical cooling over the past three decades, compared to the observations (see also Thompson et al., 2012; Santer et al., 2013). Over the Antarctic, the simulated cooling trend over the 1979–2012 period is more consistent with observations than over the shorter 1979–2005 period (Charlton-Perez et al., 2013; Santer et al., 2013). At high latitudes, there are

large differences between the pattern of zonal mean trends in the models and satellite observations (Thompson et al., 2012), which may reflect trends in the circulation (see Section 4.3.2.1).

For the high latitude Southern Hemisphere in particular, modeling studies have shown that stratospheric ozone depletion is the main driver of polar temperature trends in the lower stratosphere region during austral spring and summer (e.g., McLandress et al., 2011; Polvani et al., 2011b). The comparison of CCMs carried out as part of CCMVal-2 (SPARC CCMVal, 2010) concluded that the ensemble mean temperature showed too strong a cooling between 1969–1998, as compared with observations reported by Thompson and Solomon (2002), which has been used as a benchmark in this type of study. Recently, Young et al. (2013b) compared several different sets of radiosondes and found a cooling trend in November at 100 hPa in the range of −3.8 to −4.7 K decade^{-1} for the same period, around 50% larger than that reported by Thompson and Solomon (2002). Comparing over different periods with several observational data sets, Calvo et al. (2012) and Young et al. (2013b) concluded that the ensemble mean of both CCMVal-2 and CMIP5 exhibits cooling trends for the Southern Hemisphere lower stratosphere polar cap that are not significantly different from observations, although there is a large spread for individual models (Figure 4-4), and those underestimating ozone depletion also underestimate the temperature trends (Young et al., 2013b). Lower stratosphere temperature trends for the Southern Hemisphere polar cap are also characterized by zonal asymmetries in September and October (e.g., Lin et al., 2009). However, while Wang and Waugh (2012) found that CCMs forced with observed sea surface temperatures (SSTs) can qualitatively reproduce the observed seasonal pattern of lower stratospheric temperature variations, there is a large contribution from internal variability, and the pattern of the trends can differ substantially between different realizations from the same model. This is consistent with a large role for internal variability in generating the observed seasonal and spatial pattern of trends.

Over the recent past, global mean lower stratospheric temperatures calculated from simulations with individual forcings (Figure 4-5) suggest that ozone changes (or equivalently ODSs) are the dominant driver of lower stratospheric cooling, with greenhouse gas increases making a smaller cooling contribution, and volcanic aerosol driving episodic warming following large volcanic eruptions (Eyring et al., 2006; Ramaswamy et al., 2006; Dall'Amico et al., 2010; Gillett et al., 2011; Lott et al., 2013). An analysis of five CMIP5 model simulations of the combined response to all major anthropogenic and natural influences shows they are able to reproduce the observed evolution of global mean lower stratospheric temperature reasonably well, although with the caveats mentioned above (Figure 4-5). The

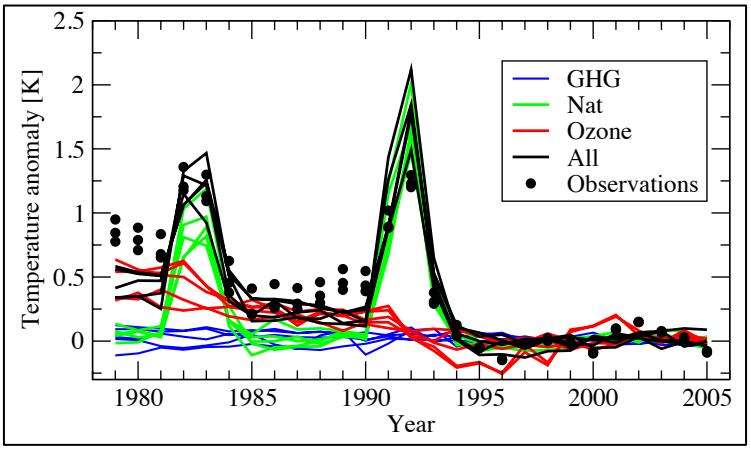

Figure 4-5. Time series of observed (black dots) and simulated global mean (82.5°S–82.5°N) synthetic MSU lower stratosphere temperature anomalies in a subset of CMIP5 simulations forced with anthropogenic and natural forcings (black), well mixed greenhouse gases (blue), natural forcings (green) and stratospheric and tropospheric ozone (red). Anomalies are calculated relative to 1996–2005. Ensemble means of the following models are shown: CCSM4, CESM1-CAM5, CanESM2, GISS-E2-H, GISS-E2-R. Adapted from Ramaswamy et al. (2006) and Bindoff et al. (2013).

models generally capture the step-like temperature reduction after episodic warming from major volcanic eruptions but the overall cooling trend (−0.29 ± 0.03 K decade^{-1}) from 1979–2005 is slightly less than observed (–0.34 ± 0.05 K decade^{-1}). Simulated changes in stratospheric and tropospheric ozone alone lead to much larger lower stratospheric temperature trends (–0.20 ± 0.04 K decade^{-1}) than increases in GHGs (–0.01 ± 0.03 K decade^{-1}). Simulations with individual forcings have also been used to examine the drivers of temperature trends in the tropical lower stratosphere. Polvani and Solomon (2012) suggested that the observed seasonal cycle of tropical lower stratospheric temperature trends correlates well with the seasonal cycle of tropical ozone trends, although these appear to be largely driven by trends in the BDC (Lamarque and Solomon, 2010; Mclandress et al., 2010) (see Section 4.3.2).

Such individual forcing simulations may also be used to attribute observed changes in stratospheric temperature by regressing observed changes onto the patterns of response simulated by the models in an attribution analysis. Gillett et al. (2011) used output from the CCMVal-2 simulations to partition observed MSU lower stratospheric temperature trends into components attributable to changes in GHGs, ODSs, and natural forcings. They found that both natural forcings and ODSs contributed significantly to the observed lower stratospheric cooling over the 1979–2005 period, with the influence of ODSs dominating, whereas the influence of greenhouse gas changes was not detectable in the observations. In the mid and upper stratosphere, Gillett et al. (2011) could detect the response to combined anthropogenic forcing (ODSs + GHGs) and natural forcings in SSU measurements, but the GHG and ODS influences were not separately detectable. However, conclusions related to the SSU data should be treated as tentative due to the large uncertainties in these observations, as discussed above. The attribution of temperature trends using one model was found to be sensitive to the height of the model top (Mitchell et al., 2013), though Charlton-Perez et al. (2013) did not find significant differences between lower stratospheric temperature trends in high-top and low-top CMIP5 models.

An important driver of the future evolution of stratospheric temperatures is the relative rate of increase of GHGs and stratospheric ozone. Relative to present day, the recovery of the ozone layer will act to warm the stratosphere over future decades. Increasing GHGs both cool the stratosphere radiatively and induce changes in the stratospheric mean meridional circulation, as discussed in Section 4.3.2. Hence, the projected GHG and ozone changes oppose each other and their relative importance in future projections varies across scenarios and models (Figure 4-6). Projected temperature changes also vary both regionally and with altitude. In the tropics, models simulate a stratospheric cooling trend that is larger at higher altitudes (e.g., Oman et al., 2010) as a result of increasing GHGs. They also exhibit tropical cooling (Figure 4-6) which increases with the magnitude of the GHG forcing. At high latitudes, the future response in the lower stratosphere exhibits seasonal structure. For the Southern Hemisphere high latitudes, warming is projected in late spring and early summer, and cooling in winter. The Northern Hemisphere high latitudes are projected to warm in winter and early spring although the trends are not statistically significant.

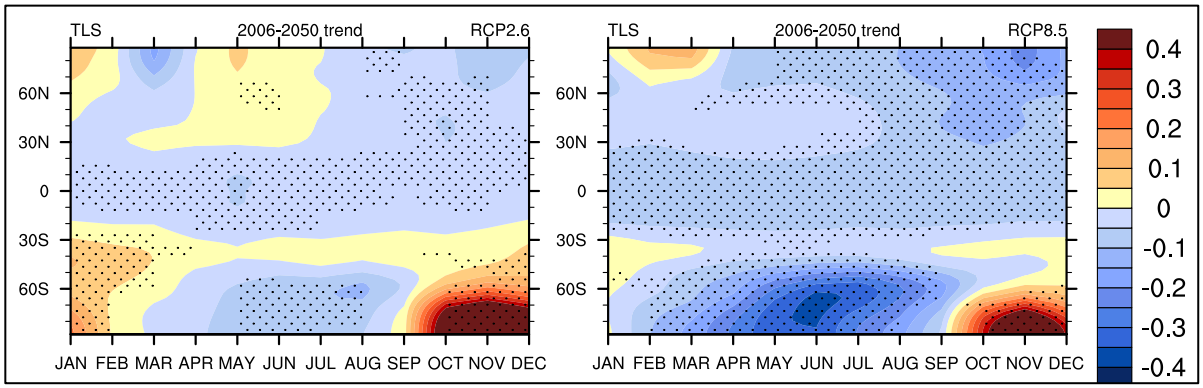

Figure 4-6. CMIP5 multi-model mean zonal mean lower stratospheric temperature trends (K per decade) over the period 2006–2050 under the low emissions scenario, RCP2.6 (*left*) and the high emissions scenario, RCP8.5 (*right*). Multi-model mean trends significant at the 5% level are stippled.

4.3.2 Stratospheric Meridional Circulation

4.3.2.1 Observations

Since the 2010 Ozone Assessment, many studies have advanced our understanding of the stratospheric meridional circulation (the so-called Brewer-Dobson circulation, BDC) and its changes. While before 2010 most of the focus of the investigations was on the changes in the tropical upwelling in the lower stratosphere, recent studies have highlighted the importance of differentiating two branches of the stratospheric circulation, the shallow and deep branches (Plumb 2002; Birner and Bönisch 2011; Bönisch et al., 2011). The shallow branch appears in the lowermost stratosphere with rising air in the tropics and descending air in the subtropics and middle latitudes, while the deep branch reaches the upper stratosphere and the descending branches extend to the mid and high latitudes, shown schematically in Figure 4-7. Birner and Bönisch (2011) compared these two branches of the Brewer-Dobson circulation and found that the deep branch was characterized by a much longer transit time (defined as the time an air parcel needs to be transported from the entry point at the tropical tropopause to a given arrival location), smaller integrated mass flux, and stratospheric entry latitudes closer to the equator. As the circulation is driven by wave dissipation, and different waves dissipate in different regions, the type of waves driving the shallow and deep branches differs.

It is now well established across many different model simulations that a strengthening of the BDC is simulated in response to increasing GHG concentrations through changes in wave dissipation driven by climate change (e.g., Butchart, 2014). Ozone changes on regional and seasonal scales also modulate changes in the meridional circulation at these scales through changes in local radiative heating, temperature, and zonal wind patterns, impacting wave-mean flow interactions (e.g., Lin and Fu, 2013). As pointed out in the last Ozone Assessment (Forster and Thompson et al., 2011), trends in the BDC are not easy to detect in observations because trends are small and thus difficult to separate from natural variability, and the BDC cannot be measured directly with available observations, so needs to be inferred from changes in other variables such as the latitudinal distribution of temperature, the amplitude of the quasi-biennial oscillation (QBO), chemical constituents, and the estimated age of air.

Based on the out-of-phase relationship between temperature changes in the tropics and high latitudes, the 2010 Ozone Assessment noted that observed changes in temperature are consistent with an acceleration of the BDC in the lower stratosphere (e.g., Thompson and Solomon, 2009; Fu et al., 2010). This has been corroborated recently by studies of radiosonde data sets (Free, 2011; Young et al., 2012) and satellite data (Young et al., 2012), although the role of decadal variability in the apparent trend and the possible role of changes in the seasonal cycle of the circulation are not clear yet. Kawatani and

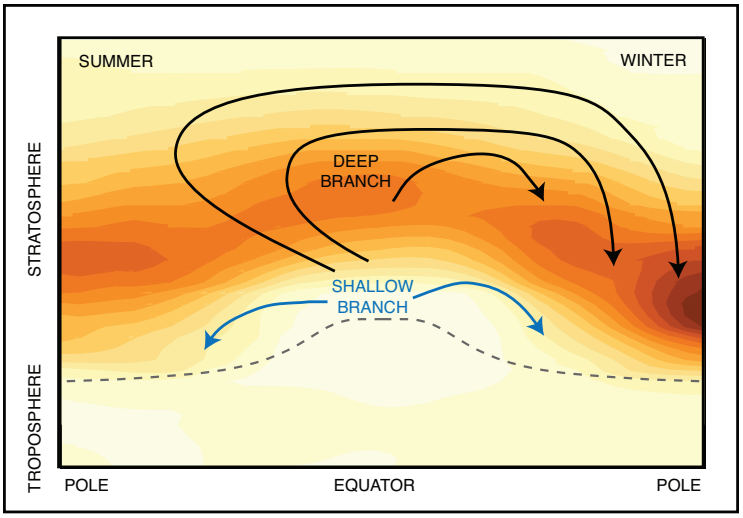

Figure 4-7. Schematic illustration of the shallow and deep branches of the Brewer-Dobson circulation in the stratosphere at solstices. Also shown is the meridional cross section of Northern Hemisphere winter ozone density (color shading, with darker shades indicating larger ozone concentrations, based on the Bodeker et al. (2013) climatology), and the approximate location of the tropopause (dashed curve). Adapted from Plumb (2002) and IPCC/TEAP (2005).

Hamilton (2013) found a significant decrease in the amplitude of the QBO at 70hPa between 1953 and 2013 based on radiosonde zonal wind measurements at near-equatorial stations and attributed it to an increased upwelling in the lowermost stratosphere that hampered the downward penetration of the QBO into this region. At higher levels in the stratosphere, Young et al. (2012) used the Met Office SSU data to diagnose a strengthening of the Northern Hemisphere branch of the BDC in December and the Southern Hemisphere branch of the BDC in August over 1979–2005, but only after removing year-to-year variability. However, as noted in Section 4.3.1.1, the Met Office SSU temperature trends have a different latitudinal structure to the NOAA STAR data (Thompson et al., 2012), meaning that the BDC trend inferred from each data set would be different. Thus, there are large uncertainties in the changes in the upper branch of the BDC inferred from temperature observations.

In addition to inferences made from observed temperature variations, changes in the BDC can also be inferred from measurements of chemical species. Decreasing ozone in the lowermost tropical stratosphere has been measured by satellite instruments and ozonesondes from 1985 to 2010 (Randel and Thompson, 2011; Sioris et al., 2014), consistent with an acceleration of the BDC in the lower stratosphere. However, the early years of the record are subject to substantial observational uncertainties (Solomon et al., 2012). Several recent studies using shorter records, subject to large interannual variability, are not long enough to corroborate such trends. More details on tropical ozone changes can be found in Chapter 2 (Section 2.3.5.3).

Recently, Stiller et al. (2012) presented new age-of-air estimates derived from more than 10^6 SF_6 profiles retrieved from the Michelson Interferometer for Passive Atmospheric Sounding (MIPAS) limb emission mid-infrared spectrometer for 2002–2010, with almost global coverage and about 3 km vertical resolution. Stiller et al. (2012) show that trends of differing sign occur at different levels in the stratosphere. In the lower stratosphere, their results show a decrease in age of air consistent with an acceleration of the BDC. As discussed in the last Ozone Assessment, Engel et al. (2009) found no significant decrease in the mean age of air above 24 km based on measurements of CO_2 and SF_6. In the middle and upper stratosphere, the results of Stiller et al. (2012) corroborate those of Engel et al. (2009) for northern midlatitudes, showing a statistically robust increase in age of air in that region, consistent with a weakening of the deep branch of the BDC there, in contrast to the strengthening inferred from stratospheric temperatures (Young et al., 2012).

As also discussed in the 2010 Ozone Assessment, inhomogeneities in observations and reanalysis products complicate the diagnosis of long-term trends in reanalysis data (e.g., Iwasaki et al., 2009). The new generation of reanalysis products, however, do show some improvements (e.g., for ERA-Interim reanalysis data as discussed by Dee et al. (2011) and Monge-Sanz et al. (2012)). Using ERA-Interim reanalysis data, changes in the BDC circulation were investigated based on the Transformed Eulerian Mean residual circulation (Sevior et al., 2011) and age of air with transport models of different complexity (Monge-Sanz et al., 2013; Diallo et al., 2012). Seviour et al. (2012) found that trends in the BDC inferred from tropical upwelling in the lower stratosphere were dependent on the altitude and tropical latitudes considered. Statistically significant trends in the lower stratosphere were found by Seviour et al. (2011) and Diallo et al. (2012) consistent with an enhancement of the BDC in this region, while Monge-Sanz et al. found significant changes above 25 km in the Northern Hemisphere that were consistent with a weakening of the deep branch of the BDC in the Northern Hemisphere and in broad agreement with findings by Engel et al. (2009) and Stiller et al. (2012). However, Diallo et al. (2012) found little or no statistical significance in the changes in age of air above 20 km (in agreement with Bönisch et al., 2011).

In summary, changes in temperature, ozone, and age of air all agree in showing an acceleration of the tropical upwelling in the lowermost stratosphere (shallow branch) and, as discussed in Section 4.3.2.2, this change is consistent with that simulated by climate models. However, the behavior of the trends in the BDC in the middle and upper stratosphere is not as clear, as temperature changes (albeit from only one data set) indicate a strengthening of the deep branch while BDC changes inferred from age of air point to no change or even weakening of the deep branch.

4.3.2.2 SIMULATED PAST AND FUTURE CHANGES

In the 2010 Ozone Assessment, it was assessed that chemistry-climate models consistently simulate an acceleration of the BDC in response to increasing GHG concentrations, although most studies had focused on the lower stratosphere. More recent modeling studies all consistently simulate an acceleration of the BDC in response to increasing GHG concentrations in past and future simulations (e.g., Butchart, 2014). The 2010 Ozone Assessment highlighted a primary caveat associated with the non-statistically significant trend found in stratospheric age-of-air estimates from SF_6 and CO_2 measurements (Engel et al., 2009) and also noted difficulties in comparing the tropical upwelling and its forcings across different studies because of the different definitions used (e.g., fixed latitudes versus turnaround latitudes, where the residual vertical velocity changes sign), and in quantifying the role of parameterized gravity waves (versus resolved waves) in models, especially in the lower stratosphere. Since the last Ozone Assessment, new research has clarified some of these issues.

New studies demonstrated that observational results of Engel et al. (2009) may not be inconsistent with simulated stratospheric circulation changes and that BDC changes in climate models agree with new observational age-of-air measurements in the lower stratosphere (Stiller et al., 2012). Ray et al. (2010) were able to reproduce the observed age of air and ozone trends over the last 30 years in their simple model assuming a small strengthening of the mean circulation in the lower stratosphere and a moderate weakening of the mean circulation in the middle and upper stratosphere. Garcia et al. (2011) identified issues associated with using natural species, with non-uniform growth rates, as proxies for trends in the stratospheric circulation. Their CCM was able to simulate non-statistically significant trends in age of air, as observed by Engel et al. (2009), when it was sampled sparsely as in the observations, demonstrating the large uncertainty in trends determined from sparsely sampled data.

Recent studies have confirmed that the role of parameterized gravity waves in driving modeled changes in tropical upwelling is larger in the middle and upper stratosphere (Bunzel and Schmidt et al., 2013; Oberländer et al., 2013; Palmeiro et al., 2014). This is in agreement with previous results from Garcia and Randel (2008) and McLandress and Shepherd (2009). In the lowermost stratosphere, orographic wave forcing dominates over non-orographic contributions and the trend in orographic gravity wave forcing is larger in the subtropics than in the deep tropics (McLandress and Shepherd, 2009). Thus the contribution of orographic gravity waves to the total trend in tropical upwelling is larger when the turnaround latitudes are used to compute the upwelling (e.g., McLandress and Shepherd, 2009) instead of using fixed latitudes encompassing the deep tropics (e.g., Calvo and Garcia, 2009).

Understanding of the role of resolved waves in driving the tropical upwelling has advanced. New individual modeling studies indicate that resolved waves are the main driver of the trend in tropical upwelling in the lower stratosphere (Bunzel and Schmidt, 2013; Oberländer et al., 2013; Palmeiro et al., 2014; Okamoto et al., 2011) while the role of orographic gravity waves seems to be largely dependent on the model. Previous multi-model studies already highlighted the large spread in the contribution of both types of waves to the trend (e.g., Butchart et al., 2010), which could be in part explained by the compensation between resolved and parameterized orographic wave driving found in this region (Cohen et al., 2013; Sigmond and Shepherd, 2014 and references therein). The fact that representation of parameterized waves varies between models hampers a systematic multi-model comparison to assess the degree of consensus in the role of resolved versus parameterized waves.

The contribution of stationary and transient waves to the trend in the shallow branch tropical upwelling varies with latitude in models. The contribution of stationary waves dominates in the deep tropics, whereas transient waves are more important at higher latitudes in the subtropics (Garny et al., 2011; Shepherd and McLandress, 2011). This explains discrepancies found in previous studies, because the contribution of these waves is expected to be different depending on how the tropical upwelling is defined (in the deep tropics or between the turnaround latitudes).

It is still difficult to attribute changes in wave forcing to changes in wave propagation or wave generation, because changes in both processes are hard to disentangle in a free-running climate model. Garny et al. (2011) found that warmer tropical SSTs under increasing GHGs cause a strengthening of the

subtropical jets and changes in deep convection affecting latent heat release, which modulate the wave propagation and wave generation, respectively, although the former dominates in their model. Shepherd and McLandress (2011) propose that critical-layer control of Rossby wave breaking (Randel and Held, 1991) is the mechanism that explains the simulated changes in wave drag that ultimately force the strengthened tropical upwelling in the lower stratosphere. The tropospheric warming in response to climate change leads to a strengthening and upward displacement of the upper flanks of the subtropical jets in the lower stratosphere (e.g., Garcia and Randel, 2008), which causes the critical layers on the equatorward side of the jets to move upward and the Rossby wave drag to occur at higher altitudes and further equatorward, allowing more Rossby wave activity to penetrate into the subtropical lower stratosphere. This mechanism can also explain the simulated increase in parameterized lower-stratospheric orographic gravity wave drag (e.g., Li et al., 2008; McLandress and Shepherd, 2009) as an upward shift of the wave-breaking levels due to the strengthened upper flank of the subtropical jets.

As discussed above, a few recent studies have been devoted to exploring the behavior of the deep branch of the circulation and understanding its driving mechanisms in future climates (Hardiman et al., 2013; Palmeiro et al., 2014; Lin and Fu, 2013; Oberländer et al., 2013). A strengthening of the deep branch of the circulation has been found in response to increasing GHG concentrations in CCMs (Lin and Fu, 2013) and in "high top" CMIP5 models (i.e., those with their lid above 1 hPa; Hardiman et al., 2013; Palmeiro et al., 2014; Figure 4-8). In addition, changes in the width of the tropical upwelling region have been found to vary with height, so that the upwelling region narrows below 20 hPa and widens above 20 hPa (Hardiman et al., 2013; also compare black and red lines in Figure 4-8). This indicates that different mechanisms might operate in forcing the changes in each branch of the circulation. Changes in the

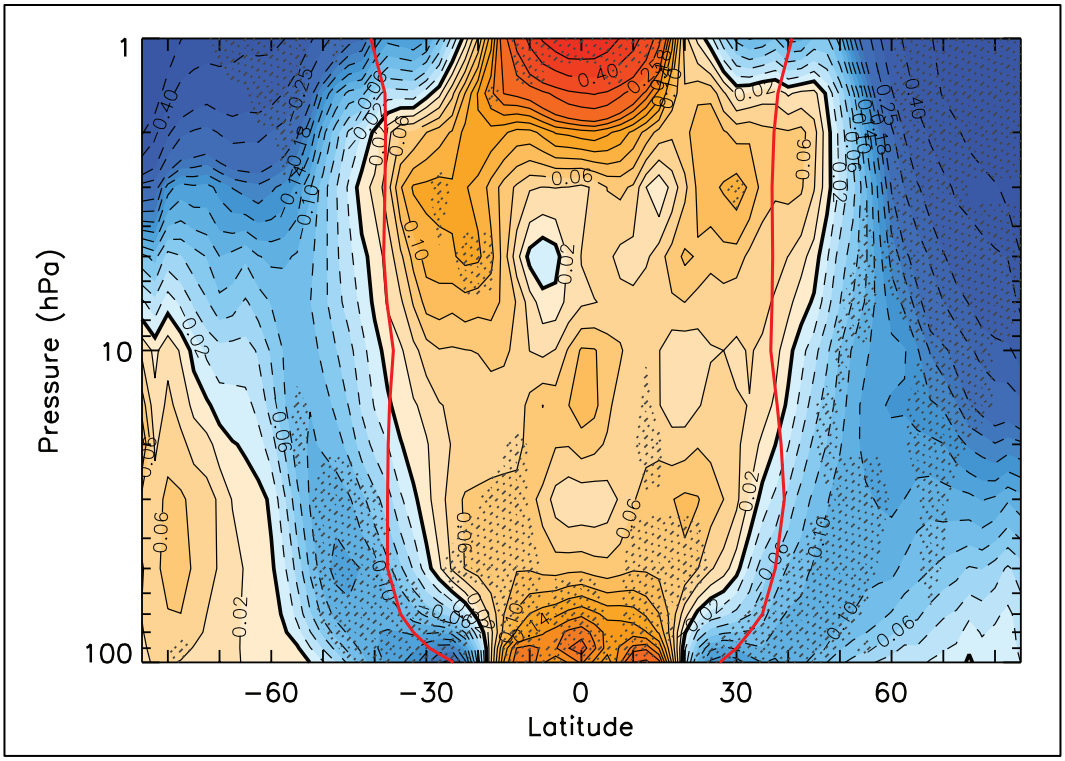

Figure 4-8. Multi-model mean CMIP5 simulated differences in annual mean residual vertical velocity (mm/s) in RCP8.5, 2080–2099 climatology minus 2006–2025 climatology. Solid/Dashed contours show positive/negative values (increases/decreases in residual vertical velocity). Stippling denotes regions where 90% of models show a statistically significant change in residual vertical velocity at the 5% level. Red lines denote the position of the turnaround latitudes (where residual vertical velocity is zero) for the 2006–2025 climatology. Adapted from Hardiman et al. (2013).

dissipation of parameterized gravity waves appear to be the key to explaining the acceleration of the deep branch of the BDC under climate change (Oberländer et al., 2013; Palmeiro et al., 2014), although there is no consensus in the type of gravity waves involved. Thus, modeling evidence is currently too limited to assess the contribution of gravity waves to the deep branch of the circulation in the upper stratosphere.

Overall, studies have found that the projected increase in the tropical upwelling in the upper stratosphere is robust across models and balanced by an increase in extratropical downwelling. In the Northern Hemisphere, a robust increase in downwelling is simulated at high latitudes throughout the entire stratosphere (Figure 4-8) while in the Southern Hemisphere, the increased downwelling mainly occurs at midlatitudes although the agreement across models is not as robust. Reduced downwelling is simulated over the Antarctic in austral spring and summer, driving the annual mean behavior in this region. Recent studies have shown that the reduced downwelling is in response to future ozone recovery (Hardiman et al., 2013; Palmeiro et al., 2014; Lin and Fu, 2013), in agreement with the enhanced downwelling in austral summer found in response to ozone depletion (e.g., Manzini et al., 2003; Li et al., 2008) but in contrast with McLandress and Shepherd (2009), who found reduced downwelling in the future in Antarctic spring in response to increasing GHGs.

In summary, modeling studies show an acceleration of the shallow and deep branches of the BDC with climate change. In the lower stratosphere, these results are in agreement with observations from changes in temperature, trace gases, and age of air, which all agree in showing an intensification of the BDC in this region. In the middle and upper stratosphere, changes in the deep branch of the BDC inferred from changes in temperatures, trace gases, and age-of-air observations are uncertain. Further research is needed to assess the changes in the BDC in the middle and upper stratosphere and the underlying mechanisms.

4.3.3 Stratospheric Zonal Flow

The characteristics of the stratospheric zonal flow, and in particular the stratospheric polar vortices, play an important role in determining polar ozone concentrations and in the dynamical coupling between the stratosphere and troposphere. Changes in the zonal flow and vortices can have an impact on tropospheric climate. The observed changes in vortex characteristics, the cause of these changes, and projected future changes are discussed in Chapter 3 of this Assessment, and are only briefly reviewed here.

In general, there is larger interannual variability in the characteristics of the Arctic vortex than the Antarctic vortex. However, as discussed in Chapter 3, there has been an increase in the year-to-year variability in both hemispheres in recent years, with increased variability in lower stratospheric polar temperatures (Figure 3-1) and the breakup date of the vortices (Figure 3-2). Also, whereas there were few Arctic major sudden warmings during the 1990s, there were many during the first decade of the 21st century (Chapter 3). In the Antarctic there has been a trend toward a stronger vortex (e.g., stronger zonal flow; see Figure 4-10) and later breakup dates since 1980 (Figure 3-2). In most recent years the vortex broke up in early to mid-December, although the 2012 vortex broke up in mid-November.

The variability in the strength and lifetime of the polar vortices is connected to similar variability in planetary wave activity, since there is generally a stronger, longer-lasting vortex in winters with lower mean winter eddy heat flux (see Section 3.3.3). However, whether changes in wave activity and the resulting vortex strength are due to natural variability or the response to anthropogenic forcing is generally not known. An exception is the strengthening and delay in breakup date of the Antarctic vortex, which is due primarily to diabatic cooling associated with the Antarctic ozone hole (see Section 4.3.1).

Climate model simulations also show a strengthening of the Antarctic vortex during the latter part of the 20th century in response to stratospheric ozone depletion, and a weakening in spring as ozone recovers (Figures 4-6, 4-10). The simulations show a shift to later breakup dates in the latter part of the 20th century and then a return to earlier breakup dates (e.g., McLandress et al., 2010; Deushi and Shibata 2011; Shaw et al., 2011; Wilcox et al., 2013; Orr et al., 2013). There is some indication of a shift toward later final warming dates in the latter half of the 21st century for a high GHG emission scenario (Wilcox et

al., 2013). However, Sheshadri et al. (2014) found that a delayed stratospheric final warming could not explain the trend in Southern Hemisphere tropospheric zonal mean zonal wind in recent decades (see Section 4.4).

In contrast to the clear trends in the Antarctic, models generally show small, insignificant trends in Arctic polar temperatures and vortex breakup dates over the 21st century (CCMVal 2010; Hitchcock et al., 2009; Langematz et al., 2014).

4.4 EFFECTS OF PAST CHANGES IN STRATOSPHERIC OZONE ON THE TROPOSPHERE AND SURFACE

The influence of stratospheric ozone change on Southern Hemisphere tropospheric and surface climate has been analyzed and investigated in an increasingly mature body of research, with its signature now well documented (e.g., recent reviews of Thompson et al., 2011; Previdi and Polvani, 2014; Canziani et al., 2014). We focus here on what has been learned since the 2010 Ozone Assessment (Forster and Thompson et al., 2011), notably, improved quantification of the relative roles of ozone and GHGs in driving observed Southern Hemisphere circulation changes. Consistent with the last Assessment, ozone depletion is assessed to be the dominant driver of austral summer (December-January-February, DJF) atmospheric circulation changes over the last several decades. We begin by assessing the effects of stratospheric ozone changes on the tropospheric circulation, followed by an assessment of the resultant impacts on surface climate, the ocean, and sea ice.

4.4.1 Tropospheric Circulation Effects

The Southern Hemisphere

As described in the previous section, the primary effect of stratospheric ozone depletion is to produce a strong cooling in the lower stratosphere over the Antarctic in austral spring. Simulations indicate that this cooling acts to strengthen and shift the Southern Hemisphere tropospheric midlatitude jet poleward in austral summer, and to drive an increase in the Southern Annular Mode (SAM) index corresponding to decreases in sea level pressure over high latitudes and increases over midlatitudes. We first evaluate the observed evidence for the impact of ozone depletion on the tropospheric circulation followed by an assessment of the current understanding of the mechanisms through which this shift occurs. We note that here and elsewhere in this chapter, we use the term "midlatitude jet" to refer to the band of strong westerly winds, climatologically centered around 50°S, which are associated with synoptic-scale eddies (i.e., typical storms in the midlatitudes). The latitude of the midlatitude jet is generally defined as the location of the maximum zonal mean westerly winds at 850 hPa. This definition is used because it distinguishes the Southern Hemisphere midlatitude jet from the upper-level subtropical jet that is present in some seasons.

The SAM is the leading mode of variability in the extratropical circulation and the SAM index gives an indication of changes in the characteristics of the midlatitude jet, though there is not necessarily a one-to-one relationship between SAM index anomalies and variations in the strength or location of the midlatitude jet. Whereas changes in the jet strength and location can only be determined from reanalysis data sets, the SAM index can be calculated from sea level pressure observations, which are available over a longer period. After 1979, there is generally good agreement between the SAM index calculated from station observations and that calculated from reanalyses, whereas prior to 1979 some reanalyses are known to have deficiencies (Marshall, 2003). Since a longer period is often used in model attribution studies, two periods are discussed here. Figure 4-9 shows trends in the SAM index from station observations of sea level pressure (based on an update of Marshall, 2003) for 1979–2012 (which encompasses the satellite era) and 1958–2012 (which begins at the International Geophysical Year). The largest seasonal trends are found in DJF over both periods and significant trends (shown in red) are observed

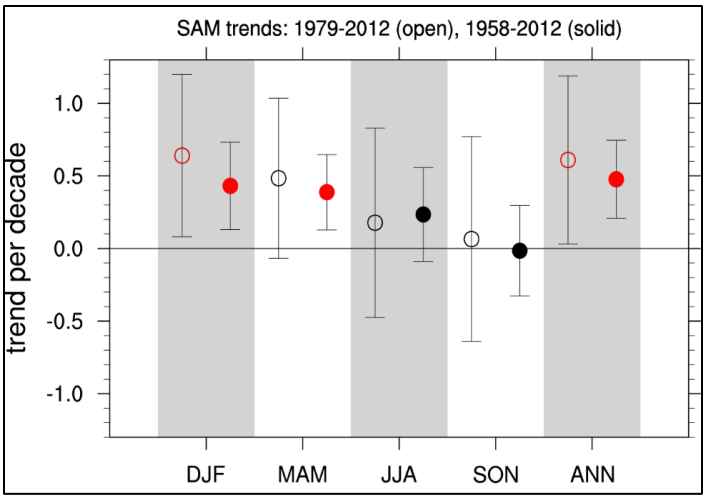

Figure 4-9. SAM trends per decade calculated over 1979–2012 (open circles) and 1958–2012 (closed circles) from the seasonal and annual data of Marshall (2003; http://www.nerc-bas.ac.uk/icd/gjma/sam.html). Error bars indicate the 95% confidence interval of the trends with the auto-correlation accounted for. Trends significant at the 5% level based on a two-sided t-test are colored red. The SAM index is dimensionless (Marshall, 2003).

in the annual mean and DJF for 1979–2012 and in the annual mean, DJF, and March-April-May (MAM) for 1958–2012.

The connection of these surface changes to the stratosphere is evident in Figure 4-10a, which shows the austral summer climatology and trends in the zonal mean zonal winds over the period 1979–2005 in one reanalysis data set (Eyring et al., 2013). There is a clear asymmetry between the Northern and Southern Hemisphere trends over this period, with the largest wind changes in the Southern Hemisphere stratosphere. These features lend support to ozone depletion being the dominant cause of the Southern Hemisphere trends, and these trends are well captured by the CMIP5 historical experiments (see Box 2-2 in Chapter 2 of this Assessment), driven by natural and anthropogenic forcings including ozone depletion (Figure 4-10b).

Swart and Fyfe (2012) analyzed recent trends in surface wind stress over the Southern Ocean in various reanalyses (Figure 4-11). They report no statistically significant trends in the annual mean midlatitude jet location (defined based on surface wind stress) over the 1979–2010 period, but note the existence of a significant poleward shift in austral summer (DJF), which is found consistently across six reanalysis data sets. They find that the Southern Hemisphere DJF midlatitude jet has shifted poleward by -0.7 ± 0.5 degrees latitude per decade, averaged across the different reanalyses (their Figure 3). Swart and Fyfe (2012) also report a *strengthening* of the midlatitude jet in the annual mean and in DJF, but the large spread across the reanalyses in Figure 4-11 precludes a confident assessment of this metric.

A recent study by Lee and Feldstein (2013) also found a dominant role for ozone depletion in summertime extratropical circulation trends in the ERA-Interim reanalyses in the last few decades. These authors applied a cluster analysis technique to zonal mean zonal wind data, identified trends in the occurrence frequency of two of the clusters, and by simply comparing the patterns of zonal mean wind anomalies associated with each cluster with the simulated response to GHGs and ozone from other studies, inferred that changes in occupation frequency of one cluster were due to GHG changes and changes in the occurrence frequency of the other were due to ozone depletion. Based on this, they inferred that ozone depletion has contributed about 50% more than increasing GHGs toward the jet shift in austral summer. Son et al. (2013) and Bandoro et al. (2014) further showed that stratospheric ozone variability can change the tropospheric circulation on interannual timescales.

Since the previous Ozone Assessment, several modeling studies have compared the influence of ozone depletion and GHGs on the tropospheric circulation. McLandress et al. (2011), performed transient simulations with a coupled-chemistry stratosphere-resolving model with a fully coupled (non-eddy resolving) ocean; Polvani et al. (2011b), performed time-slice integrations with a much simpler atmosphere-only (low-top) climate model, with prescribed ozone concentrations, sea surface temperatures, and sea ice; while Gillett et al. (2013) and Fyfe et al. (2012) compared sea level pressure trends in CMIP5 simulations that included GHG changes only and ozone (stratospheric and tropospheric) changes only. Considering spatio-temporal patterns of sea level pressure change over the whole globe and for all four

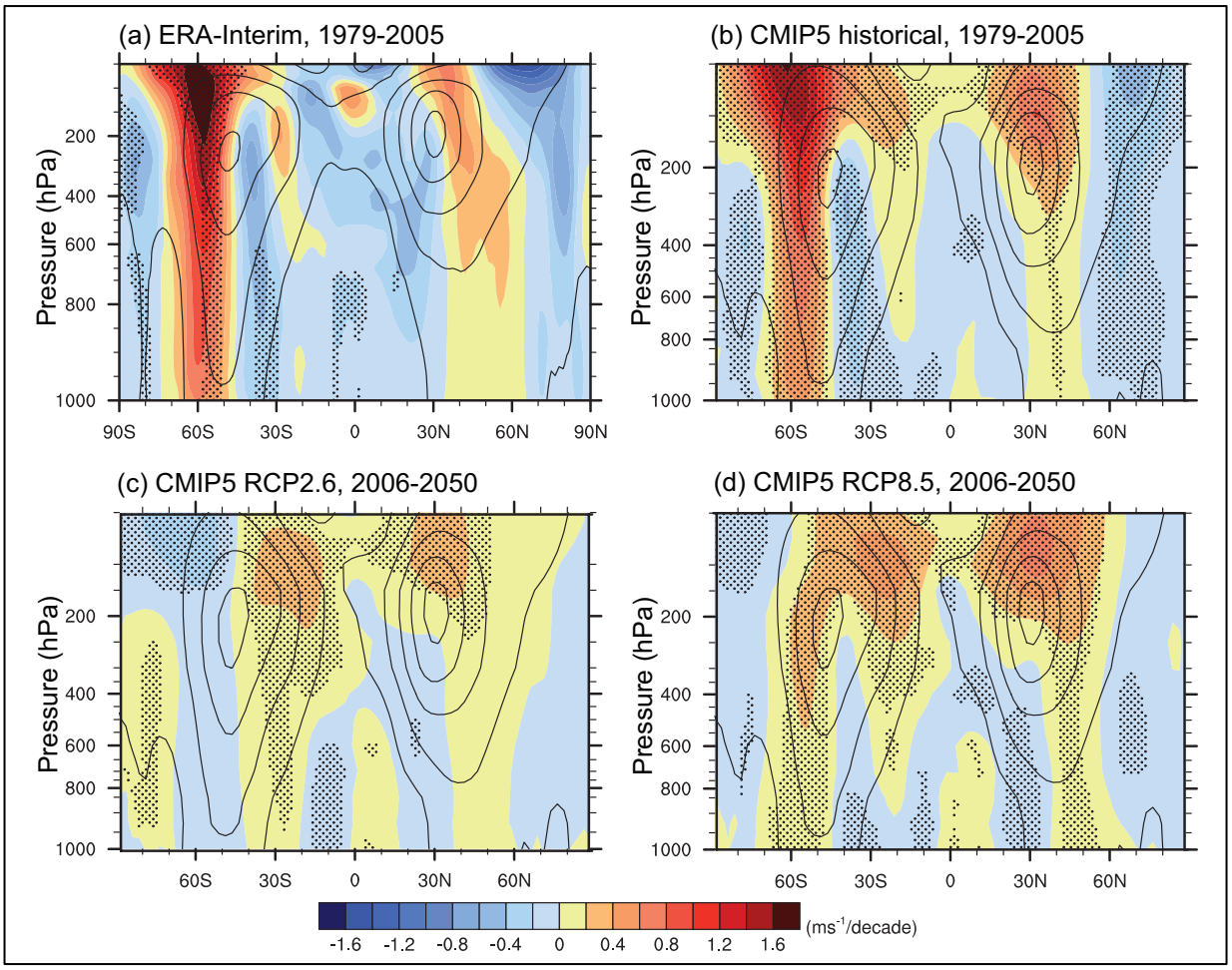

Figure 4-10. Long-term mean (thin black contour) and linear trend (color) of zonal mean DJF zonal winds for (a) ERA-interim over 1979–2005; (b) the mean of the CMIP5 historical experiments over 1979–2005; (c) CMIP5 RCP2.6 multi-model mean over 2006–2050 and (d) CMIP5 RCP8.5 multi-model mean over 2006–2050. Contour intervals of climatological wind are 10 m s^{-1} starting from −20 m s^{-1}. Trends that are statistically significant at the 5% level are stippled. Adapted from Eyring et al. (2013).

seasons, Gillett et al. (2013) separately detected the influence of ozone changes and GHG changes in observations, using attribution techniques that employ the distinctive patterns of response to each forcing simulated by CMIP5 models. Gillett et al. (2013) also examined seasonal SAM trends across the CMIP5 individual forcing simulations (see Figure 4-12). In all studies apart from Fyfe et al. (2012), simulations showed that the shift in the latitude of the midlatitude jet and the SAM index trend in DJF were considerably larger in response to stratospheric ozone depletion than in response to GHG changes over the last fifty years or so (McLandress et al., 2011; Polvani et al., 2011b; Gillett et al., 2013). Fyfe et al. (2012) find a comparable contribution of GHGs and ozone to trends in their DJF sea level pressure index over 1957–2010, although they note that the prescribed ozone forcing used in their simulations may be weaker than observed.

In seasons other than DJF, the relative amplitude of the circulation response to anthropogenic and natural forcings depends on the metric used and on the period over which trends are calculated. Observations and most models show smaller SAM trends in these seasons, and simulations show a relatively uniform response to GHGs in all months (e.g., Staten et al., 2012; Gillett et al., 2013). In MAM, when the observed SAM index trends are significant over longer timescales (Figure 4-9), Polvani et al. (2011b) and McLandress et al. (2011) find larger contributions from GHGs compared to ozone depletion,

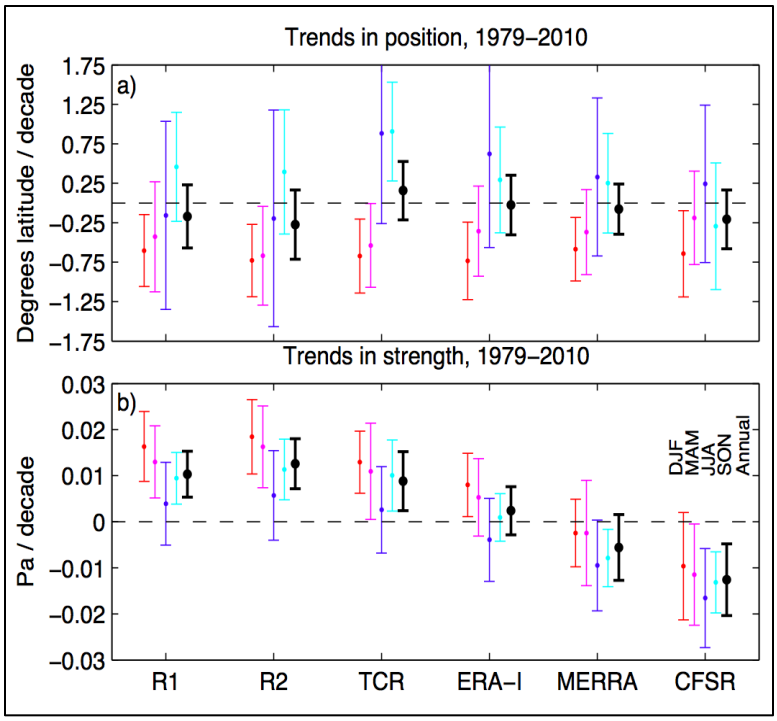

Figure 4-11. Historical trends in the Southern Hemisphere surface westerly wind-stress jet position (a) and strength (b). Trends are computed over the period 1979–2010 from six reanalysis products: NCEP-NCAR Reanalysis 1 (R1), NCEP-DOE Reanalysis 2 (R2), ECMWF ERA-Interim Reanalysis (ERA-I), NOAA-CIRES Twentieth Century Reanalysis Version 2 (TCR), NASA Modern Era-Retrospective Analysis for Research and Applications (MERRA), and NCEP Climate Forecast System Reanalysis (CFSR); the analysis has been adapted from Swart and Fyfe (2012) to include the NASA MERRA and NCEP CFSR data sets that were not included in the main text. The error bars show the 95% confidence interval of the trends, where auto-correlation has been accounted for. Trends are computed for seasonal means and annual means of the zonal-mean zonal wind-stress. Adapted from Swart and Fyfe (2012).

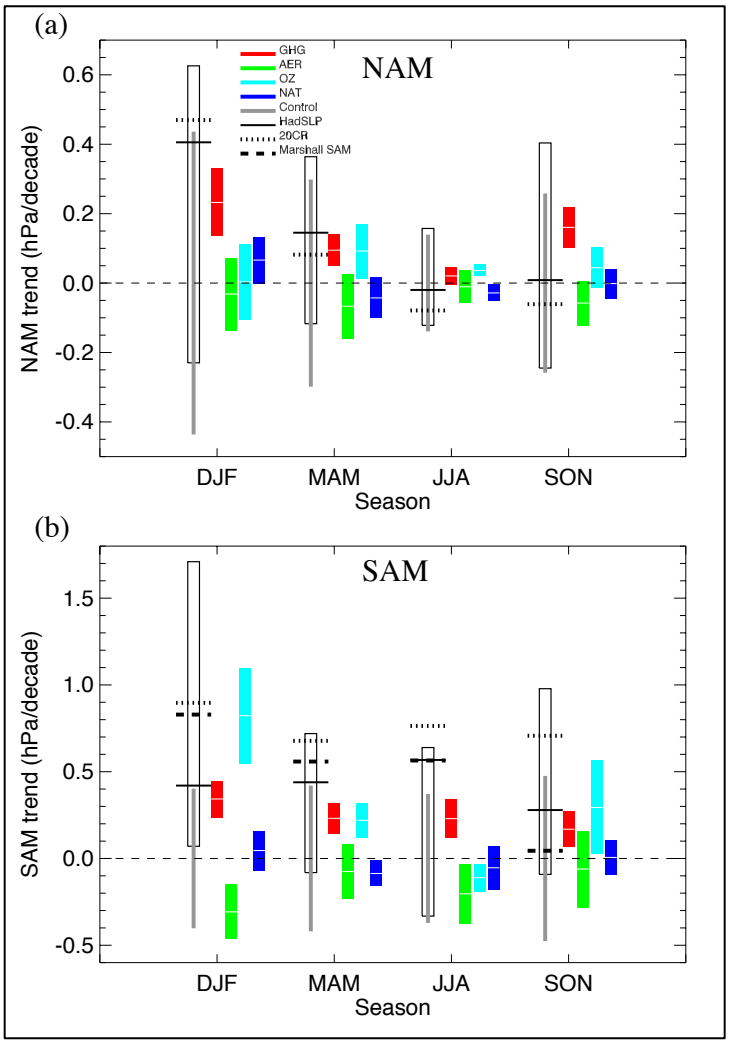

Figure 4-12. Simulated and observed trends in the Northern Annular Mode and Southern Annular Mode indices. Observed trends in the (a) NAM and (b) SAM over the period 1951–2011 are shown for each season based on HadSLP2 / HadSLP2r_lowvar (solid line), the 20th Century Reanalysis (dotted), and in the case of the SAM, the Marshall SAM index over the period 1958–2011 (dashed). No normalization was used when computing the annular mode indices. Gray bars show the 5–95% centered range of trends in the control simulations. Colored boxes show the ensemble mean and its 5–95% confidence range for the simulated response to GHGs, aerosols (AER), tropospheric and stratospheric ozone changes (OZ), and natural forcings (NAT), based on available individual forcing simulations. Black boxes show the 5–95% range of trends simulated in response to ALL forcings. Note the different scales on (a) and (b). Adapted from Gillett et al. (2013).

while Staten et al. (2012) and Gillett et al. (2013) suggest comparable contributions from both (see Figure 4-12). A comparable contribution of GHGs and ozone is also found in annual mean trends in the SAM in studies where it was diagnosed (Sigmond et al., 2011; Staten et al., 2012), consistent with earlier studies (e.g., Arblaster and Meehl, 2006; Shindell and Schmidt, 2004). Recent modeling studies suggest that the response to other forcings is weaker, though aerosol changes may have driven opposing, negative trends in the SAM (Gillett et al., 2013; Xie et al., 2013).

In summary, the contribution of Antarctic ozone depletion to the observed increase in the Southern Annular Mode index in austral summer is substantially larger in most models than the contribution from greenhouse gas increases over the past three to five decades. The role of ozone depletion is largest in summer. Observations and models suggest smaller Southern Annular Mode trends in other seasons. In most models, GHGs drive consistently positive trends in the SAM across the seasonal cycle and likely contribute partially to the observed changes seen.

In the Southern Hemisphere midlatitudes, in association with the shift of the jet, several additional impacts of stratospheric ozone depletion, beyond those already mentioned in the previous Ozone Assessment have now been documented. Ndarana et al. (2012) reported a large increase in summertime Rossby wave breaking events on the equatorward side of the tropospheric midlatitude jet in the Southern Hemisphere (and weak decreases on the poleward side), over the last 30 years in meteorological analyses. Such events are of interest because they are often linked to weather extremes and stratosphere-troposphere exchange of trace gases. Using model integrations with single forcings, Ndarana et al. (2012) showed that trends consistent with the reanalyses are simulated in response to stratospheric ozone depletion. Using the same model integrations, Grise et al. (2014) showed how ozone depletion can also cause a significant poleward shift in the position of midlatitude storms over the Southern Ocean, indicating that the storm tracks are tightly linked with the position of the midlatitude jet.

Recent studies have shown that the impact of stratospheric ozone depletion is not confined to the mid to high latitudes but extends well into the low latitudes. Notably, new studies have shown that ozone depletion has likely contributed to a broadening of the Hadley Cell in austral summer (McLandress et al., 2011; Polvani et al., 2011b; Min and Son, 2013), confirming the tentative conclusion of the last Ozone Assessment (Forster and Thompson et al., 2011; Son et al., 2010). This is illustrated in Figure 4-13, which shows a broad variety of simulated circulation metrics exhibit substantial trends in austral summer, in a model forced with stratospheric ozone changes alone (via changes in ODSs). Note, in particular, the Hadley cell width in panel (d), and how the ozone forcing yields a much stronger broadening than greenhouse gas forcing, over the period 1960–2005. The response of the Hadley Cell width to ozone depletion has also been detected in observations in austral summer by Min and Son (2013), using several reanalyses and CMIP3 and CMIP5 models. Nonetheless, large observational uncertainties remain and the observed trend in the Hadley Cell width is considerably larger than that simulated in response to ozone and GHG changes by climate models (Quan et al., 2013; Min and Son, 2013; Lucas et al., 2013, 2014). Understanding of the influence of stratospheric ozone depletion on the low-latitude atmospheric circulation has also improved since the last Ozone Assessment. Although the direct response to polar ozone depletion is primarily a shift of the jet in the midlatitudes, the width of the tropical circulation is very tightly coupled to the position of the jet in austral summer (Kang and Polvani, 2011).

In spite of the modeling and observational evidence that stratospheric ozone depletion affects the tropospheric circulation, a precise mechanism linking stratospheric ozone loss to the jet shift is still the subject of active research. Experiments with simplified atmospheric models (e.g., Polvani and Kushner, 2002, and Butler et al., 2010) have established that the impact of ozone depletion on the troposphere is effected through a cooling of the lower polar stratosphere, which is associated with anomalously strong westerly winds that alter the wave driving of the stratosphere, producing a positive anomaly in potential vorticity. It is well accepted that the balanced response of the troposphere to this positive potential vorticity anomaly is an acceleration of the zonal flow on the poleward flank of the storm track, consistent with the sign of the observed shift in the circulation (e.g., Hartley et al., 1998; Thompson et al., 2006). It is unlikely, however, that this balanced response is sufficiently large to explain the magnitude of the observed circulation shift.

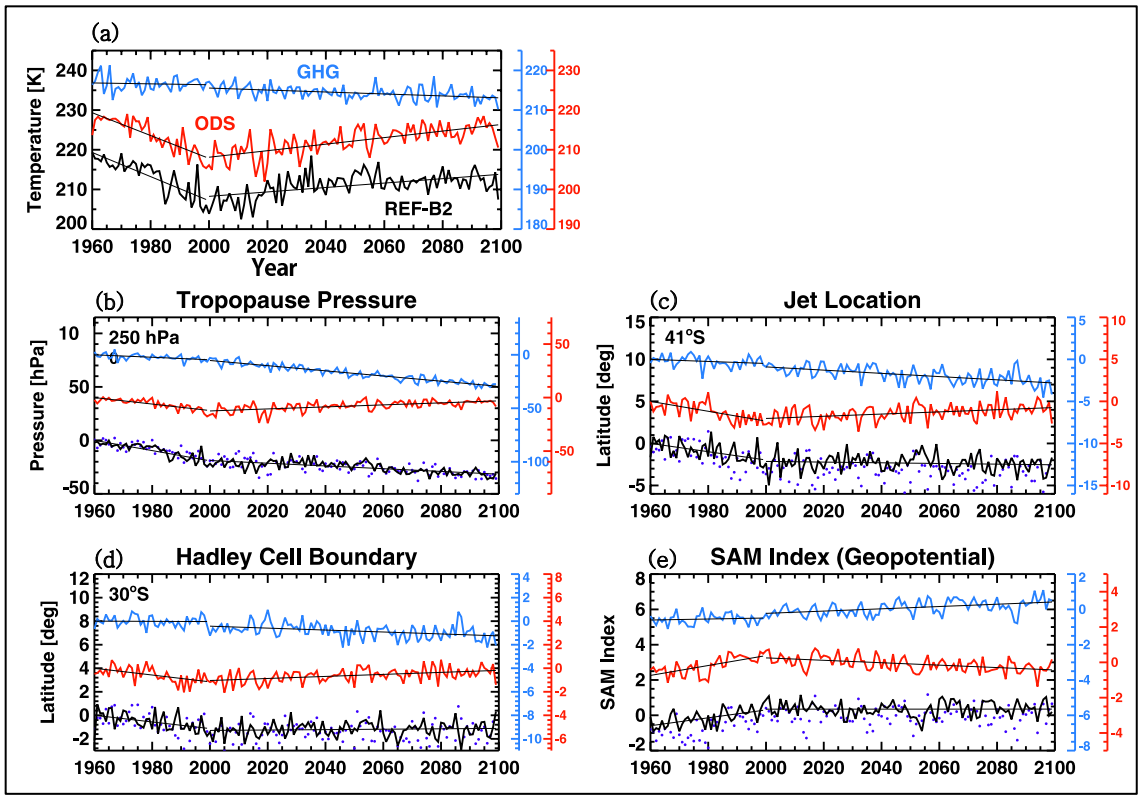

Figure 4-13. Time series of (a) 100-hPa temperature for October–January area-averaged over 70° to 90°S, (b) DJF tropopause pressure anomaly averaged over 45° to 90°S, (c) DJF jet-location anomaly defined by the latitude of 850-hPa zonal-mean zonal wind maximum, (d) DJF Hadley cell boundary anomaly defined as the zero-crossing latitude of 500-hPa mass streamfunction, and (e) DJF SAM-index anomaly derived from 850-hPa geopotential. The REF-B2 (black), ODS (red), and GHG (blue) simulations denote an experiment with time-varying ODS and GHG concentrations, an experiment with time-varying ODS concentration but GHG concentrations fixed at 2000 values, and an experiment with time-varying GHG concentration and ODS concentrations fixed at 2000 values, respectively. The sum of the GHG and ODS responses is denoted by purple dots. The straight lines are linear fits computed from 1960 to 1999 and 2000 to 2099. The red and blue curves are shifted with respect to the black; their color-coded axes are given on the right. In (b-d), anomalies are computed with respect to 1960 baselines; the average baseline (i.e., average of the REF-B2, ODS, and GHG baselines) is shown in the top-left corner of each panel. The 1960 baseline has not been removed from the SAM index time series. Adapted from McLandress et al. (2011).

Studies with idealized atmospheric models in particular suggest that tropospheric eddy feedbacks amplify the impact of stratospheric cooling, and so play a critical role in the mechanism (Kushner and Polvani, 2004; Song and Robinson, 2004); a number of pathways for the lower stratosphere to directly influence tropospheric eddies have been proposed. Several mechanisms focus on the direct influence of the lower stratosphere on tropospheric eddy momentum fluxes: linear theories consider the propagation and refraction of synoptic waves (Limpasuvan and Hartmann, 2000; Chen and Held, 2007; Simpson et al., 2009), while nonlinear mechanisms focus on the wave breaking itself (Wittman et al., 2004; Kunz et al., 2009). Other studies have focussed on the impact of stratospheric anomalies on the generation of wave activity through baroclinic instability, which in turn drives changes in the eddy momentum fluxes (Rivière, 2011; Thompson and Birner, 2012).

Crook et al. (2008) and Waugh et al. (2009) find that the zonal structure of ozone loss amplifies its impact on the troposphere, suggesting a role for planetary-scale wave interactions. The potential for constructive and destructive interferences between forced and climatological planetary waves has been shown to impact coupling between the stratosphere and troposphere in the Northern Hemisphere (Smith et al., 2010), and there is evidence that the ozone hole has modified planetary wave coupling in the Southern Hemisphere (Shaw et al., 2011).

Tropospheric eddy feedbacks have been observed in the jet response in comprehensive model studies (McLandress et al., 2011; Orr et al., 2012), but Garfinkel et al. (2013) illustrate the difficulty in separating and confirming many of the proposed mechanisms, even in an idealized atmospheric model. Tropospheric eddy feedbacks overwhelm the initial perturbation generated by the stratosphere, controlling the ultimate amplitude of the response. Both comprehensive and idealized models tend to overestimate the strength of the tropospheric eddy feedbacks (e.g., Gerber et al., 2010), complicating the effort to connect model-based analysis to the real atmosphere. A number of studies have also noted the equatorward bias in the position of the Southern Hemisphere DJF midlatitude jet in the CMIP3 and CMIP5 models compared to the reanalyses (Wilcox et al., 2012, Swart and Fyfe, 2012), which may impact their response to stratospheric ozone changes (Sigmond and Fyfe, 2014). Swart and Fyfe (2012) find this bias has somewhat improved from CMIP3 to CMIP5. Despite these uncertainties and the lack of clarity on the mechanism, the influence of stratospheric ozone on the troposphere is robust across a range of comprehensive and idealized atmospheric models.

The Northern Hemisphere

The last Ozone Assessment assessed that no robust linkages between stratospheric ozone depletion and tropospheric circulation had been established in the Northern Hemisphere, consistent with the relatively weak ozone depletion observed in the Arctic (see, e.g., Figure 3-4). However, Morgenstern et al. (2010) find a weak but significant anticorrelation between Northern Hemisphere column ozone and the NAM index in spring (March-May, MAM) in the CCMVal-2 models, suggesting that in these models Arctic ozone depletion drives an increase in the NAM index in MAM. The CMIP5 models also exhibit an increase in the NAM index in MAM in response to combined changes in stratospheric and tropospheric ozone (Figure 4-12), though simulations with one model suggest that this response may be driven by tropospheric ozone changes (Gillett et al., 2013). No statistically significant trend in the NAM index has been observed in MAM (e.g., Gillett et al., 2013). Thus our assessment remains that no robust link between stratospheric ozone depletion and Northern Hemisphere circulation has been established.

4.4.1.1 SURFACE IMPACTS

An important development since the previous Ozone Assessment has been the improved understanding of the influence of ozone depletion on Southern Hemisphere precipitation. The effect of ozone depletion on midlatitude precipitation is directly related to the position of the midlatitude jet, and has been documented in a number of studies (e.g., Fyfe et al., 2012; Previdi and Polvani, 2014). What has become apparent more recently is that ozone depletion may also be impacting precipitation in the subtropics, notably the latitudinal band 15–35°S (Kang et al., 2011). Over this region a positive trend in precipitation has been observed over the last decades of the 20th century during austral summer (Kang et al., 2011; Previdi and Polvani, 2014).

The connection between observed Southern Hemisphere precipitation changes and the SAM trends in austral summer is illustrated in Figure 4-14, which shows the DJF zonal mean observed GPCP (Global Precipitation Climatology Project) precipitation trend over both land and ocean points over the period 1979–2000. Note how most of the observed precipitation changes (red) are linearly congruent with the SAM (blue; see caption for details). This is particularly the case for the midlatitude zone. The subtropical trends are less significant, with more year-to-year variability in that latitude band compared to higher

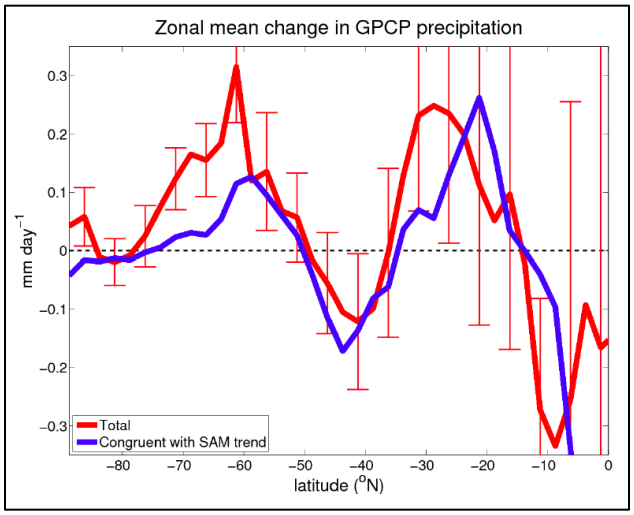

Figure 4-14. Zonal-mean change in GPCP (Global Precipitation Climatology Project) DJF precipitation during 1979–2000. The total precipitation change is plotted in red, and is based on the linear trend in the seasonal-mean precipitation at each latitude. The component of the precipitation change that is linearly congruent with the SAM trend is plotted in blue. This is calculated by regressing the seasonal detrended precipitation onto the SAM index and multiplying by the trend in the SAM. Error bars show the plus and minus one standard deviation range of the detrended seasonal-mean data, providing an indication of the year-to-year precipitation variability. From Previdi and Polvani (2014).

latitudes, yet are also largely congruent with the observed positive trend in the SAM index. Attribution of precipitation trends to SAM trends on more regional scales is more difficult. For example, the observed summer rainfall increases in subtropical northern Australia are larger than can be explained by the SAM changes alone (Hendon et al., 2007; Thompson et al., 2011).

Kang et al. (2011), using models forced with ozone depletion alone, showed that the precipitation response in austral summer was consistent with that observed and resulted from an expansion of the tropical circulation in their simulations. This moves the downwelling branch of the tropical circulation poleward, which results in enhanced upwelling in the subtropics and hence enhanced precipitation, in austral summer. A recent regional study by Gonzalez et al. (2013), contrasting models forced with ozone depletion and increasing GHGs, suggested that ozone depletion is a driver of observed precipitation increases in South East South America in austral summer, with its effect comparable to that due to increasing GHGs. Fyfe et al. (2012) identified a poleward shift in Southern Hemisphere extratropical austral summer precipitation from merged reanalysis and satellite-based observations that was inconsistent with simulated internal variability, but consistent with the simulated response to anthropogenic and natural forcings. In individual forcing simulations from one model, they found that both GHGs and ozone depletion contributed to a shift in precipitation consistent with that observed, with their influence partially opposed by the response to aerosols.

Previous Ozone Assessments have noted that the observed warming of the Antarctic Peninsula and cooling observed over the rest of continental Antarctica observed in austral summer are largely congruent with the positive trend in the SAM, suggesting that ozone depletion has contributed to these trends (e.g., Forster and Thompson et al., 2011). Since the last Ozone Assessment, several studies have directly examined the surface temperature trends simulated in response to ozone changes in coupled ocean-atmosphere models. Consistent with the last Ozone Assessment, McLandress et al. (2011) simulate cooling over eastern Antarctica and warming over western Antarctica in austral summer in response to ozone depletion. Sigmond and Fyfe (2010) also simulate a weak cooling over the Antarctic interior in austral summer in response to ozone depletion, but no significant response over the Antarctic Peninsula. They simulate a maximum surface temperature response to ozone depletion over the Southern Ocean at around 60°S in late winter where a pronounced warming is associated with the simulated decrease in sea ice extent (Section 4.4.1.3). In the annual mean, Bitz and Polvani (2012) also simulate the largest surface temperature response to ozone depletion over the high latitude Southern Ocean at around 60°S, in standard and high-resolution models. Over Antarctica itself, the simulated surface temperature response is small in the annual mean in their simulations. Thus recent studies find that in models at least, the largest annual mean surface temperature response to ozone depletion is not over Antarctica itself, but warming over the high latitude Southern Ocean. Other studies have noted the summertime contribution of the positive SAM trend to surface warming over southern Africa (Manatsa et al., 2013) and Patagonia

(Thompson et al., 2011) and the mitigation of warming in central-east Australia (Hendon et al., 2007), with a recent study suggesting springtime ozone losses can be directly implicated in these impacts (Bandoro et al., 2014).

4.4.1.2 OCEAN IMPACTS

As discussed above, observations show a strengthening and poleward shift of the band of maximum surface wind stress over the southern oceans since 1979 (Figure 4-11), largest in austral summer. Modeling evidence indicates that in summer, stratospheric ozone depletion has been the dominant driver of these changes, with greenhouse gas increases and stratospheric ozone making comparable contributions in the annual mean (see discussion above). The westerly wind stress plays a fundamental role in driving the oceanic circulation, including creating (via so-called Ekman transport) a region of divergence and upwelling on the poleward side of the surface wind maximum, and convergence and downwelling equatorward of the maximum. As discussed in the 2010 Ozone Assessment (Forster and Thompson et al., 2011), given the observed trends in the surface wind stress, one expects an enhancement of this Ekman response, causing increased upwelling of deep waters south of the Antarctic Circumpolar Current (ACC), increased northward surface flow at the latitude of the ACC, and increased downwelling north of the ACC. Recent observational and modeling studies have considerably improved our understanding of the response of the southern oceans to changing winds.

We first consider changes in the southern subtropical oceans (~15–45^{o}S), where observations show increases in the horizontal circulation, and transport consistent with the increase in maximum wind stress (and wind stress curl). Analysis of satellite altimetry and ship and float hydrographic data shows an increase in the strength of the southern subtropical horizontal circulation ("gyres") from the early 1990s to early 2000s that agrees with the expected response to the increase in the wind stress curl (Roemmich et al., 2007; Cai, 2006). Model simulations indicate that at least half of the changes in DJF are induced by Antarctic ozone depletion (Cai and Cowan, 2007). This intensification of the subtropical gyres and associated changes in Ekman-driven downwelling north of the ACC would be expected to contribute to more rapid transport of surface waters into the interior ("ventilation") of the upper southern subtropical oceans. Recent analysis of repeat measurements of chlorofluorocarbons (CFCs) in the southern oceans shows such an increase in ventilation, with a decrease in the mean age of water at the subtropical thermocline between the early 1990s and mid-late 2000s (Waugh et al., 2013; Figure 4-15). The mean age of ocean water is analogous to the mean age of stratospheric air, and is defined as the mean time for transport from the surface to the interior ocean. Further, there is quantitative agreement in observed changes in wind stress curl, gyre strength, and subtropical age, with all changing by around 20–30% (Waugh, 2014).

The new analysis of ocean CFC measurements also indicates decadal changes in the ventilation of the subpolar southern oceans, but with an increase in the mean age between the early 1990s and mid-late 2000s (Huhn et al., 2013; Waugh et al., 2013; Figure 4-15). This increase is consistent with theoretical considerations and modeling studies, which (as discussed in the last Assessment) indicate that an intensification of the surface winds will lead to an intensification in the meridional overturning circulation, with an increase of upwelling in subpolar waters and an increase in downwelling in subtropical waters. The increase in subpolar upwelling will bring up more deep, old waters that mix with surrounding waters and increase the ages in subpolar waters. The contrast between the decrease in age in subtropical waters and increase in subpolar waters inferred from CFC observations is also found in modeling studies (Bryan et al., 2006; Gnanadesikan et al., 2007; Waugh, 2013).

An intensification of surface winds is also expected to lead to changes in subsurface ocean temperatures. A subsurface warming is observed below and north of the ACC (around 40–60°S), and this is consistent with a poleward shift of the temperature structure (Böning et al., 2008; Gille, 2008; Cai et al., 2010). However, the extent to which the Southern Ocean warming is caused by shifting of the ACC versus other processes, such as an acceleration of poleward heat flux caused by the increasing eddy intensity (Hogg et al., 2008), is currently unclear. A subsurface warming, extending deepest in the midlatitudes, is

also found in modeling studies examining the impact of ozone depletion on Antarctic sea ice (Sigmond and Fyfe, 2010; Bitz and Polvani, 2012; Smith et al., 2012), as described in Section 4.4.1.3 below.

The above observational and modeling studies present a consistent picture for the ocean's response to increasing surface wind stress, with intensification of the subtropical horizontal (gyre) and the meridional overturning circulations, more rapid ventilation of the subtropical waters but older subpolar waters, and a subsurface warming. However, large uncertainties remain. This is in part due to limited historical oceanic data that prevents observational quantification of the (potentially large) natural decadal variability. An additional complication is the role of oceanic mesoscale (10–50 km scale) eddies. As discussed in the 2010 Ozone Assessment, these play an important role in the ocean response to changing forcing, but the climate models used to examine ozone impacts generally do not explicitly resolve these eddies and it is uncertain how much the effect of eddies oppose the direct wind-forced acceleration of the zonal flow (e.g., ACC transport) and overturning circulation. However, there has been recent progress in testing these ideas, and we now have a better understanding of the Southern Ocean eddy field and circulation response to changing winds. Theoretical arguments have been made that indicate that an invariant ACC transport (eddy saturation) is dynamically distinct from an invariant overturning circulation (eddy compensation), and one does not imply the other (Meredith et al., 2012). These arguments have been tested with various eddy permitting and eddy resolving models with different configurations, and it has been found that in the eddy saturated limit, only partial compensation of the overturning circulation is expected in response to decadally-changing winds (Meredith et al., 2012; Morrison and Hogg, 2013; Farneti et al., 2010). Widely used parameterizations for the role of mesoscale eddies have typically failed to capture this response adequately, though recent improvements in their implementation have shown progress (Hofmann and Morales Maqueda, 2011; Gent and Danabasoglu, 2011). Investigations are continuing, including into what sets the level of (incomplete) eddy compensation, and hence the magnitude of the overturning response to changing winds (Abernathey et al., 2011). These advances in understanding imply that an increase in Southern Ocean overturning (and corresponding changes in the ventilation) in response to changing winds is a reasonable expectation.

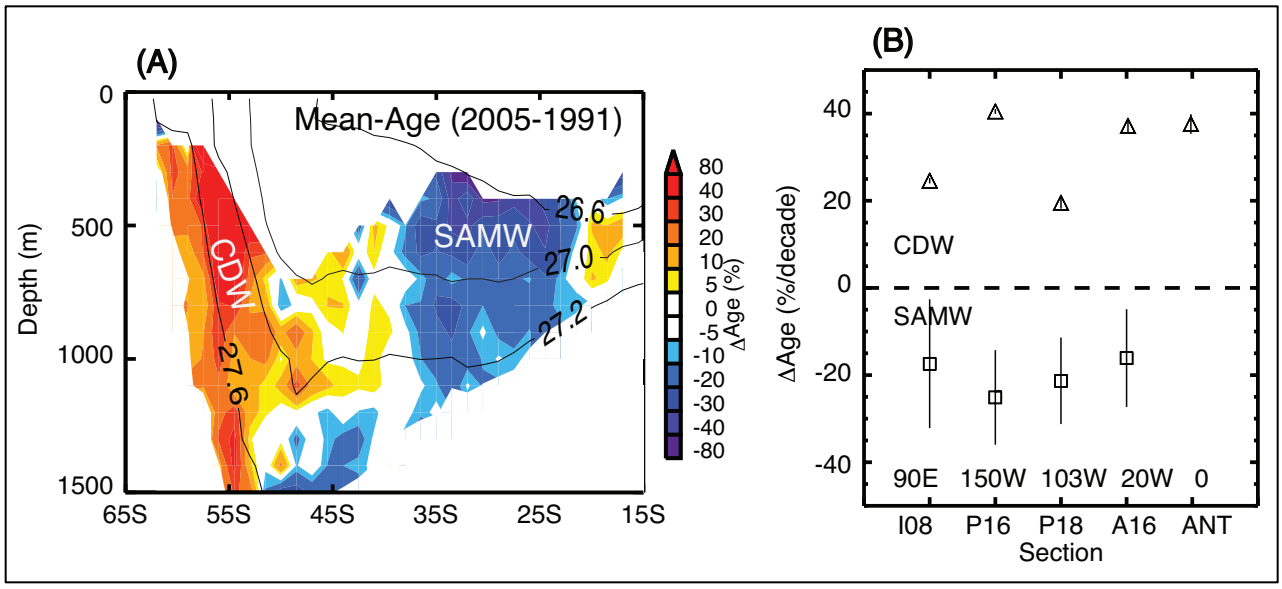

Figure 4-15. (a) Depth-latitude cross-sections of the change in mean age of ocean water between 1991 and 2005 based on CFC-12 measurements along 150°W. (b) Difference in mean age, expressed as percentage change per decade relative to age from original cruise, for circumpolar deep water (CDW) and Subantarctic Mode Water (SAMW) water masses for the repeat sampling of meridional sections at 90°E, 150°W, 103°W, 20°W, and 0°E. Adapted from Waugh et al. (2013) and Huhn et al. (2013).

Ocean carbon

The southern oceans play a critical role in the oceanic uptake of atmospheric carbon dioxide, and, as discussed in the last Assessment, there is evidence that the intensification and poleward shift of the surface winds has led to a reduction in the CO_2 uptake in Antarctic waters. This reduction is linked to more transport of carbon-rich deep waters to the surface, which decreases the surface air-sea gradients and oceanic uptake. An increase in the upwelling of carbon-rich deep waters is consistent with the increase in the age of subpolar water discussed above. However, the southern oceans are very poorly sampled (especially for carbon), and there are large uncertainties in the estimates of the carbon uptake.

In a recent study, Lenton et al. (2013) compared estimates of 1990–2009 Southern Ocean air-sea CO_2 fluxes from several different methods, including a synthesis of surface ocean observations, five ocean biogeochemical models coupled to ocean general circulation models, eleven atmosphere inversions, and ten ocean inversions (the atmospheric inversions estimate carbon fluxes from atmospheric CO_2 measurements, while the ocean inversions estimate fluxes from ocean measurements). They show large interannual variability in the air-sea fluxes (up to 25% of annual mean) and some substantial differences between fluxes inferred using different methods. In particular, there is a large spread in the 1990–2009 trends, with atmospheric inversions generally showing a slowdown in the uptake (broadly consistent with Le Quéré et al., 2007), while the ocean biogeochemical models indicate an uptake consistent with the growth of atmospheric CO_2 (i.e., no slow-down). Further complicating the picture, recent observational studies indicate large zonal variations in the ocean uptake of carbon (Sallée et al., 2012), and the changes in the efficiency of the Southern Ocean sink may not be zonally uniform (Lenton et al., 2013). Given the poor sampling in southern oceans, the zonal and interannual variability, and large uncertainties in all methods, longer data records will be needed to determine if there are any trends in the oceanic uptake of CO_2 (and even then it may not be possible to determine if these trends are linked to stratospheric ozone depletion).

4.4.1.3 SEA ICE IMPACTS

Significant increases in Antarctic sea ice extent of 2.5 ± 2.0% have been observed in austral summer from 1979–2012 (Vaughan et al., 2013). The sea ice trends vary regionally, with large increases in the Ross Sea and decreases in the Bellingshausen and Amundsen seas (Vaughan et al., 2013). At the time of the 2010 Assessment, the influence of stratospheric ozone trends on Antarctic sea ice was unclear, with some studies arguing that ozone depletion might be responsible for the observed positive trends in Antarctic sea ice extent (e.g., Turner et al., 2009), leading the last Assessment to conclude that there was some evidence that the ozone-induced summer SAM trend had caused the summer increase in Antarctic sea ice extent (Forster and Thompson et al., 2011). However, the studies assessed in the last Assessment focused on the relationship between sea ice and the SAM on monthly timescales, instead of on how stratospheric ozone changes affect sea ice on decadal timescales. Since the last Ozone Assessment, Simpkins et al. (2012) argued, based on observations, that the increase in sea ice extent is not linked to the trend in the SAM and several studies have now explicitly addressed the question of how stratospheric ozone depletion affects Antarctic sea ice.

The first of these studies is by Sigmond and Fyfe (2010); they contrasted time-slice model integrations before and after the formation of the ozone hole and concluded that ozone depletion would result in a reduction of Antarctic sea ice extent. The second is a study by Bitz and Polvani (2012), which also contrasted model runs with and without an ozone hole; they confirmed the results of Sigmond and Fyfe (2010) and corroborated them by using an eddy-resolving ocean model. This same result was further strengthened by the study of Smith et al. (2012), who used a fully coupled chemistry-climate model to study the effect of ozone recovery on sea ice. Finally, Sigmond and Fyfe (2014) found that a decrease in annual mean sea ice extent was simulated in response to ozone changes over the 1951–2005 period in all five CMIP5 models with ozone-only simulations available. The ozone-induced strengthening of the

Southern Ocean overturning circulation (Section 4.4.1.2) is found to enhance the upwelling of warm water beneath the mixed-layer and enhance convection, driving upper ocean warming (Section 4.4.1.2) and decreases in sea ice extent in all seasons (Bitz and Polvani, 2012).

Thus, in all models that have isolated the impact of stratospheric ozone depletion, Antarctic sea ice extent declines in all seasons. However, confidence in the simulated response to ozone depletion is limited by the fact that even with all major forcings, climate models on average simulate a decrease in sea ice extent (Turner et al., 2013; Zunz et al., 2013), whereas observations show Antarctic sea ice extent to have increased (albeit at a rather small rate) over the observational period (Parkinson and Cavalieri, 2012; Vaughan et al., 2013). Some studies have found that the observed positive trend is within the range of simulated trends, perhaps just reflecting a multi-decadal natural variation (Polvani and Smith, 2013; Zunz et al., 2013; Mahlstein et al., 2013), though Turner et al. (2013) and Zunz et al. (2013) also note the difficulties the models have in reproducing both the climatological and interannual variability of the observed sea ice extent. Another hypothesis is that the observed sea ice growth is due to enhanced freshwater input from dynamic mass loss (Bintanja et al., 2013), which is not included in the models, though this effect may not be large enough to explain the discrepancy (Swart and Fyfe, 2013). Overall, as concluded in the IPCC Fifth Assessment Report, the fundamental cause for the observed sea ice increase remains unknown and there is low confidence in the scientific understanding of this trend (Bindoff et al., 2013).

4.4.2 Radiative Effects

Stratospheric ozone exerts an influence on the troposphere directly by affecting the longwave and shortwave irradiances in the troposphere. Since 2000, a limited number of studies have investigated the radiative effects of stratospheric ozone concentration change, as assessed in previous IPCC and Ozone Assessments. These assessments have all reached similar conclusions, that stratospheric ozone depletion since 1979 likely contributes a net negative radiative forcing of around −0.05 W m^{-2} ± 0.1 W m^{-2} (e.g., Myhre et al., 2013). For context the forcing from CO_2 changes over 1979–2010 was 0.8 W m^{-2} (Myhre et al., 2013). The sign of the ozone forcing remains uncertain due to uncertainties from: i) quantifying ozone changes near the tropopause where the relative forcing is strongest; ii) cancellation between positive shortwave and negative longwave forcing, and iii) the dominant role of stratospheric adjustment in contributing a negative longwave forcing. Because of these factors considerable uncertainties remain when deriving forcing from observations and these uncertainties impact the testing of model-derived forcings. The radiative forcing from stratospheric ozone change is comparable in magnitude to that from changes in stratospheric water vapor due to methane oxidation (discussed in Section 4.2.2), which is assessed to be 0.07 (0.02–0.12) W m^{-2} in the IPCC Fifth Assessment Report (Myhre et al., 2013). Changes in stratospheric water vapor due to changes in transport or circulation are considered to be a feedback rather than a forcing by Myhre et al. (2013).

Hassler et al. (2013) compared stratospheric ozone forcings derived from different observation-based data sets over 1979–1997 and found a factor of four difference in net globally averaged radiative forcing (−0.03 W m^{-2} to −0.12 W m^{-2}; Figure 4-16). Uncertainties in derived ozone trends, corresponding to differences between data sets, at both high latitudes and over the equator lead to uncertainties in forcing, and to uncertainties in the simulated response to ozone changes. This uncertainty is illustrated in Figure 4-16 where the mean forcing derived from models (−0.04 ± 0.06 W m^{-2}) is similar to the forcings derived using the SPARC (Stratosphere-troposphere Processes and their Role in Climate; Cionni et al., 2011) data set but smaller than those derived from the BDBP (Binary Database of Profiles; Bodeker et al., 2013) data set. There is also additional uncertainty introduced by the radiative transfer and stratospheric adjustment method (compare the two dashed lines in Figure 4-16). The weaker ozone and radiative forcing trends in the SPARC data set, used in many CMIP5 simulations (Eyring et al., 2013), could lead to an underestimate of the magnitude of the simulated response to ozone changes in many CMIP5 models, although it is not clear whether simulations forced with the BDBP data set could lead to overestimates in the response (e.g., Solomon et al., 2012).

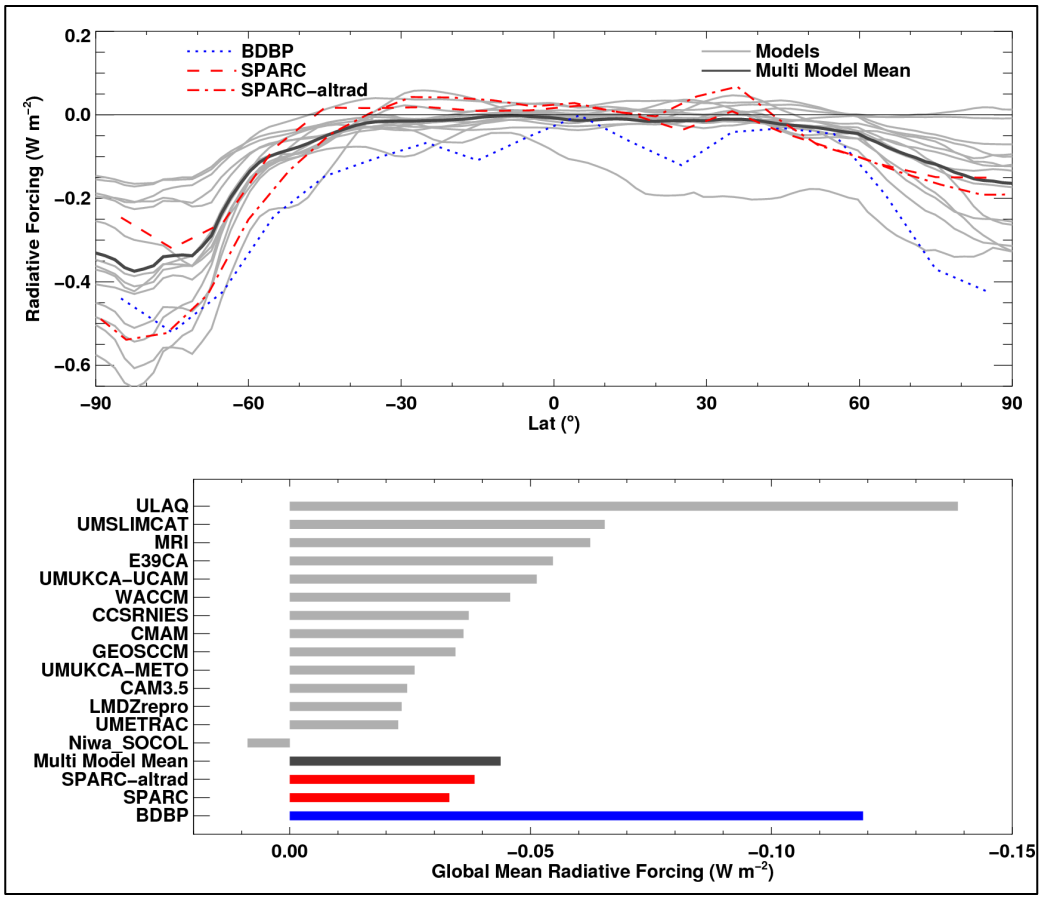

Figure 4-16. *Top:* Annual mean radiative forcing due to stratospheric ozone changes between 1979–1981 and 1995–1997 averages for the BDBP (solid blue line), and the SPARC (dashed red lines) ozone data sets (reproduced from Hassler et al., 2013). Two different radiation and stratospheric adjustment schemes are used with the SPARC data to give a measure of methodological uncertainty. Model forcings are calculated using their ozone fields with a single radiation scheme (CAMRT- J.F. Lamarque). Calculations for CAM3.5, CCSRNIES, CMAM, E39CA, GEOSCCM, LMDZrepro, MRI, Niwa_SOCOL, ULAQ, UMETRAC, UMSLIMCAT, UMUKCA-METO, UMUKCA-UCAM, WACCM CCMVAL-2 models are shown, as well as the multi-model mean. *Bottom:* Same as above but for the global average.

Previous Ozone Assessments have considered the radiative forcing due to stratospheric ozone concentration changes, but this is not necessarily the same as the ozone forcing from ODS emissions, as both ODSs and stratospheric precursors such as methane can affect stratospheric ozone concentrations (see Section 4.4.3). Further, ODS emissions can induce changes in ozone in both the stratosphere and troposphere (see Section 4.4.3). Therefore, as discussed in the IPCC Fifth Assessment Report (Myhre et al., 2013), progress has been made toward merging observation and model results (e.g., Søvde et al., 2011; Shindell et al., 2013a) to derive the radiative forcing from ozone changes due to ODS emissions, considering effects on both tropospheric and stratospheric ozone. There have also been ongoing multi-model intercomparison efforts (e.g., Shindell et al., 2013b; Conley et al., 2013; Stevenson et al., 2013) that help to assess the uncertainties in the ozone radiative forcing. The net radiative forcing due to stratospheric and tropospheric ozone changes induced by ODSs relative to preindustrial levels was calculated to be −0.26 W m^{-2} based on simulations of the Oslo CTM2 (Søvde et al., 2011) and −0.28 W m^{-2} based on simulations of the GISS-E2-R model (Shindell et al., 2013a). Based on these two studies, Myhre et al. (2013) assess the radiative forcing from the effect of ODSs on ozone to be –0.15 (–0.3 to 0.0) W m^{-2} from 1750 to 2010. The best estimate was assessed to be smaller than the estimates of Søvde et al. (2011) and Shindell et al. (2013a) because the models used in those studies had stronger

stratospheric ozone radiative forcing than the Atmospheric Chemistry and Climate Model Intercomparison Project (ACCMIP) multi-model mean (Myhre et al., 2013). About three-quarters of the ozone forcing from ODS emissions results from ozone changes in the stratosphere. The indirect changes in tropospheric ozone account for the other quarter (Shindell et al., 2013a).

The IPCC Fifth Assessment Report (Myhre et al., 2013) also uses effective radiative forcings to quantify the drivers of climate change. This effective radiative forcing goes beyond the traditional definition of radiative forcing and is defined to additionally account for the forcing from rapid cloud and circulation adjustments in the troposphere, not associated with global mean climate change. Myhre et al. (2013) assumed that any rapid adjustment associated with ozone was small and the effective radiative forcing matched the radiative forcing quoted above, i.e., any indirect forcings from cloud changes were small. However, some studies suggest otherwise. Grise et al. (2013) find a cloud radiative forcing due to the fact that the modeled poleward jet shift caused by the ozone hole moves the Southern Hemisphere clouds poleward, exposing the surface to higher insolation on average. In their model this effect contributed a positive indirect radiative forcing of +0.25 W m^{-2} averaged over the Southern Hemisphere in the annual mean (and around +0.2 W m^{-2} in the global mean). Their result is subject to considerable uncertainty and would likely be model dependent. A further possible effect relates to the modification of surface wind driven sea salt fluxes and thereby cloud condensation nuclei and clouds (Korhonen et al., 2010; Struthers et al., 2013). Korhonen et al. (2010) show that this could be of a similar magnitude, but is a cooling effect (–0.7 W m^{-2} over the 50°S to 65°S latitude band in the summer, and around −0.1 W m^{-2} in the global mean). Therefore, it is expected that Southern Hemisphere effective forcings exist due to shifts in the midlatitude jet. These are of indeterminate sign, could exert a large local forcing, and could be of a comparable magnitude to the direct ODS-induced ozone radiative forcing in the global mean.

In summary ODS emissions likely contributed a small negative radiative forcing of −0.15 ± 0.15 W m^{-2} in 2010 due to ozone. However, the possibility of a similarly sized adjusted forcing from circulation-driven cloud changes leads to an effective radiative forcing from ODSs of undetermined sign. The regional nature of this adjusted forcing could be important for Southern Hemisphere climate change.

4.4.3 Chemistry Effects

Ozone levels in the troposphere are affected by natural and anthropogenic emissions of reactive compounds, the prevailing climate, and the influence of the stratosphere. At the global scale, the impact of these drivers on tropospheric ozone is assessed by examining its budget terms, with production from in situ photochemistry and a net influx from the stratosphere (via stratosphere-troposphere exchange, STE), and loss from in situ chemistry and deposition to surfaces (e.g., Wild, 2007). The role of stratospheric change for tropospheric ozone is both direct and indirect. The direct influence is via changes in the net influx of stratospheric ozone, mediated by increases or decreases in stratospheric ozone concentrations and changes in the patterns and strength of the stratospheric transport and circulation (e.g., the BDC) that bring ozone to the troposphere (e.g., Hegglin and Shepherd, 2009). The indirect influence is mainly through stratospheric ozone-modulated changes in UV radiation and the subsequent impacts on tropospheric photochemistry (e.g., Tang et al., 2011), although stratospherically driven tropospheric climate changes could have an additional small impact. Changes in tropospheric ozone and the UV flux are important because these have impacts on all chemically active tropospheric constituents, including impacting air quality (Tang et al., 2011; Lin et al., 2012) and the lifetimes of chemically active GHGs such as methane (Voulgarakis et al., 2013).

Global chemistry models remain the main tools for understanding the tropospheric ozone budget (see Box 2-2 in Chapter 2 of this Assessment). A major improvement to many chemistry-climate models since the last Assessment is the merging of tropospheric and stratospheric chemistry schemes (e.g., Naik et al., 2013; Shindell et al., 2013c), enabling studies that examine impacts and feedbacks between the two domains. Ten of the fifteen models used to assess preindustrial to projected future ozone changes in the Atmospheric Chemistry and Climate Model Intercomparison Project (ACCMIP) (Young et al., 2013a)

included a chemistry scheme appropriate for both stratospheric and tropospheric chemical processes, although there was a broad range in the complexity of the schemes (the number of species simulated ranged from 16 to 130). However, despite the overall increase in complexity of the models, simulations of present day tropospheric ozone do not differ markedly from those considered in the 2010 Ozone Assessment (see also Stevenson et al., 2006), including in their ability to reproduce the seasonal and geographical features in ozone observations (Myhre et al., 2013; Young et al., 2013a).

Since the 2010 Ozone Assessment, there have been several model studies examining the drivers of past tropospheric composition that explicitly consider the influence of stratospheric ozone change caused by ODSs (John et al., 2012; Lang et al., 2012; Shindell et al., 2013c; Young et al., 2013a; Reader et al., 2013). Lang et al. (2012) examined the changes between 1960 and 2005, using sensitivity simulations to isolate the role of ODS changes between those periods. They found that, in the absence of other changes, the increase of ODSs between 1960 and 2005 reduced ozone concentrations globally, with the chemically induced reduction of stratospheric ozone resulting in a decreased net ozone influx to the troposphere of 5.4% in the Northern Hemisphere and 21.6% in the Southern Hemisphere. The decrease in STE ozone flux was slightly offset by an ODS-driven increase in the strength of the meridional circulation, which increases the STE mass flux (Oman et al., 2009) (see also Section 4.3.2.2). John et al. (2012) note the importance of decreased stratospheric ozone in decreasing methane lifetime in the last decades of the 20th century (through enhanced UV increasing the concentration of the hydroxyl radical, OH), but do not quantify the effect.

The main focus of the other studies is on the drivers of preindustrial (PI; ~1850) to present-day changes. All three studies (Shindell et al., 2013c; Young et al., 2013a; Reader et al., 2013) report a much lower tropospheric ozone column/burden in the PI (reduced 25–30% compared to present day), driven by the lower ozone precursor emissions in the past. Shindell et al. (2013c) found that the net stratospheric influx of ozone into the troposphere was ~25% greater in their PI simulation. Such an increase might indeed be expected, given the higher stratospheric ozone concentrations and the lower tropospheric ozone concentrations (meaning a higher *net* import of ozone into the troposphere), although the range of changes in the net stratospheric influx reported by Young et al. (2013a) (~0–50%) shows that there is little agreement on the magnitude of this impact. Reader et al. (2013) suggest that the combined increase in tropospheric ozone (through precursor emission increases) and decrease in stratospheric ozone since the PI means that the global total ozone column has changed little.

Overall, the move by many groups toward combined troposphere-stratosphere chemistry-climate models allows better characterization of the links between the two domains, albeit with the caveat that it is hard to unambiguously assign magnitudes to individual drivers in such an interrelated system. While most models agree that ODS-driven ozone depletion has reduced the magnitude of the net stratospheric influx of ozone into the troposphere, our assessment of the magnitude of the effect is hampered by the range of stratospheric treatments in different models (i.e., fully interactive to passive/prescribed), which is likely one driver of inter-model variability in the results. Furthermore, improvements in measurement techniques will be needed to better constrain STE processes in models (Tang and Prather, 2012), although new observational analyses are providing insights into the main locations of STE events (Jin et al., 2013), which will be valuable for future validations.

4.5 EFFECTS OF FUTURE CHANGES IN STRATOSPHERIC OZONE ON THE TROPOSPHERE AND SURFACE

This section assesses the climate impacts of future variations in stratospheric ozone over the next century. It follows an identical structure to Section 4.4, discussing the climate impacts from a radiative, dynamical, and chemistry perspective. Earlier chapters have outlined future projections of stratospheric ozone for the globe (Chapter 2) and polar regions (Chapter 3). These projections involve a complex interaction between projected changes in GHGs, ODSs, and the climate system. While a declining stratospheric halogen loading is expected to lead to an increase in stratospheric ozone, GHG changes will

also influence ozone concentrations through direct chemical effects, climate-induced changes in chemistry, and changes in the stratospheric circulation.

The studies assessed incorporate climate model results from a number of intercomparison projects. These include experiments run under new scenarios of future emissions named Representative Concentration Pathways (RCPs) that were developed in preparation for the IPCC Fifth Assessment Report. Box 4-1 gives a description of the RCPs and how they differ from the Special Report on Emissions Scenarios (SRES) scenarios considered in the 2010 Ozone Assessment.

4.5.1 Tropospheric Circulation Effects

It is now well established that the Southern Hemisphere circulation response to the anticipated ozone recovery is largely opposite to that resulting from ozone depletion in the past (Section 4.4.1), offsetting GHG-induced circulation change in the austral summer. This offsetting effect may then result in a much weaker rate of Southern Hemisphere circulation change, and associated impacts, in the next few decades than in the recent past. In this section the possible effects of stratospheric ozone recovery on Southern Hemisphere climate are assessed, updating the 2010 Ozone Assessment by integrating recent findings. Since projected circulation changes are all assessed from climate models and many models exhibit biases, for example in the climatological jet location, projected circulation changes are subject to considerable uncertainty. In line with Section 4.4.1, overall assessments are focused on the Southern Hemisphere especially over austral summer, DJF, when ozone-related tropospheric climate changes are strongest. The potential impact of ozone recovery on the Northern Hemisphere climate is only briefly assessed. The benefit of the Montreal Protocol is also documented by considering recent simulations of the effects of unregulated ODS emissions.

The Southern Hemisphere

Since the 2010 Ozone Assessment significant progress has been made in our understanding of stratospheric ozone-related Southern Hemisphere climate change in the future. A number of studies have been conducted either by performing climate model sensitivity tests with and without stratospheric ozone recovery (Shindell and Schmidt, 2004; Perlwitz et al., 2008; Karpechko et al., 2010; McLandress et al., 2011; Polvani et al., 2011a; Arblaster et al., 2011; Staten et al., 2012; Watson et al., 2012) or by examining multi-model projections of the CMIP3 (Miller et al., 2006; Son et al., 2009), CCMVal-2 (Son et al., 2010), and CMIP5 models where stratospheric ozone concentration is prescribed or predicted internally (Swart and Fyfe, 2012; Eyring et al., 2013; Barnes et al., 2014; Gerber and Son, 2013).

Figure 4-13 summarizes the overall climate effects of stratospheric ozone recovery as simulated by the Canadian CCM (CMAM) under the SRES A1B GHG emission scenario (McLandress et al., 2011). Although this is based on single model's experiments, these experiments are qualitatively consistent with results that were reported by Polvani et al. (2011a) based on simulations from the CAM3 model. In the absence of other climate forcing, the increase in stratospheric ozone concentration since 2000 (red lines) warms the stratosphere, with a maximum warming in the Antarctic lower stratosphere during austral spring and summer (Figure 4-13a, Figure 4-6). This warming reduces the temperature lapse rate near the tropopause, lowering polar tropopause height and increasing tropopause pressure (Figure 4-13b). The polar warming also reduces the meridional temperature gradient in the upper troposphere and lower stratosphere that will likely lead to a weakening of the Antarctic polar vortex. As discussed in Section 4.4.1 and shown in Figure 4-13c, the wind change is not limited to the upper troposphere and lower stratosphere. A significant response is also simulated near the surface. Specifically, the midlatitude jet is simulated to shift equatorward in response to ozone recovery. This change strongly projects onto the negative polarity of the SAM. Recent studies have shown that the latitudinal shift of the austral-summer jet is mostly eddy-driven (Lorenz and DeWeaver, 2007; Butler et al., 2010; McLandress et al., 2011) and highly correlated with the long-term trend of the southern edge of the Southern Hemisphere Hadley Cell

Box 4-1. Representative Concentration Pathways

Future anthropogenic emission projections typically follow a scenario approach based on a set of assumed socio-economic choices that may be expected over the next century. In the lead-up to the Intergovernmental Panel on Climate Change (IPCC) Fifth Assessment Report, the scientific community, for the first time in 12 years, developed new scenarios for climate change research. These Representative Concentration Pathways (RCPs) differ from the previous Special Report on Emissions Scenarios (SRES) scenarios in that they are concentration scenarios based around general characteristics of radiative forcing at 2100, rather than emissions scenarios (van Vuuren et al., 2011). This allowed both emission and socio-economic scenarios to be developed in parallel.

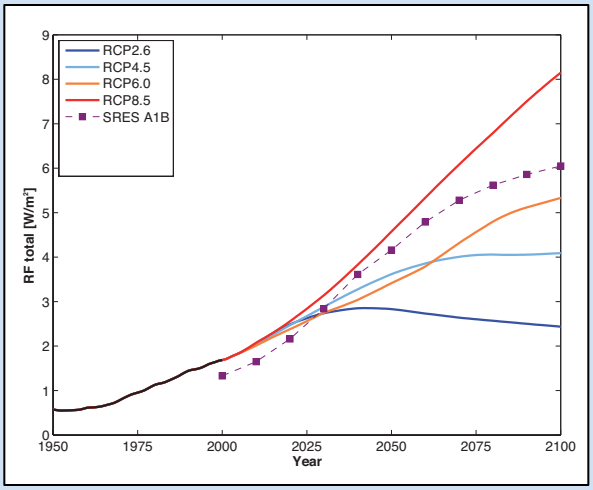

Box 4-1: Figure 1. Historical and projected total anthropogenic radiative forcing (RF; W m^{-2}) relative to preindustrial (~1765) between 1950 and 2100 for the SRES A1B and RCP scenarios. Adapted from Cubasch et al. (2013).

For the Coupled Model Intercomparison Project-Phase 5 (CMIP5), four pathways were chosen from the existing literature to span a range of radiative forcing in 2100 which are outlined in Figure 1: RCP2.6 (peak and decline; 2.6 W m^{-2}), RCP4.5 (stabilization without over-shoot; 4.5 W m^{-2}), RCP6.0 (stabilization without over-shoot; 6.0 W m^{-2}), and RCP8.5 (rising; 8.5 W m^{-2}). By 2100, the radiative forcing of the SRES A1B scenario, used in most of the chemistry-climate model simulations assessed in SPARC CCMVal (2010), is closest to RCP6.0. The RCPs explicitly define emissions and concentrations of GHGs (Figure 2), aerosols, tropospheric ozone precursors, and land-use change. They do not give specific guidance on variations in natural forcings, such as volcanic eruptions and solar input for the future, however most CMIP5 models included some form of the 11-year solar cycle in their RCP simulations while returning volcanic aerosols to zero or preindustrial background volcanic aerosol values (Collins et al., 2013). Emissions of most ozone-depleting substances follow the A1 scenario (WMO, 2003), which has a similar trajectory to the adjusted A1 halon scenario used in the 2010 Ozone Assessment, and is identical for all RCPs. See Meinshausen et al. (2011) for more details.

The main set of climate model simulations underlying the IPCC Fifth Assessment Report were those included in CMIP5. For models without interactive chemistry, the International Global Atmospheric Chemistry (IGAC) and Stratosphere-troposphere Processes and Their Role in Climate (SPARC) communities developed an ozone concentrations database covering the period 1850–2100 (Cionni et al., 2011). For the future period, zonal mean stratospheric ozone concentrations in this database were computed from the average of 13 CCMVal-2 models run under the SRES A1B scenario. Thus, the stratospheric ozone concentrations are identical for each RCP. Tropospheric ozone was based on the CAM3.5 chemistry-climate model (Lamarque et al., 2011). Eyring et al. (2013) document the implementation of ozone forcing in each model that participated in CMIP5. Of the 46 models assessed, a little over half prescribed ozone concentrations from the IGAC/SPARC database and the others used either semi-offline or interactive chemistry. For the latter, the ozone concentrations were simulated interactively under the four RCPs, providing some variation in stratospheric ozone across scenarios and models. The CMIP5 ozone projections are within the spread of those from the CCMVal-2 models used in the 2010 Ozone Assessment.

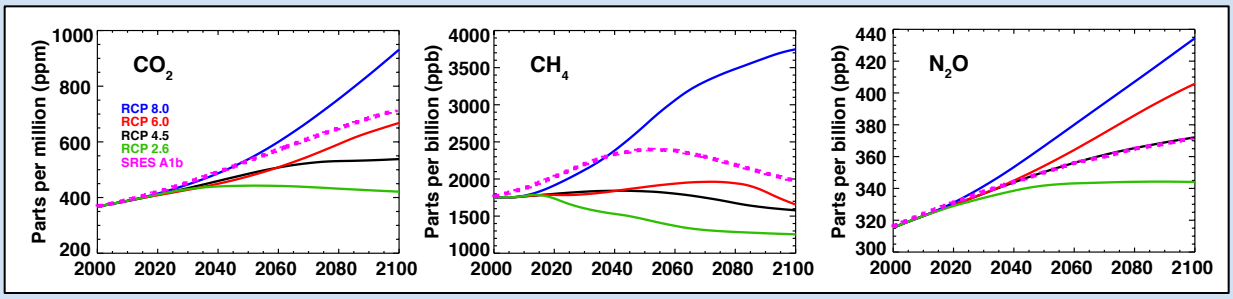

Box 4-1: Figure 2. Concentrations of CO_2, CH_4, and N_2O under the four RCPs and the SRES A1B scenario.

(Son et al., 2009; Kang and Polvani, 2011; Gerber and Son, 2013). Although weak, this equatorward shift of the Hadley Cell edge is evident in Figure 4-13d.

All of these projected changes are essentially opposite to those resulting from stratospheric ozone depletion in the past (compare 1960–2000 and 2001–2099 trends in Figure 4-13). More importantly, they oppose atmospheric circulation changes associated with ongoing GHG increases (blue lines in Figure 4-13). As a result, Southern Hemisphere summer circulation changes in the next few decades are likely to be much weaker than those in the late 20th century (black lines in Figure 4-13).

The relative importance of GHG increases and ozone recovery for the simulated future midlatitude jet shift depends on the GHG emissions scenario and season. Multi-model analyses using the CMIP5 models (e.g., Swart and Fyfe, 2012; Eyring et al., 2013; Barnes et al., 2014) have shown that in austral summer the Southern Hemisphere circulation effects of stratospheric ozone recovery in the first half of 21st century likely overwhelm those of GHG increases under a low GHG emissions scenarios, e.g., RCP2.6 (Box 4-1), as shown in Figures 4-10c and 4-17a. In the RCP8.5 scenario, which has high GHG emissions, the influence of GHGs likely dominates (Figures 4-10d, 4-17a), whereas near cancellation is simulated under moderate emission scenarios such as RCP4.5 and RCP6.0 (Box 4-1). In austral winter (JJA), the jet shift is weaker and scales with the strength of the GHG emissions (Figure 4-17b). Differences in radiative forcing between RCP scenarios are small in the near term (Box 4-1), and hence the difference in projected jet trends between RCP scenarios may not be significant until the middle of 21st century (Figure 4-17; Simpkins and Karpechko, 2012).

Projected changes in the Southern Hemisphere midlatitude jet are also dependent on the Antarctic lower stratosphere ozone trend itself. The CCMVal-2 and CMIP5 models with interactive chemistry exhibit a range in future projections of stratospheric ozone. For example, the dates when global-mean total column ozone returns to its 1980 values vary by about 20 years between CCMVal-2 models (Eyring et al., 2010; see also Section 2.4 of Chapter 2 of this Assessment). Consideration of the effects of differing ODS emissions scenarios, and the effects of solar and volcanic forcing changes, would further increase this spread (see Sections 2.4 and 5.4 of Chapters 2 and 5 of this Assessment).

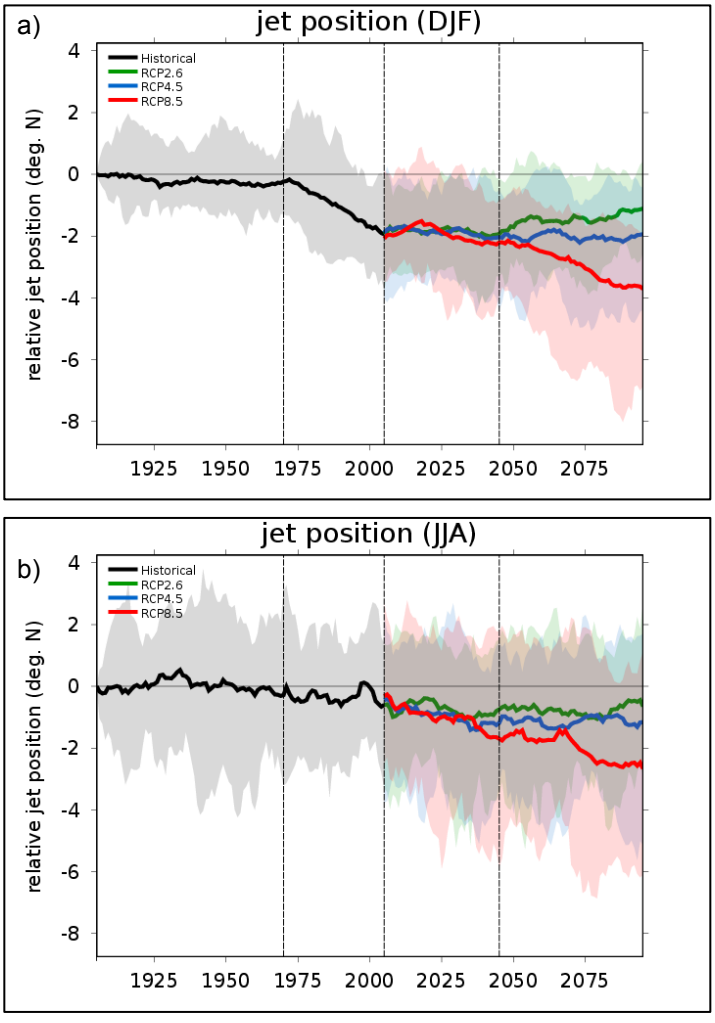

Figure 4-17. Time series of the CMIP5 Southern Hemisphere DJF (panel a) and JJA (panel b) jet position anomalies relative to the 1900–1910 value in the historical simulations and three climate scenario simulations (RCP8.5, RCP4.5, and RCP2.6). Thick lines show the multi-model means and shading indicates the model spread. Time series have been smoothed using a 10-year moving average filter. Adapted from Barnes et al. (2014).

The degree of simulated cancellation between ozone-related and GHG-related climate changes further depends on climate sensitivity (Arblaster et al., 2011; Watson et al., 2012). For the same GHG emissions scenario, upper tropospheric tropical temperature changes differ widely between models (bottom panel of Figure 4-18) partly because of uncertainties in physical parameterizations of atmospheric processes (e.g., Watson et al., 2012). Likewise the same ODS emissions scenario results in different Antarctic ozone and lower stratospheric temperature trends in different models (top panel of Figure 4-18). These uncertainties in tropical upper troposphere and polar lower stratosphere temperature changes, or uncertainties in equator-to-pole temperature gradient changes in the upper troposphere and lower stratosphere, contribute to the uncertainty in projections of future Southern Hemisphere climate change in austral summer (Lorenz and DeWeaver, 2007; Wilcox et al., 2012; Gerber and Son, 2013; Harvey et al., 2013). In general a larger poleward shift of the midlatitude jet is associated with a larger temperature gradient change in the upper troposphere and lower stratosphere (e.g., Wilcox et al., 2012). Even for models with similar climate sensitivity, the atmospheric and surface climate response to external forcings can differ substantially, in part due to differing biases in the mean state (Kidston and Gerber, 2010; Son et al., 2010), since the mean state bias is correlated with the projected Southern Hemisphere midlatitude jet change (Kidson and Gerber, 2010; Son et al., 2010; Simpson et al., 2012; Sigmond and Fyfe, 2014). The projected circulation change is typically larger if the climatological jet is biased equatorward. However, the causal relationship is not clear as there are other deficiencies in climate models. For example, Simpson

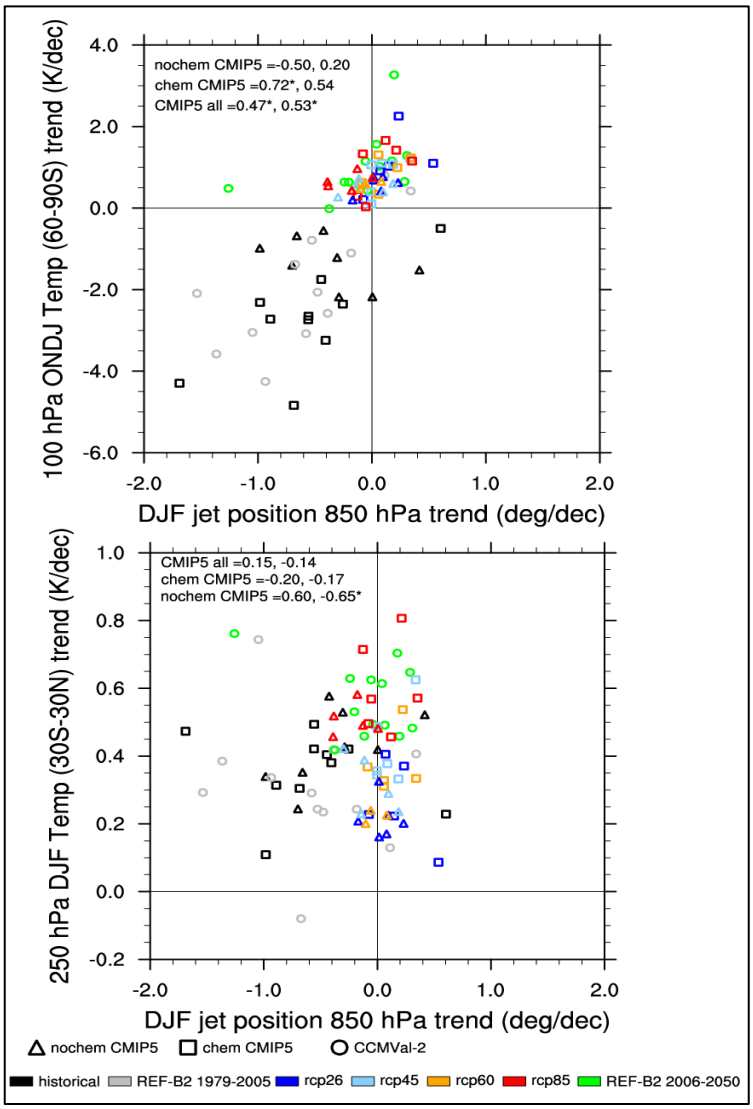

Figure 4-18. The relationship between the trends of the latitudinal location of the DJF near-surface westerly maximum and (*top*) ONDJ polar lower-stratospheric temperature trends and (*bottom*) DJF tropical upper-tropospheric temperature trends. The trends are calculated over 1979–2005 for the past (black or gray) and 2006–2050 for the future (different colors for various GHG emissions scenarios). Both CCMVal-2 (circles) and CMIP5 models (squares for the models with interactive chemistry and triangles for models without it) are used. The correlation between the two variables is computed for all CMIP5 models and for the subset of CMIP5 models with and without interactive chemistry for the past (first number) and for the future (second number). The correlation coefficients that are statistically significant at the 95% confidence level are indicated with an asterisk. Adapted from Eyring et al. (2013).

et al. (2013) showed that the CMIP5 models do not have realistic planetary wave-zonal mean flow feedback, overestimating the time scale of SAM anomalies. This bias in eddy feedback can introduce more uncertainty in future Southern Hemisphere climate changes.

The Northern Hemisphere

Hu et al. (2011) recently argued that the anticipated recovery of stratospheric ozone will substantially enhance tropospheric and surface warming in the first half of the 21st century. They examined CMIP3 models with and without ozone recovery and suggested that ozone-induced tropospheric warming will be strongest during winter in the extratropical Northern Hemisphere, despite the fact that ozone recovery will be strongest in the Southern Hemisphere during springtime. This surprising result was shown by Previdi and Polvani (2012) and McLandress et al. (2012) to be caused not by stratospheric ozone forcing but by different responses of the climate models to GHG forcing. By examining the same two groups of models in GHG-only simulations, Previdi and Polvani (2012) found essentially the same result as Hu et al. (2011), clearly attributing the differences to climate sensitivity. McLandress et al. (2012) further confirmed that Northern Hemisphere surface temperature response to stratospheric ozone recovery is negligible in their coupled chemistry-climate model integrations.

4.5.1.1 SURFACE IMPACTS

Projected future tropospheric circulation changes are accompanied by surface climate changes, as were past changes (Section 4.4.1.1). These include changes in sea level pressure, surface air temperature, and precipitation (McLandress et al., 2011; Polvani et al., 2011a). In response to ozone recovery, sea level pressure is projected to increase in high latitudes and decrease in midlatitudes in austral summer, consistent with the negative SAM trend. This will likely change Antarctic surface temperature (Son et al., 2009), but projected changes are relatively small (e.g., McLandress et al., 2011). Hydro-climate systems are also projected to change in response to ozone recovery in austral summer. Specifically the ozone-induced equatorward shift of the surface wind and the associated storm track in summer is expected to drive high-latitude drying and midlatitude moistening (Purich and Son, 2012; Polvani et al., 2011a) and potentially modify the frequency of extreme precipitation events (Purich and Son, 2012; Kang et al., 2013). Projected ozone-induced precipitation and circulation changes approximately cancel GHG-induced changes in the mid and high latitudes of the Southern Hemisphere in summer under the SRES A1B scenario over the 2000–2060 period (Polvani et al., 2011a).

4.5.1.2 OCEAN IMPACTS

The possible influences of stratospheric ozone recovery on the southern oceans have been discussed in the literature, based mainly on past climate simulations (Forster and Thompson et al., 2011). However, a few recent studies have directly addressed this issue using CCMs coupled with coarse-resolution ocean and sea-ice models (Sigmond et al., 2011; Smith et al., 2012).

The equatorward shift and weakening of surface westerlies, or negative SAM trend, simulated in response to ozone recovery will tend to reverse the changes in the southern oceans due to ozone depletion (discussed in Section 4.4.1.2). For example, ozone recovery is expected to reduce northward Ekman transport in the austral summer, weaken the meridional overturning circulation, and weaken the baroclinic component of the ACC (e.g., Figure 4-19). While this effect may be overestimated in some simulations because of unresolved mesoscale eddies, these circulation changes are expected to offset GHG-induced changes to some degree (Sigmond et al., 2011).

There is uncertainty in the timescales of response of different aspects of the ocean circulation to changes in the wind stress. The Ekman response to a change in winds will be almost instantaneous, but the contributions due to eddies will increase over time on a timescale of decades (Meredith and Hogg,

2006; Screen et al., 2009). Changes due to advection of surface perturbations (due to the wind stress change) into the interior ocean will also take longer than the instantaneous Ekman response. Thus there will likely be a delay between changes in the wind stress and changes in the ocean circulation, with the delay depending on the relative role of Ekman and eddy responses in causing changes in a particular aspect of the circulation. For example, the simulations in Sigmond et al. (2011) showed a delay of around 20 years in the response of the ACC to changes in the surface wind stress (see Figure 4-19).

There have been no studies of the impact of ozone recovery on the oceanic uptake of CO_2, but it is likely there will be a reversal of the impact of ozone depletion.

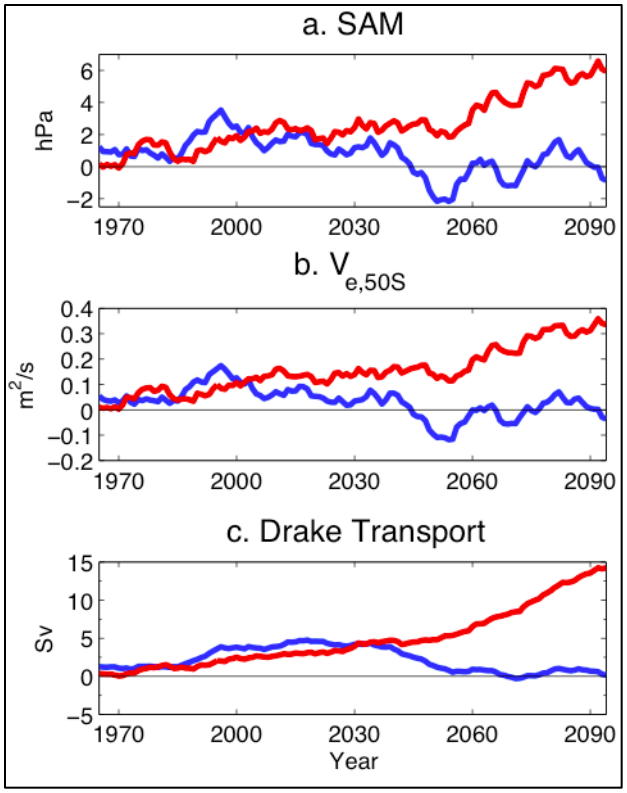

Figure 4-19. Annual mean response to GHG (red) and ODS forcings (blue) of (a) the SAM index, (b) the zonal-mean meridional Ekman transport at 50°S, and (c) the zonal transport through the Drake passage. The time series are smoothed with an 11-year moving average. Three sets of CMAM experiments (GHG, ODS, and control simulations) are used in this figure, each with three ensemble members simulating the 1960–2100 period. The GHG simulation is forced with time-varying GHGs and fixed ODSs at 1960 levels. Conversely, the ODS simulation is forced with time-varying ODSs and other GHGs at 1960 levels. The control simulation is forced with time-varying ODSs and GHGs. To account for model drift, the response to the ODS forcing is defined as the difference between the control and GHG simulations. Likewise GHG-related response is defined as the difference between the control and ODS simulations. Updated from Sigmond et al. (2011).

4.5.1.3 Sea Ice Impacts

Smith et al. (2012) showed that ozone recovery is projected to slow down the Antarctic sea ice decline that is projected in response to GHG increases. This compensation, which results from modulation of the Ekman transport and upper-ocean temperature near the Antarctic continent (Sigmond and Fyfe, 2010; Smith et al., 2012), is found to occur in all seasons because of the long-term memory of ocean temperature. However, this result, which is largely opposite to the simulated Antarctic sea ice response to ozone depletion (Section 4.4.1.3), is based on a single model experiment coupled with a coarse-resolution ocean model. Verification of this result will require further evaluations using high-resolution ocean models.

4.5.1.4 The World Avoided by the Montreal Protocol

The ozone-related climate changes described above are all based on the successful regulation of ODS emissions in accordance with the Montreal Protocol (considered here together with its Amendments and adjustments). However, it is pertinent to ask, what would have happened if the Montreal Protocol had

not been implemented? In other words, what is the benefit of the Montreal Protocol and actions taken so far? Climate models suggest that continued accumulation of ODSs in the absence of the Montreal Protocol would have led to a collapse of the global ozone layer by the mid-21st century. For example, recent studies suggest a decrease of global total ozone from about 315 DU in 1974 to about 110 DU in 2065 in the absence of the Montreal Protocol (Newman et al., 2009; Garcia et al., 2012). Because ODSs are effective GHGs (e.g., Velders et al., 2007; WMO, 2011), increasing ODS concentrations would also enhance surface warming. The combined effects of lower-stratospheric cooling by continued ozone depletion and tropospheric warming by increased ODS emissions would then drive much stronger climate changes in both the Southern Hemisphere and Northern Hemisphere in the 21st century than those simulated in the latter half of the 20th century (Morgenstern et al., 2008; Newman et al., 2009; Wu et al., 2013).

A series of modeling studies, the so-called "world avoided" simulations, have recently been performed either by increasing the concentration of ODSs in CCMs (Morgenstern et al., 2008; Newman et al., 2009; Garcia et al., 2012) or by prescribing unregulated ODSs and corresponding ozone concentrations in an atmospheric general circulation model (AGCM) (Wu et al., 2013). Such simulations show significant stratospheric cooling in the next 20–50 years, with a maximum cooling in the Antarctic lower stratosphere in response to the increased ODS concentrations (e.g., Wu et al., 2013). This cooling would maintain the polar vortex year-round by the mid-21st century (Newman et al., 2009), resulting in no final warming in the Southern Hemisphere stratosphere. Simulated tropospheric warming due to the direct radiative effects of the ODSs would also be substantial. For example, Garcia et al. (2012) found surface warming of over 2 K in response to enhanced ODSs in the tropics, 6 K in the Arctic, and about 4 K in Antarctic from 2000 to 2070 (Figure 4-20). This is of comparable magnitude to GHG warming under the RCP4.5 scenario (Garcia et al., 2012), indicating that global warming over next few decades could have been doubled in the absence of the Montreal Protocol.

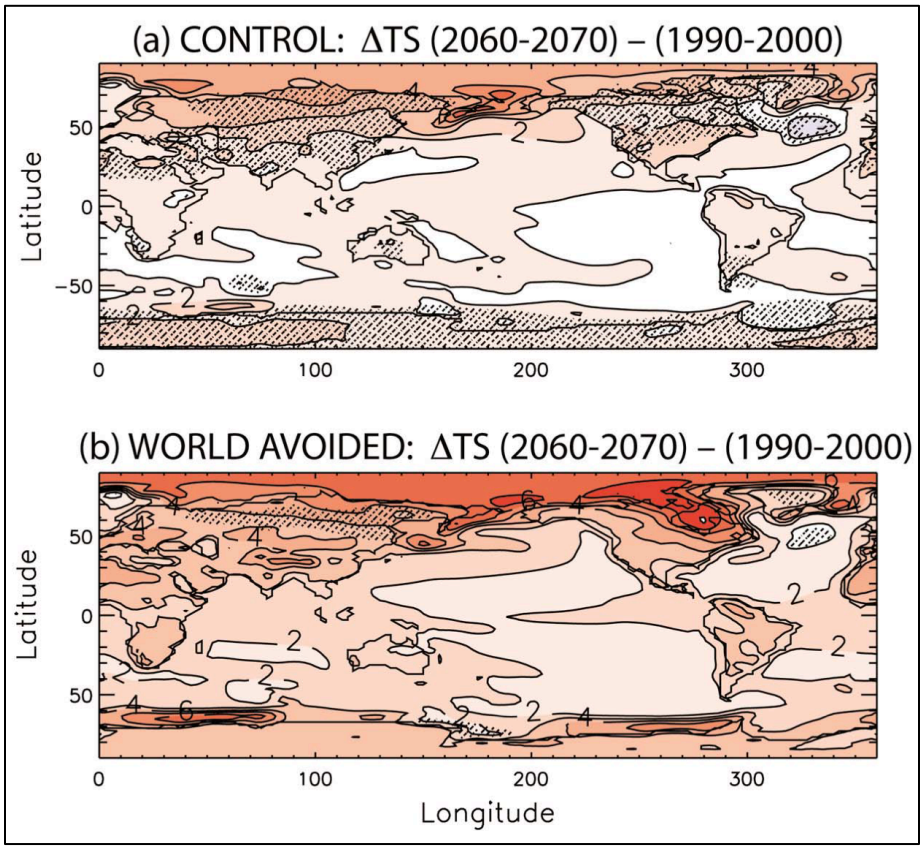

Figure 4-20. Surface temperature change (K) between the decades of 1990–2000 and 2060–2070 in the (a) control and (b) world-avoided simulations. The former is driven by RCP 4.5 and an ODS emissions scenario that is based on the Montreal Protocol. However, in the latter, ODS emissions are not regulated until 2070. Changes in the stippled regions are not significant at the 95% confidence level. From Garcia et al. (2012).

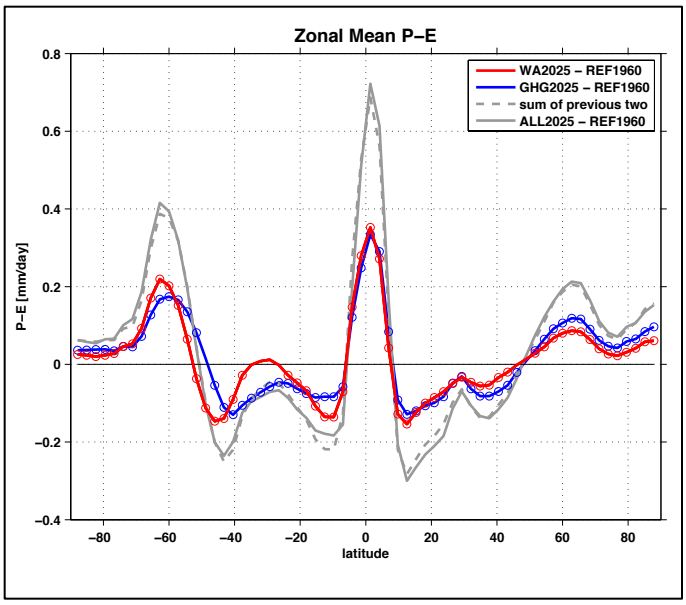

Figure 4-21. The precipitation minus evaporation (P-E) change between a reference simulation (REF1960) and a simulation with increased ODSs but fixed GHGs (WA2025; red), a simulation with GHG increases only (GHG2025; blue), the sum of the two (gray dashed), and a simulation with both ODS and GHG increases (ALL202; gray solid line). In REF1960, CO_2, CH_4, N_2O, CFC-11, CFC-12, and O_3 concentrations are prescribed at levels corresponding to the year 1960. In WA2025, the concentrations of CFC-11, CFC-12, and stratospheric O_3 are increased from the reference level to the world-avoided levels, averaged over the decade 2020–29. In GHG2025 the concentrations of CO_2, CH_4, and N_2O are increased by approximately 37%, 66%, and 15%, respectively, relative to the reference level. Updated from Wu et al. (2013).

Focusing on near-future climate impacts, Wu et al. (2013) examined atmospheric and surface responses to unregulated ODS emissions in the 2020s. They showed that not only the Southern Hemisphere, but also the tropics and Northern Hemisphere would experience substantial hydro-climate changes in the absence of the Montreal Protocol (Figure 4-21; Wu et al., 2013). As the ODS concentration increases, tropical and extratropical wet regions become wetter, whereas subtropical dry regions become drier in both hemispheres (red line in Figure 4-21). These changes in global precipitation minus evaporation (P-E) are of comparable magnitude to those associated with the increase in other GHGs alone (blue line in Figure 4-21). This result suggests that hydro-climate change by 2025 would be almost doubled in the absence of the Montreal Protocol, highlighting the importance of the Montreal Protocol in mitigating future climate change.

4.5.2 Radiative Effects

Stratospheric ozone forcing is very sensitive to the altitude of ozone change, and GHG increases as well as future circulation changes are expected to influence the distribution of ozone. Therefore, as stratospheric chlorine levels decline, stratospheric ozone is not expected to return to its 1970 or preindustrial spatial distribution or total column. As a result, the stratospheric ozone radiative forcing does not simply scale with stratospheric chlorine loading and would not be expected to return to zero in the future (Portmann et al., 2012). Bekki et al. (2013) found a large spread between CCMVal-2 models, with radiative forcing due to stratospheric ozone staying negative in some models but increasing by up to +0.25 W m^{-2} by 2100 in others. On average the multi-model mean showed an increase in forcing to +0.06 W m^{-2} by 2100 from a value of −0.05 W m^{-2} today. The spread is driven by differences in modeled ozone change near the tropopause. The expected high-altitude increase in ozone would have little effect on forcing.

4.5.3 Chemistry Effects

Kawase et al. (2011), a single model study, and the ACCMIP multi-model study of Young et al. (2013a) present the most detailed account of the 21st century tropospheric ozone projections under the RCP scenarios (see Box 4-1), supported by complementary findings of Lamarque et al. (2011), Shindell

et al. (2013b), and – for the CMIP5 models – Eyring et al. (2013). These model studies find that tropospheric ozone changes over the 21st century are dominated by changes in precursor emissions (oxides of nitrogen, carbon monoxide, and volatile organic compounds) (see Lamarque et al., 2011, 2013). A decrease in the tropospheric ozone burden is found for the RCP2.6, 4.5, and 6.0 simulations, driven by falling emissions of ozone precursors. RCP8.5 simulations project ozone increases throughout the troposphere, partially driven by the near doubling of methane concentrations by 2100 (compared to the present day), and occurring in spite of the decreasing emissions prescribed for the other ozone precursors. In these studies, the expected recovery of stratospheric ozone concentrations, due to reduced ODSs, combines with an enhanced STE, due to the projected strengthening of the BDC (Section 4.3.2.2), to somewhat negate the tropospheric ozone decrease in RCP2.6, 4.5, and 6.0, and enhance the increase in RCP8.5.

Both Kawase et al. (2011) and Young et al. (2013a) quantify the increases in the net influx of stratospheric ozone to the troposphere for the RCPs. For 2100, Kawase et al. (2011) report net influx increases of 45%, 80%, 111%, and 109% compared to the present day for RCP2.6, 4.5, 6.0, and 8.5 respectively (RCP8.5 has a lower net influx due to the large tropospheric ozone increases). The ACCMIP models (Young et al., 2013a) exhibit a wide range of net influx increases: 14–90% and 24–139% for RCP2.6 and 8.5, respectively. Using different climate and emissions scenarios (and neglecting changes in ozone precursor emissions), Zeng et al. (2010) separated the impacts on the net stratospheric ozone influx from increasing GHG concentrations (strengthening the BDC) and from ozone recovery, finding that approximately half their overall 43% increase in the influx by 2100 was attributable to each factor. Moreover, the combined impact of ozone recovery and a strengthened BDC was enough to cancel the reduction in tropospheric ozone due to climate change (from enhanced water vapor, leading to more ozone destruction; e.g., Johnson et al. (2001). Morgenstern et al. (2014) found a 33% increase in the net stratospheric influx by 2050, caused predominantly by ozone recovery.

The range of stratospheric influx changes between models is related to: different treatments of the stratosphere, such as whether the model explicitly calculates stratospheric ozone concentrations or uses an offline stratospheric ozone data set; what the vertical extent and resolution of the stratosphere is in the model, which may influence how the modeled circulation responds to GHG forcing; and the magnitude of the troposphere-stratosphere gradient in ozone concentrations, which is important since we are concerned with the *net* ozone influx from STE. Furthermore, different tropopause definitions can affect comparisons between studies. Despite the inter-model differences, there is general agreement in the spatial patterns of tropospheric ozone change that are qualitatively attributable to an increased stratospheric influx between models, such as enhanced ozone in the upper troposphere (at the flanks of the jets), and a quasi-zonal increase in the midlatitude tropospheric ozone column (Kawase et al., 2011; Eyring et al., 2013; Stevenson et al., 2013; Young et al., 2013a).

As with past changes (Section 4.4.3), the potential impacts of projected stratospheric ozone change through UV attenuation have received less attention. Model studies by Voulgarakis et al. (2013) and Morgenstern et al. (2014) (correcting Morgenstern et al., 2013) investigated OH and methane lifetime changes, finding a significant impact of the modeled stratospheric ozone column changes on the mean tropospheric OH concentration (mediated through ozone photolysis), suggesting that differences in stratospheric ozone could contribute to the model spread in methane lifetimes.

Overall, simulations are in agreement that stratospheric ozone recovery and climate change (through circulation impacts) mean that the net influx of stratospheric ozone could become a more important term in the tropospheric ozone budget. Simulations also agree on the broad spatial patterns of an enhanced stratospheric input, but there remains a large degree of uncertainty in the magnitude of the impact. Models are beginning to include more interactive processes relevant for understanding the role of stratospheric change on tropospheric composition (e.g., stratospheric chemistry, interactive photolysis calculations), but it remains to be seen whether an ensemble of models with more consistent processes will reduce or increase the inter-model spread.

POLICY-RELEVANT INFORMATION

There is further evidence that Antarctic ozone depletion has influenced the Southern Hemisphere surface climate and ocean.

The Antarctic ozone hole was first linked to changes in the tropospheric circulation in the early 2000s. In the decade or so since, a strong case has been built for the dominance of ozone depletion in driving the Southern Hemisphere summertime circulation changes in recent decades. A poleward shift in the circulation, including the position of the midlatitude jet and storm tracks, has been observed in austral summer. Since the last Ozone Assessment, the contribution of ozone depletion to Southern Hemisphere summertime circulation changes over the past three to five decades has been better quantified and shown to be considerably larger than that from greenhouse gases, in most studies. No robust link between stratospheric ozone changes and Northern Hemisphere tropospheric climate has been found, consistent with the conclusions of the previous Ozone Assessment.

The ozone hole impacts the Southern Hemisphere tropospheric circulation by cooling the polar lower stratosphere in spring, which increases the gradient in temperature between the equator and pole. While the precise mechanism by which this then shifts the tropospheric midlatitude jet poleward is still unclear, such a response is robustly simulated in models. New research has found that ozone depletion has likely contributed to the observed expansion of the Southern Hemisphere Hadley Cell, with models simulating an associated pattern of increased summertime precipitation in the subtropics. An improved understanding of the role of ocean eddies in the response of the Southern Ocean to observed wind stress changes (partly due to ozone depletion) has also been gained, and models and observations provide evidence that these wind stress changes have strengthened the overturning circulation in the Southern Ocean. This may have led to a reduction in the amount of carbon uptake by the Southern Ocean, but large uncertainties remain in both observing and simulating this process. Additional research since the previous Ozone Assessment has shown that coupled models simulate a decrease in hemispheric-mean Antarctic sea-ice extent in response to ozone depletion. However, there is low confidence in this model result because these models also simulate a decrease in Antarctic sea-ice extent when driven by all major anthropogenic and natural forcings, in contrast to the small observed increase since 1979. Figure 4-22 schematically summarizes the impact of ozone depletion on the climate system.

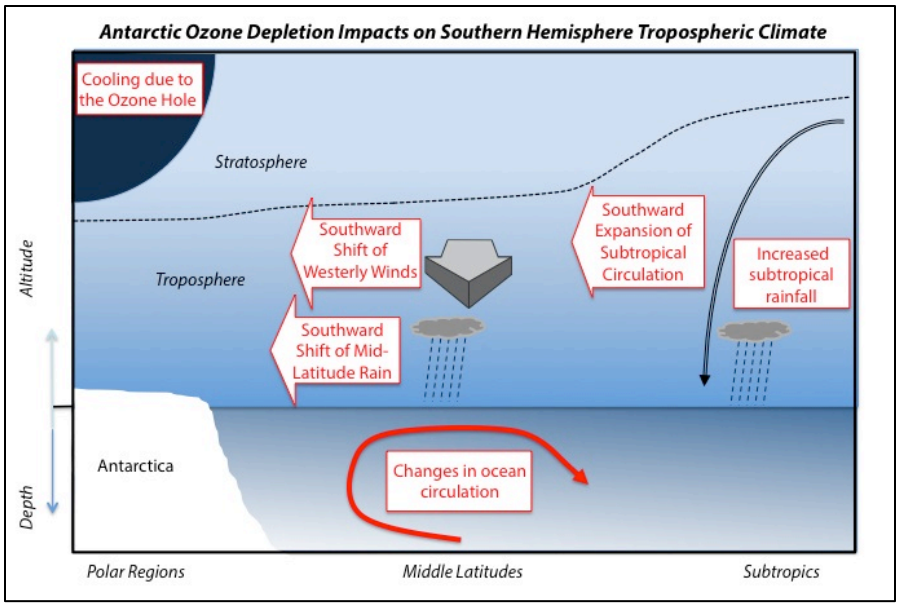

Figure 4-22. Schematic illustration of Southern Hemisphere climate impacts in austral summer associated with Antarctic ozone depletion. Ozone depletion has cooled the Antarctic stratosphere, very likely shifting the region of strong westerly winds and associated rainfall southward in the summer. These changes in midlatitude winds have likely led to changes in the ocean circulation. Ozone depletion has also likely contributed to a southward expansion of the tropical circulation in summer, and may have increased subtropical rainfall.

With the ozone hole expected to recover over coming decades, the climate impacts of stratospheric ozone change in the future will be opposite to those of the past. Meanwhile, GHGs are projected to keep increasing, driving circulation effects that oppose those of ozone recovery. Hence, climate model simulations show that summer trends in the Southern Hemisphere tropospheric circulation over the next fifty years will likely be weaker than those over the past few decades. New simulations since the last Ozone Assessment have allowed an assessment of the impacts of ozone recovery under various scenarios of future emissions, compared to the single emissions scenario previously assessed. In all scenarios, ozone recovery acts to weaken the circulation changes induced by greenhouse gases alone. In a scenario with low greenhouse gas emissions, ozone recovery is found to dominate the Southern Hemisphere summer circulation changes, shifting the midlatitude jet equatorward.

Stratospheric ozone changes are the dominant driver of globally averaged cooling in the lower stratosphere.

Stratospheric temperature changes are important indicators of the impact of anthropogenic emissions on climate. There is robust evidence that changes in composition in the stratosphere have resulted in radiative cooling of the stratosphere over the past three decades. Weather balloons have been providing vertically resolved temperatures since 1958 but are sparse geographically and only cover the lower stratosphere. Hence, most of the information about stratospheric temperature change comes from satellite measurements. Satellite observations provide good global coverage of the stratosphere since the late 1970s but have coarser vertical resolution than the balloon data.

New research since the previous Ozone Assessment has led to a better understanding of the uncertainties in stratospheric temperature changes. Lower stratospheric temperature trends have been analyzed by numerous groups and, while some differences exist between data sets, a global cooling of approximately 1°C over the 1979–2012 period is found across these data sets. For the middle and upper stratosphere, however, only one data set was available at the time of the 2010 Ozone Assessment, making estimates of uncertainty difficult. An additional analysis of the Stratospheric Sounding Unit (SSU) satellite measurements published in 2012 tells quite a different story from the previous data set. While both data sets show global cooling, the new data set shows a cooling almost twice as large as the original analysis in the middle stratosphere. Comparison with modeled trends provided little insight into the cause of these differences, though planned updates to the data sets may help to resolve some of the discrepancies.

Since the previous Ozone Assessment, a number of carefully designed model experiments have been undertaken to quantify the contribution of ozone depletion to recent climate change. Based on these and earlier experiments, cooling in the lower stratosphere over Antarctica in spring and summer has been clearly attributed to Antarctic ozone depletion by multiple studies. In the tropics, one study suggests that ozone depletion is the main driver of lower stratospheric cooling there, though uncertainties in ozone concentrations used to force the models are tightly linked to uncertainties in the temperatures. Globally, several studies have shown that ozone changes are the dominant driver of lower stratospheric cooling.

New estimates of global mean ozone radiative forcing due to emissions of ozone-depleting substances, which account for stratospheric ozone change and its indirect effect on tropospheric ozone, indicate a stronger surface cooling effect than that due to stratospheric ozone changes alone.

Radiative forcing — the net change in the energy balance at the tropopause due to an imposed perturbation — has been further developed within the IPCC Fifth Assessment Report. A new term "Effective Radiative Forcing" was defined to encompass rapid adjustments in the troposphere as well as the traditional stratospheric adjustment. This quantity is more closely associated with the resulting temperature changes. Radiative forcings are assessed at 2010.

This Assessment, for the first time, considers the radiative forcing from the effects of ODS emissions on ozone, including impacts on both tropospheric and stratospheric ozone, which is assessed to

be −0.15 [−0.3 to 0] W m^{-2}. Approximately three-quarters of this radiative forcing results from ozone changes in the stratosphere. There is also the possibility of an induced forcing from rapid adjustment effects on clouds, associated with ozone-driven changes in the Southern Hemisphere tropospheric circulation, and a second possible effect due to ozone-induced wind changes increasing sea salt aerosol over the Southern Ocean. These rapid adjustments could be of a comparable size to the direct ozone radiative forcing and could be of either sign. Overall, this makes the sign of the Effective Radiative Forcing, which includes such adjustments, unknown at present.

Estimates of radiative forcing are very sensitive to the latitudinal and vertical distribution of ozone. Observations and models suggest that increasing greenhouse gases have accelerated the shallow branch of the Brewer-Dobson circulation, leading to a decrease of lower stratospheric ozone in the tropics and an increase in midlatitudes, with additional impacts on tropospheric ozone. A further acceleration of the Brewer-Dobson circulation is projected due to future greenhouse gas increases. This implies that the distribution of ozone will not recover to its pre-depletion spatial state, which has implications for projections of radiative forcing. Model estimates for stratospheric ozone radiative forcing by 2100 are highly uncertain, ranging from slightly negative to exceeding +0.25 W m^{-2} under a high greenhouse gas emissions scenario.

REFERENCES

Abernathey, R., J. Marshall, and D. Ferreira, The dependence of Southern Ocean meridional overturning on wind stress, *J. Phys. Oceanogr*., *41*, 2261-2278, doi: 10.1175/JPO-D-11-023.1, 2011.

Arblaster, J.M., G.A. Meehl, and D.J. Karoly, Future climate change in the Southern Hemisphere: Competing effects of ozone and greenhouse gases, *Geophys. Res. Lett.*, *38*, L02701, doi: 10.1029/2010GL045384, 2011.

Bandoro, J., S. Solomon, A. Donohoe, D. Thompson, and B. Santer, Influences of the Antarctic ozone hole on Southern Hemisphere summer climate change, *J. Clim.*, *27* (16), 6245-6264, doi: 10.1175/JCLI-D-13-00698.1, 2014.

Barnes, E.A., N.W. Barnes, and L.M. Polvani, Delayed Southern Hemisphere climate change induced by stratospheric ozone recovery, as projected by the CMIP5 models, *J. Clim.*, *27*, 852-867, doi: 10.1175/JCLI-D-13-00246.1, 2014.

Bekki, S., A. Rap, V. Poulain, S. Dhomse, M. Marchand, F. Lefevre, P.M. Forster, S. Szopa, and M.P. Chipperfield, Climate impact of stratospheric ozone recovery, *Geophys. Res. Lett.*, *40*, 2796–2800, doi: 10.1002/grl.50358, 2013.

Bindoff, N.L., and P.A. Stott (Coordinating Lead Authors), K. Mirle AchutaRao, M. Allen, N. Gillett, D. Gutzler, K. Hansingo, G. Hegerl, Y. Hu, S. Jain, I. Mokhov, J. Overland, J. Perlwitz, R. Sebbari, and X. Zhang (Lead Authors), Detection and attribution of climate change: From global to regional, Chapter 10 in *Climate Change 2013: The Physical Science Basis. Contribution of Working Group I to the Fifth Assessment Report of the Intergovernmental Panel on Climate Change*, edited by T.F. Stocker, D. Qin, G.-K. Plattner, M. Tignor, S.K. Allen, J. Boschung, A. Nauels, Y. Xia, V. Bex and P.M. Midgley, Cambridge University Press, Cambridge, UK, and New York, NY, USA, 2013.

Bintanja, R., G.J. van Oldenborgh, S.S. Drijfhout, B. Wouters, and C.A. Katsman, Important role for ocean warming and increased ice-shelf melt in Antarctic sea-ice expansion, *Nature Geosci.*, *6*, 376-379, doi: 10.1038/ngeo1767, 2013.

Birner, T., and H. Bönisch, Residual circulation trajectories and transit times into the extratropical lowermost stratosphere, *Atmos. Chem. Phys.*, *11*, 817-827, doi: 10.5194/acp-11-817-2011, 2011.

Bitz, C.M., and L.M. Polvani, Antarctic climate response to stratospheric ozone depletion in a fine resolution ocean climate model, *Geophys. Res. Lett.*, *39*, L20705, doi: 10.1029/2012GL053393, 2012.

Bodeker, G.E., B. Hassler, P.J. Young, and R.W. Portmann, A vertically resolved, global, gap-free ozone database for assessing or constraining global climate model simulations, *Earth Syst. Sci. Data*, *5*, 31-43, doi: 10.5194/essd-5-31-2013, 2013.

Böning C.W., A. Dispert, M. Visbeck, S.R. Rintoul, and F.U. Schwarzkopf, The response of the Antarctic Circumpolar Current to recent climate change, *Nature Geosci*., *1*, 864-869, doi: 10.1038/ngeo362, 2008.

Bönisch, H., A. Engel, Th. Birner, P. Hoor, D.W. Tarasick, and E.A. Ray, On the structural changes in the Brewer-Dobson Circulation after 2000, *Atmos. Chem. Phys.*, *11*, 3937-3948, doi: 10.5194/acp-11-3937-2011, 2011.

Bryan, F.O., G. Danabasoglu, P.R. Gent and K. Lindsay, Changes in ocean ventilation during the 21st century in the CCSM3, *Ocean Model.*, *15*, 141-156, doi: 10.1016/j.ocemod.2006.01.002, 2006.

Bunzel, F., and H. Schmidt, The Brewer-Dobson circulation in a changing climate: Impact of the model configuration, *J. Atmos. Sci.*, *70*, 1437-1455, doi: 10.1175/JAS-D-12-0215.1, 2013.

Butchart, N., The Brewer-Dobson circulation, *Rev. Geophys*, *52* (2), 157-184, doi: 10.1002/2013RG000448, 2014.

Butchart, N., I. Cionni, V. Eyring, T.G. Shepherd, D.W. Waugh, H. Akiyoshi, J. Austin, C. Brühl, M.P. Chipperfield, E. Cordero, M. Dameris, R. Deckert, S. Dhomse, S.M. Frith, R.R. Garcia, A. Gettelman, M.A. Giorgetta, D.E. Kinnison, F. Li, E. Mancini, C. McLandress, S. Pawson, G. Pitari, D.A. Plummer, E. Rozanov, F. Sassi, J.F. Scinocca, K. Shibata, B. Steil, and W. Tian, Chemistry-climate model simulations of 21st century stratospheric climate and circulation changes, *J. Clim*., *23* (20), 5349-5374, doi: 10.1175/2010JCLI3404.1, 2010.

Butler, A.H., D.W.J. Thompson, and R. Heikes, The steady-state atmospheric circulation response to climate change-like thermal forcings in a simple general circulation model, *J. Clim.*, *23*, 3474-3496, doi: 10.1175/ 2010JCLI3228.1, 2010.

Cai, W., Antarctic ozone depletion causes an intensification of the Southern Ocean super-gyre circulation, *Geophys. Res. Lett*., *33*, L03712, doi: 10.1029/ 2005GL024911, 2006.

Cai, W., and T. Cowan, Trends in Southern Hemisphere circulation in IPCC AR4 models over 1950–99: Ozone depletion versus greenhouse forcing, *J. Clim*., *20* (4), 681-693, doi: 10.1175/JCLI4028.1, 2007.

Cai, W., T. Cowan, S. Godfrey, and S. Wijffels, Simulations of processes associated with the fast warming rate of the southern mid-latitude ocean, *J. Clim.*, *23*, 197-206, doi: 10.1175/2009JCLI3081.1, 2010.

Calvo, N., and R.R. Garcia, Wave forcing of the tropical upwelling in the lower stratosphere under increasing concentrations of greenhouse gases, *J. Atmos. Sci*., *66* (10), 3184-3196, doi: 10.1175/2009JAS3085.1, 2009.

Calvo, N., R.R. Garcia, D.R. Marsh, M.J. Mills, D.E. Kinnison, and P.J. Young, Reconciling modeled and observed temperature trends over Antarctica, *Geophys. Res. Lett*., *39*, L16803, doi: 10.1029/2012GL052526, 2012.

Canziani, P.O., A. O'Neill, R. Schofield, M. Raphael, G.J. Marshall, and G. Redaelli, World climate research programme special workshop on climatic effects of ozone depletion in the southern hemisphere, *Bull. Amer. Meteorol. Soc.*, *95*, ES101-ES105, doi: 10.1175/BAMS-D-13-00143.1, 2014.

Charlton-Perez, A.J., M.P. Baldwin, T. Birner, R.X. Black, A.H. Butler, N. Calvo, N.A. Davis, E.P. Gerber, N. Gillett, S. Hardiman, J. Kim, K. Krüger, Y.-Y. Lee, E. Manzini, B.A. McDaniel, L. Polvani, T. Reichler, T.A. Shaw, M. Sigmond, S.-W. Son, M. Toohey, L. Wilcox, S. Yoden, B. Christiansen, F. Lott, D. Shindell, S. Yukimoto, and S. Watanabe, On the lack of stratospheric dynamical variability in low-top versions of the CMIP5 models, *J. Geophys. Res*., *118*, 2494-2505, doi: 10.1002/jgrd.50125, 2013.

Chen, G., and I.M. Held, Phase speed spectra and the recent poleward shift of Southern Hemisphere surface westerlies, *Geophys. Res. Lett.*, *34*, L21805, doi: 10.1029/2007GL031200, 2007.

Ciais, P., and C. Sabine (Coordinating Lead Authors), G. Bala, L. Bopp, V. Brovkin, J. Canadell, A. Chhabra, R. DeFries, J. Galloway, M. Heimann, C. Jones, C. Le Quéré, R.B. Myneni, S. Piao, and P. Thornton (Lead Authors), Carbon and other biogeochemical cycles, Chapter 6 in *Climate Change 2013: The Physical Science Basis. Contribution of Working Group I to the Fifth Assessment Report of the Intergovernmental Panel on Climate Change*, edited by T.F. Stocker, D. Qin, G.-K. Plattner, M. Tignor, S.K. Allen, J. Boschung, A. Nauels, Y. Xia, V. Bex, and P.M. Midgley, Cambridge University Press, Cambridge, UK, and New York, NY, USA, 2013.

Cionni, I., V. Eyring, J.F. Lamarque, W.J. Randel, D.S. Stevenson, F. Wu, G.E. Bodeker, T.G. Shepherd, D.T. Shindell, and D.W. Waugh, Ozone database in support of CMIP5 simulations: Results and corresponding radiative forcing, *Atmos. Chem. Phys.*, *11*, 11267-11292, doi: 10.5194/acp-11-11267-2011, 2011.

Collins, M., and R. Knutti (Coordinating Lead Authors), J. Arblaster, J.-L. Dufresne, T. Fichefet, P. Friedlingstein, X. Gao, W.J. Gutowski, T. Johns, G. Krinner, M. Shongwe, C. Tebaldi, A.J. Weaver, and M. Wehner (Lead Authors), Long-term climate change: Projections, commitments and irreversibility, Chapter 12 in *Climate Change 2013: The Physical Science Basis. Contribution of Working Group I to the Fifth Assessment Report of the Intergovernmental Panel on Climate Change*, edited by T.F. Stocker, D. Qin, G.-K. Plattner, M. Tignor, S.K. Allen, J. Boschung, A. Nauels, Y. Xia, V. Bex and P.M. Midgley, Cambridge University Press, Cambridge, UK, and New York, NY, USA, 2013.

Conley, A.J., J.-F. Lamarque, F. Vitt, W.D. Collins, and J. Kiehl, PORT, a CESM tool for the diagnosis of radiative forcing, *Geosci. Model Dev.*, *6*, 469-476, doi: 10.5194/gmd-6-469-2013, 2013.

Crook, J.A., N.P. Gillett, and S.P.E. Keeley, Sensitivity of Southern Hemisphere climate to zonal asymmetry in ozone, *Geophys. Res. Lett.*, *35*, L07806, doi: 10.1029/2007GL032698, 2008.

Cubasch, U., and D. Wuebbles (Coordinating Lead Authors), D. Chen, M.C. Facchini, D. Frame, N. Mahowald, and J.-G. Winther (Lead Authors), Introduction, Chapter 1 in *Climate Change 2013: The Physical Science Basis. Contribution of Working Group I to the Fifth Assessment Report of the Intergovernmental Panel on Climate Change*, edited by T.F. Stocker, D. Qin, G.-K. Plattner, M. Tignor, S.K. Allen, J. Boschung, A. Nauels, Y. Xia, V. Bex, and P.M. Midgley, Cambridge University Press, Cambridge, UK, and New York, NY, USA, 2013.

Dall'Amico, M., P.A. Stott, A.A. Scaife, L.J. Gray, K.H. Rosenlof, and A.Y. Karpechko, Impact of stratospheric variability on tropospheric climate change, *Clim. Dyn.*, *34*, 399-417, doi: 10.1007/s00382-009-0580-1, 2010.

Dee, D.P., S.M. Uppala, A.J. Simmons, P. Berrisford, P. Poli, S. Kobayashi, U. Andrae, M.A. Balmaseda, G. Balsamo, P. Bauer, P. Bechtold, A.C.M. Beljaars, L. van de Berg, J. Bidlot, N. Bormann, C. Delsol, R. Dragani, M. Fuentes, A.J. Geer, L. Haimberger, S.B. Healy, H. Hersbach, E.V. Hólm, L. Isaksen, P. Kållberg, M. Köhler, M. Matricardi, A.P. McNally, B.M. Monge-Sanz, J.-J. Morcrette, B.-K. Park, C. Peubey, P. de Rosnay, C. Tavolato, J.-N. Thépaut, and F. Vitart, The ERA-Interim reanalysis: Configuration and performance of the data assimilation system, *Quart. J. Roy. Meteorol. Soc.*, *137*, 553-597, doi: 10.1002/qj.828, 2011.

Dessler, A.E., M.R. Schoeberl, T. Wang, S.M. Davis, and K.H. Rosenlof, Stratospheric water vapor feedback, *Proc. Natl. Acad. Sci.*, *110*, 18087-18091, doi: 10.1073/pnas.1310344110, 2013.

Deushi, M., and K. Shibata, Impacts of increases in greenhouse gases and ozone recovery on lower stratospheric circulation and the age of air: Chemistry-climate model simulations up to 2100, *J. Geophys. Res.*, *116*, D07107, doi: 10.1029/2010JD015024, 2011.

Diallo, M., B. Legras, and A. Chédin, Age of stratospheric air in the ERA-Interim, *Atmos. Chem. Phys*., *12*, 12133-12154, doi: 10.5194/acp-12-12133-2012, 2012.

Engel, A., T. Möbius, H. Bönisch, U. Schmidt, R. Heinz, I. Levin, E. Atlas, S. Aoki, T. Nakazawa, S. Sugawara, F. Moore, D. Hurst, J. Elkins, S. Schauffler, A. Andrews, and K. Berine, Age of stratospheric air unchanged within uncertainties over the past 30 years, *Nature Geosci.*, *2*, 28-31, doi: 10.1038/GEO388, 2009.

Eyring, V., N. Butchart, D.W. Waugh, H. Akiyoshi, J. Austin, S. Bekki, G.E. Bodeker, B.A. Boville, C. Brühl, M.P. Chipperfield, E. Cordero, M. Dameris, M. Deushi, V.E. Fioletov, S.M. Frith, R.R. Garcia, A. Gettelman, M.A. Giorgetta, V. Grewe, L. Jourdain, D.E. Kinnison, E. Mancini, E. Manzini, M. Marchand, D.R. Marsh, T. Nagashima, P.A. Newman, J.E. Nielsen, S. Pawson, G. Pitari, D.A. Plummer, E. Rozanov, M. Schraner, T.G. Shepherd, K. Shibata, R.S. Stolarski, H. Struthers, W. Tian, and M. Yoshiki, Assessment of temperature, trace species, and ozone in chemistry-climate model simulations of the recent past, *J. Geophys. Res.*, *111*, D22308, doi: 10.1029/2006JD007327, 2006.

Eyring, V., I. Cionni, J.-F. Lamarque, H. Akiyoshi, G.E. Bodeker, A.J. Charlton-Perez, S.M. Frith, A. Gettelman, D.E. Kinnison, T. Nakamura, L.D. Oman, S. Pawson, and Y. Yamashita, Sensitivity of 21st century stratospheric ozone to greenhouse gas scenarios, *Geophys. Res. Lett.*, *37*, L16807, doi: 10.1029/2010GL044443, 2010.

Eyring, V., J.M. Arblaster, I. Cionni, J. Sedlacek, J. Perlwitz, P.J. Young, S. Bekki, D. Bergmann, P. Cameron-Smith, W. Collins, G. Faluvegi, K.-D. Gottschaldt, L. Horowitz, D. Kinnison, J.-F. Lamarque, D.R. Marsh, D. Saint-Martin, D. Shindell, K. Sudo, S. Szopa, and S. Watanabe, Long-term changes in tropospheric and stratospheric ozone and associated climate impacts in CMIP5 simulations, *J. Geophys. Res.*, *118*, 5029-5060, doi: 10.1002/jgrd.50316, 2013.

Farneti R., T.L. Delworth, A.J. Rosati, S.M. Griffies, and F. Zeng, The role of mesoscale eddies in the rectification of the Southern Ocean response to climate change, *J. Phys. Oceanogr.*, *40*, 1539-1557, doi: 10.1175/2010JPO4353.1, 2010.

Fels, S.B., J.D. Mahlman, M.D. Schwarzkopf, and R.W. Sinclair, Stratospheric sensitivity to perturbations in ozone and carbon dioxide: Radiative and dynamical response, *J. Atmos. Sci.*, *37*, 2265-2297, doi: 10.1175/1520-0469(1980)037<2265:SSTPIO>2.0.CO;2, 1980.

Forster, P.M., and K.P. Shine, Radiative forcing and temperature trends from stratospheric ozone changes, *J. Geophys. Res.*, *102*, 10841-10855, doi: 10.1029/96JD03510, 1997.

Forster, P.M., and K.P. Shine, Stratospheric water vapour changes as a possible contributor to observed stratospheric cooling, *Geophys. Res. Lett.*, *26*, 3309-3312, doi: 10.1029/1999GL010487, 1999.

Forster, P.M., V.I. Fomichev, E. Rozanov, C. Cagnazzo, A.I. Jonsson, U. Langematz, B. Fomin, M.J. Iacono, B. Mayer, E. Mlawer, G. Myhre, R.W. Portmann, H. Akiyoshi, V. Falaleeva, N. Gillett, A. Karpechko, J. Li, P. Lemennais, O. Morgenstern, S. Oberländer, M. Sigmond, and K. Shibata, Evaluation of radiation scheme performance within chemistry climate models, *J. Geophys. Res.*, *116*, D10302, doi: 10.1029/2010JD015361, 2011.

Forster, P.M., and D.W.J. Thompson (Coordinating Lead Authors), M.P. Baldwin, M.P. Chipperfield, M. Dameris, J.D. Haigh, D.J. Karoly, P.J. Kushner, W.J. Randel, K.H. Rosenlof, D.J. Seidel, S. Solomon, G. Beig, P. Braesicke, N. Butchart, N.P. Gillett, K.M. Grise, D.R. Marsh, C. McLandress, T.N. Rao, S.-W. Son, G.L. Stenchikov, and S. Yoden, Stratospheric changes and climate, Chapter 4 in *Scientific Assessment of Ozone Depletion: 2010*, Global Ozone Research and Monitoring Project-Report No. 52, 516 pp., World Meteorological Organization, Geneva, Switzerland, 2011.

Free, M., The seasonal structure of temperature trends in the tropical lower stratosphere, *J. Clim.*, *24*, 859-866, doi: 10.1175/2010JCLI3841.1, 2011.

Free, M., and J. Lanzante, Effect of volcanic eruptions on the vertical temperature profile in radiosonde data and climate models, *J. Clim*., *22*, 2925-2939, doi: 10.1175/2008JCLI2562.1, 2009.

Fu, Q., S. Solomon, and P. Lin, On the seasonal dependence of tropical lower-stratospheric temperature trends, *Atmos. Chem. Phys*., *10*, 2643-2653, doi: 10.5194/acp-10-2643-2010, 2010.

Fueglistaler, S., Y.S. Liu, T.J. Flannaghan, P.H. Haynes, D.P. Dee, W.J. Read, E.E. Remsberg, L.W. Thomason, D.F. Hurst, J.R. Lanzante, and P.F. Bernath, The relation between atmospheric humidity and temperature trends for stratospheric water, *J. Geophys. Res.*, *118*, 1052-1074, doi: 10.1002/jgrd.50157, 2013.

Fujiwara, M., H. Vömel, F. Hasebe, M. Shiotani, S.-Y. Ogino, S. Iwasaki, N. Nishi, T. Shibata, K. Shimizu, E. Nishimoto, J.M. Valverde Canossa, H.B. Selkirk, and S.J. Oltmans, Seasonal to decadal variations of water vapor in the tropical lower stratosphere observed with balloon-borne cryogenic frost point hygrometers, *J. Geophys. Res.*, *115*, D18304, doi: 10.1029/2010JD014179, 2010.

Fyfe, J.C., N.P. Gillett, and G.J. Marshall, Human influence on extratropical Southern Hemisphere summer precipitation, *Geophys. Res. Lett.*, *39*, L23711, doi: 10.1029/2012GL054199, 2012.

Fyfe, J.C., N.P. Gillett, and F.W. Zwiers, Overestimated global warming over the past 20 years, *Nature Climate Change*, *3*, 767-769, doi: 10.1038/nclimate1972, 2013.

Garcia, R.R., and W.J. Randel, Acceleration of the Brewer-Dobson circulation due to increases in greenhouse gases, *J. Atmos. Sci.*, *65* (8), 2731-2739, doi: 10.1175/2008JAS2712.1, 2008.

Garcia, R.R., W.J. Randel, and D.E. Kinnison, On the determination of age of air trends from atmospheric trace species, *J. Atmos. Sci*., *68*, 139-154, doi: 10.1175/2010JAS3527.1, 2011.

Garcia, R.R., D.E. Kinnison, and D.R. Marsh, "World avoided" simulations with the Whole Atmosphere Community Climate Model, *J. Geophys. Res.*, *117*, D23303, doi: 10.1029/2012JD018430, 2012.

Garfinkel, C.I., D.W. Waugh, and E.P. Gerber, The effect of tropospheric jet latitude on coupling between the stratospheric polar vortex and the troposphere, *J. Clim.*, *26*, 2077-2097, doi: 10.1175/JCLI-D-12-00301.1, 2013.

Garny H., M. Dameris, W. Randel, G.E. Bodeker, and R. Deckert, Dynamically forced increase of tropical upwelling in the lower stratosphere, *J. Atmos. Sci.*, *68*, 1214-1233, doi: 10.1175/2011JAS3701.1, 2011.

Gent P.R., and G. Danabasoglu, Response to increasing Southern Hemisphere winds in CCSM4, *J. Clim.*, *24*, 4992-4998, doi: 10.1175/JCLI-D-10-05011.1, 2011.

Gerber, E.P., and S.-W. Son, Quantifying the summertime Austral jet stream and Hadley Cell response to stratospheric ozone and greenhouse gases, *J. Clim.*, *27*, 5538-5559, 2014.

Gerber, E.P., M.P. Baldwin, H. Akiyoshi, J. Austin, S. Bekki, P. Braesicke, N. Buchart, M. Chipperfield, M. Dameris, S. Dhomse, S.M. Firth, R.R. Garcia, H. Garney, A. Gettelman, S.C. Hardiman, O. Morgenstern, J.E. Nielsen, S. Pawson, T. Peter, D.A. Plummer, J.A. Pyle, E. Rozanov, J.F. Scinocca, T.G. Shepherd, and D. Smale, Stratosphere-troposphere coupling and annular mode variability in chemistry-climate models, *J. Geophys. Res.*, *115*, D00M06, doi: 10.1029/2009JD013770, 2010.

Gettelman, A., M.I. Hegglin, S.-W. Son, J. Kim, M. Fujiwara, T. Birner, S. Kremser, M. Rex, J.A. Añel, H. Akiyoshi, J. Austin, S. Bekki, P. Braesike, C. Brühl, N. Butchart, M. Chipperfield, M. Dameris, S. Dhomse, H. Garny, S.C. Hardiman, P. Jöckel, D.E. Kinnison, J.F. Lamarque, E. Mancini, M. Marchand, M. Michou, O. Morgenstern, S. Pawson, G. Pitari, D. Plummer, J.A. Pyle, E. Rozanov, J. Scinocca, T.G. Shepherd, K. Shibata, D. Smale, H. Teyssèdre, and W. Tian, Multimodel assessment of the upper troposphere and lower stratosphere: Tropics and trends, *J. Geophys. Res.*, *115*, D00M08, doi: 10.1029/2009JD013638, 2010.

Gille, S.T., Decadal-scale temperature trends in the Southern Hemisphere ocean, *J. Clim.*, *21* (18), 4749-4765, doi: 10.1175/2008JCLI2131.1, 2008.

Gillett, N.P., H. Akiyoshi, S. Bekki, P. Braesicke, V. Eyring, R. Garcia, A. Yu. Karpechko, C.A. McLinden, O. Morgenstern, D.A. Plummer, J.A. Pyle, E. Rozanov, J. Scinocca, and K. Shibata, Attribution of observed changes in stratospheric ozone and temperature, *Atmos. Chem. Phys*., *11* (2), 599-609, doi: 10.5194/acp-11-599-2011, 2011.

Gillett, N.P., J.C. Fyfe, and D.E. Parker, Attribution of observed sea level pressure trends to greenhouse gas, aerosol, and ozone changes, *Geophys. Res. Lett.*, *40*, 2302-2306, doi: 10.1002/grl.50500, 2013.

Gnanadesikan, A., J.L. Russell, and F. Zeng, How does ocean ventilation change under global warming?, *Ocean Sci.*, *3* (1), 43-53, doi: 10.5194/os-3-43-2007, 2007.

Gómez-Escolar, M., S. Fueglistaler, N. Calvo, and D. Barriopedro, Changes in polar stratospheric temperature climatology in relation to stratospheric sudden warming occurrence, *Geophys. Res. Lett*., *39*, L22802, doi: 10.1029/2012GL053632, 2012.

Gonzalez, P.L.M., L.M. Polvani, R. Seager, and G.J.P. Correa, Stratospheric ozone depletion: A key driver of recent precipitation trends in south eastern South America, *Clim. Dyn*., *42*, 1775-1792, doi: 10.1007/s00382-013-1777-x, 2013.

Grise, K.M., L.M. Polvani, G. Tselioudis, Y. Wu, and M.D. Zelinka, The ozone hole indirect effect: Cloud-radiative anomalies accompanying the poleward shift of the eddy-driven jet in the Southern Hemisphere, *Geophys. Res. Lett*., *40*, 1-5, doi: 10.1002/grl.50675, 2013.

Grise, K.M., S.-W. Son, G.P.J. Correa, and L.M. Polvani, The response of extratropical cyclones in the Southern Hemisphere to stratospheric ozone depletion in the 20th century, *Atmos. Sci. Lett.*, *15*, 29-36, doi: 10.1002/asl2.458, 2014.

Hardiman, S., N. Butchart, and N. Calvo, The morphology of the Brewer-Dobson circulation and its response to climate change in CMIP5 simulations, *Q. J. Roy. Meteorol. Soc.*, *140* (683), 1958-1965, doi: 10.1002/qj.2258, 2013.

Hartley, D.E., J.T. Villarin, R.X. Black, and C.A. Davis, A new perspective on the dynamical link between the stratosphere and troposphere, *Nature*, *391*, 471-474, 1998.

Hartmann, D.L., A.M.G. Klein Tank, and M. Rusticucci (Coordinating Lead Authors), L.V. Alexander, S. Brönnimann, Y. Charabi, F.J. Dentener, E.J. Dlugokencky, D.R. Easterling, A. Kaplan, B.J. Soden, P.W. Thorne, M. Wild, and P.M. Zhai, Observations: Atmosphere and surface, Chapter 2 in *Climate Change 2013: The Physical Science Basis. Contribution of Working Group I to the Fifth Assessment Report of the Intergovernmental Panel on Climate Change*, edited by T.F Stocker, D. Qin, G.-K. Plattner, M. Tignor, S.K. Allen, J. Boschung, A. Nauels, Y. Xia, V. Bex, and P.M. Midgley, Cambridge University Press, Cambridge, UK, and New York, NY, USA, 2013.

Harvey, B.J., L.C. Shaffrey, and T.J. Woollings, Equator-to-pole temperature differences and the extra-tropical storm track response of the CMIP5 climate models, *Clim. Dyn.*, *43*, 1171-1182, doi: 10.1007/s00382-013-1883-9, 2013.

Hassler, B., P.J. Young, R.W. Portmann, G.E. Bodeker, J.S. Daniel, K.H. Rosenlof, and S. Solomon, Comparison of three vertically resolved ozone data bases: Climatology, trends and radiative forcings, *Atmos. Chem. Phys.*, *13*, 5533-5550, doi: 10.5194/acp-13-5533-2013, 2013.

Hegglin, M.I., and T.G. Shepherd, Large climate-induced changes in stratosphere-to-troposphere ozone flux and ultraviolet index, *Nature Geosci.*, *2*, 687-691, doi: 10.1038/NGEO604, 2009.

Hendon, H.H., D.W.J. Thompson, and M.C.Wheeler, Australian rainfall and surface temperature variations associated with the Southern Hemisphere Annular Mode, *J. Clim.*, *20* (11), 2452-2467, doi: 10.1175/JCLI4134.1, 2007.

Hitchcock, P., T.G. Shepherd, and C. McLandress, Past and future conditions for polar stratospheric cloud formation simulated by the Canadian middle atmosphere model, *Atmos. Chem. Phys.*, *9* (2), 483-495, doi: 10.5194/acp-9-483-2009, 2009.

Hofmann, M., and M.A. Morales Maqueda, The response of Southern Ocean eddies to increased mid-latitude westerlies: A non-eddy resolving model study, *Geophys. Res. Lett.*, *38*, L03605, doi: 10.1029/2010GL045972, 2011.

Hogg A.M., M.P. Meredith, J.R. Blundell, and C. Wilson, Eddy heat flux in the southern ocean: Response to variable wind forcing, *J. Clim*., *21*, 608-620, 2008.

Hu, Y., Y. Xia, and Q. Fu, Tropospheric temperature response to stratospheric ozone recovery in the 21st century, *Atmos. Chem. Phys*., *11*, 7687-7699, doi: 10.5194/acp-11-7687-2011, 2011.

Huhn O., M. Rhein, M. Hoppema, and S. van Heuven, Decline of deep and bottom water ventilation and slowing down of anthropogenic carbon storage in the Weddell Sea, 1984-2011, *Deep-Sea Research I*, *76*, 66-84, doi: 10.1016/j.dsr.2013.01.005, 2013.

Hurst, D.F., S.J. Oltmans, H. Vömel, K.H. Rosenlof, S.M. Davis, E.A. Ray, E.G. Hall, and A.F. Jordan, Stratospheric water vapor trends over Boulder, Colorado: Analysis of the 30 year Boulder record, *J. Geophys. Res*., *116*, D02306, doi: 10.1029/2010JD015065, 2011.

IPCC (Intergovernmental Panel on Climate Change), *Climate Change 2013: The Physical Science Basis: Contribution of Working Group I to the Fifth Assessment Report of the Intergovernmental Panel on Climate Change*, edited by T.F. Stocker, D. Qin, G.-K. Plattner, M. Tignor, S.K. Allen, J. Boschung, A. Nauels, Y. Xia,

V. Bex, and P.M. Midgley, 1535 pp., Cambridge University Press, Cambridge, UK, and New York, NY, USA, 2013.

Iwasaki, T., H. Hamada, and K. Miyazaki, Comparisons of Brewer-Dobson circulations diagnosed from reanalyses, *J. Meteor. Soc. Jap*., *87* (6), 997-1006, 2009.

Jin, J.J., N.J. Livesey, G.L. Manney, J.H. Jiang, M.J. Schwartz, and W.H. Daffer, Chemical discontinuity at the extratropical tropopause and isentropic stratosphere-troposphere exchange pathways diagnosed using Aura MLS data, *J. Geophys. Res*., *118*, 3832-3847, doi: 10.1002/jgrd.50291, 2013.

John, J.G., A.M. Fiore, V. Naik, L.W. Horowitz, and J.P. Dunne, Climate versus emission drivers of methane lifetime against loss by tropospheric OH from 1860-2100, *Atmos. Chem. Phys*., *12*, 12021-12036, doi: 10.5194/acp-12-12021-2012, 2012.

Johnson, C.E., D.S. Stevenson, W.J. Collins, and R.G. Derwent, Role of climate feedback on methane and ozone studied with a coupled Ocean-Atmosphere-Chemistry model, *Geophys. Res. Lett*., *28*, 1723-1726, doi: 10.1029/2000GL011996, 2001.

Kang, S.M., and L.M. Polvani, The interannual relationship between the eddy-driven jet and the edge of the Hadley Cell, *J. Clim*., *24*, 563-568, doi: 10.1175/2010JCLI4077.1, 2011.

Kang, S.M., L.M. Polvani, J.C. Fyfe, and M. Sigmond, Impact of polar ozone depletion on subtropical precipitation, *Science*, *332*, 951-954, doi: 10.1126/science.1202131, 2011.

Kang, S.M., L.M. Polvani, J.C. Fyfe, S.-W. Son, M. Sigmond, and G.J.P. Correa, Modeling evidence that ozone depletion has impacted extreme precipitation in the austral summer, *Geophys. Res. Lett.*, *40*, 4054-4059, doi: 10.1002/grl.50769, 2013.

Karpechko, A.Y., N.P. Gillett, L.J. Gray, and M. Dall'Amico, Influence of ozone recovery and greenhouse gas increases on Southern Hemisphere circulation, *J. Geophys. Res*., *115*, D22117, doi: 10.1029/2010JD014423, 2010.

Kawase, H., T. Nagashima, K. Sudo, and T. Nozawa, Future changes in tropospheric ozone under Representative Concentration Pathways (RCPs), *Geophys. Res. Lett*., *38*, L05801, doi: 10.1029/2010GL046402, 2011.

Kawatani, Y., and K. Hamilton, Weakened stratospheric quasibiennial oscillation driven by increased tropical mean upwelling, *Nature*, *497*, 478-481, doi: 10.1038/nature12140, 2013.

Kidston, J., and E.P. Gerber, Intermodel variability of the poleward shift of the austral jet stream in the CMIP3 integrations linked to biases in 20th century climatology, *Geophys. Res. Lett*., *37*, L09708, doi: 10.1029/2010GL042873, 2010.

Kobayashi, S., M. Matricardi, D. Dee, and S. Uppala, Toward a consistent reanalysis of the upper stratosphere based on radiance measurements from SSU and AMSU-A, *Quart. J. Roy. Meteor. Soc.*, *135*, 2086-2099, doi: 10.1002/qj.514, 2009.

Korhonen, H., K.S. Carslaw, P.M. Forster, S. Mikkonen, N.D. Gordon, and H. Kokkola, Aerosol climate feedback due to decadal increases in Southern Hemisphere wind speeds, *Geophys. Res. Lett.*, *37*, L02805, doi: 10.1029/2009GL041320, 2010.

Kunz, T., K. Fraedrich, and F. Lunkeit, Synoptic scale wave breaking and its potential to drive NAO-like circulation dipoles: A simplified GCM approach, *Quart. J. Roy. Meteorol. Soc*., *135*, 1-19, doi: 10.1002/qj.351, 2009.

Kushner, P.J., and L.M. Polvani, Stratosphere-troposphere coupling in a relatively simple AGCM: The role of eddies, *J. Clim.*, *17* (3), 629-639, 2004.

Lamarque, J.-F., and S. Solomon, Impact of changes in climate and halocarbons on recent lower stratosphere ozone and temperature trends, *J. Clim*., *23* (10), 2599-2611, doi: 10.1175/2010JCLI3179.1, 2010.

Lamarque, J.-F., G.P. Kyle, M. Meinshausen, K. Riahi, S.J. Smith, D.P. Vuuren, A.J. Conley, and F. Vitt, Global and regional evolution of short-lived radiatively-active gases and aerosols in the Representative Concentration Pathways, *Clim. Change*, *109*, 191-212, doi: 10.1007/s10584-011-0155-0, 2011.

Lamarque, J.-F., D.T. Shindell, B. Josse, P.J. Young, I. Cionni, V. Eyring, D. Bergmann, P. Cameron-Smith, W.J. Collins, R. Doherty, S. Dalsoren, G. Faluvegi, G. Folberth, S.J. Ghan, L.W. Horowitz, Y.H. Lee, I.A. MacKenzie, T. Nagashima, V. Naik, D. Plummer, M. Righi, S.T. Rumbold, M. Schulz, R.B. Skeie, D.S. Stevenson, S. Strode, K. Sudo, S. Szopa, A. Voulgarakis, and G. Zeng, The Atmospheric Chemistry and Climate Model Intercomparison Project (ACCMIP): Overview and description of models, simulations and climate diagnostics, *Geosci. Model Dev*., *6* (1), 179-206, doi: 10.5194/gmd-6-179-2013, 2013.

Lang, C., D.W. Waugh, M.A. Olsen, A.R. Douglass, Q. Liang, J.E. Nielsen, L.D. Oman, S. Pawson, and R.S. Stolarski, The impact of greenhouse gases on past changes in tropospheric ozone, *J. Geophys. Res*., *117*, D23304, doi: 10.1029/2012JD018293, 2012.

Langematz, U., S. Meul, K. Grunow, E. Romanowsky, S. Oberländer, J. Abalichin, and A. Kubin, Future Arctic temperature and ozone: The role of stratospheric composition changes, *J. Geophys. Res.*, *119*, 2092-2112, doi:

10.1002/2013JD021100, 2014.

Le Quéré, C., C. Rodenbeck, E.T. Buitenhuis, T.J. Conway, R. Langenfelds, A. Gomez, C. Labuschagne, M. Ramonet, T. Nakazawa, N. Metzl, N. Gillett, and M. Heimann, Saturation of the Southern Ocean CO_2 sink due to recent climate change, *Science*, *316*, 1735-1738, doi: 10.1126/science.1136188, 2007.

Lee, S., and S.B. Feldstein, Detecting ozone- and greenhouse-gas-driven wind trends with observational data, *Science*, *339*, 563-567, doi: 10.1126/science.1225154, 2013.

Lenton, A., B. Tilbrook, R. Law, D. Bakker, S.C. Doney, N. Gruber, M. Hoppema, M. Ishii, N.S. Lovenduski, R.J. Matear, B.I. McNeil, N. Metzl, S.E. Mikaloff Fletcher, P. Monteiro, C. Rödenbeck, C. Sweeney, and T. Takahashi, Sea-air CO_2 fluxes in the Southern Ocean for the period 1990-2009, *Biogeosciences*, *10*, 4037-4054, doi: 10.5194/bg-10-4037-2013, 2013.

Li, F., J. Austin, and J. Wilson, The strength of the Brewer-Dobson circulation in a changing climate: Coupled chemistry-climate model stimulation, *J. Clim.*, *21* (1), 40-57, doi: 10.1175/2007.JCLI1663.1, 2008.

Limpasuvan, V., and D.L. Hartmann, Wave-maintained annular modes of climate variability, *J. Clim.*, *13*, 4414-4429, 2000.

Lin, P., and Q. Fu, Changes in various branches of the Brewer Dobson circulation from an ensemble of chemistry climate models, *J. Geophys. Res.*, *118*, 73-84, doi: 10.1029/2012JD018813, 2013.

Lin, P., Q. Fu, S. Solomon, and J.M. Wallace, Temperature trend patterns in Southern Hemisphere high latitudes: Novel indicators of stratospheric change, *J. Clim.*, *22* (23), 2009.

Lin, M., A.M. Fiore, O.R. Cooper, L.W. Horowitz, A.O. Langford, H. Levy II, B.J. Johnson, V. Naik, S.J. Oltmans, and C.J. Senff, Springtime high surface ozone events over the western United States: Quantifying the role of stratospheric intrusions, *J. Geophys. Res.*, *117*, D00V22, doi: 10.1029/2012JD018151, 2012.

Lorenz, D.J., and E.T. DeWeaver, Tropopause height and zonal wind response to global warming in the IPCC scenario integrations, *J. Geophys. Res.*, *112*, D10119, doi: 10.1029/2006JD008087, 2007.

Lott, F.C., P.A. Stott, D.M. Mitchell, N. Christidis, N.P. Gillet, L. Haimberger, J. Perlwitz, and P.W. Thorne, Models versus radiosondes in the free atmosphere: A new detection and attribution analysis of temperature, *J. Geophys. Res.*, *118*, 2609-2619, doi: 10.1002/jgrd.50255, 2013.

Lucas, C., H. Nguyen, and B. Timbal, An observational analysis of Southern Hemisphere tropical expansion, *J. Geophys. Res.*, *117*, D17112, doi: 10.1029/2011JD017033, 2013.

Lucas, C., B. Timbal, and H. Nguyen, The expanding tropics: A critical assessment of the observational and modeling studies, *WIREs Clim Change*, *5* (1), 89-112. doi: 10.1002/wcc.251, 2014.

Mahlstein I., P.R. Gent, and S. Solomon, Historical Antarctic mean sea ice area, sea ice trends, and winds in CMIP5 simulations, *J. Geophys. Res. 118* (11), 5105-5110, doi: 10.1002/jgrd.50443, 2013.

Manatsa, D., Y. Morioka, S.K. Behera, T. Yamagata, and C.H. Matarira, Link between Antarctic ozone depletion and summer warming over southern Africa, *Nature Geoscience.*, 6, 934-939, doi: 10.1038/ngeo1968, 2013.

Marshall, G., Trends in the Southern Annular Mode from observations and reanalyses, *J. Clim.*, *16* (24), 4134-4143, doi: 10.1175/1520-0442(2003)016<4134:TITSAM>2.0.CO;2, 2003.

Maycock, A.C., M.M. Joshi, K.P. Shine, A.A. Scaife, The circulation response to idealized changes in stratospheric water vapor, *J. Clim.*, *26*, 545-561, doi: 10.1175/JCLI-D-12-00155.1, 2013.

Maycock, A.C., M.M. Joshi, K.P. Shine, S.M. Davis, and K.H. Rosenlof, The potential impact of changes in lower stratospheric water vapour on stratospheric temperatures over the past 30 years, *Quart. J. Roy. Meteor. Soc.*, *140* (684), 2176-2185, doi: 10.1002/qj.2287, 2014.

McLandress, C., and T.G. Shepherd, Simulated anthropogenic changes in the Brewer-Dobson circulation, including its extension to high latitudes, *J. Clim.*, *22*, 1516-1540, doi: 10.1175/2008JCLI2679.1, 2009.

Mclandress, C., A.I. Jonsson, D.A. Plummer, M.C. Reader, J.F. Scinocca, and T.G. Shepherd, Separating the dynamical effects of climate change and ozone depletion Part I: Southern Hemisphere stratosphere, *J. Clim.*, *23*, 5002-5020, doi: 10.1175/2010JCLI3586.1, 2010.

McLandress, C., T.G. Shepherd, J.F. Scinocca, D.A. Plummer, M. Sigmond, A.I. Jonsson, and M.C. Reader, Separating the dynamical effects of climate change and ozone depletion. Part II: Southern Hemisphere troposphere, *J. Clim.*, *24*, 1850-1868, doi: 10.1175/2010JCLI3958.1, 2011.

McLandress, C., J. Perlwitz, and T.G. Shepherd, Comment on "Tropospheric temperature response to stratospheric ozone recovery in the 21st century" by Hu et al. (2011), *Atmos. Chem. Phys.*, *12*, 2533-2540, doi: 10.5194/acp-12-2533-2012, 2012.

Meinshausen, M., S.J. Smith, K.V. Calvin, J.S. Daniel, M.L.T. Kainuma, J.-F. Lamarque, K. Matsumoto, S.A. Montzka, S.C.B. Raper, K. Riahi, A. Thomson, G.J.M. Velders, and D.P.P. van Vuuren, The RCP greenhouse gas concentrations and their extensions from 1765 to 2300, *Clim. Change*, *109*, 213-241, doi: 10.1007/s10584-011-0156-z, 2011.

Meredith, M.P., and A.M. Hogg, Circumpolar response of the Southern Ocean eddy activity to a change in the Southern Annular Mode, *Geophys. Res. Lett.*, *33*, L16608, doi: 10.1029/2006GL026499, 2006.

Meredith, M.P., A.C. Naveira Garabato, A.M. Hogg, and R. Farneti, Sensitivity of the overturning circulation in the Southern Ocean to decadal changes in wind forcing, *J. Clim.*, *25*, 99-110, doi: 10.1175/2011JCLI4204.1, 2012.

Miller, R.L., G.A. Schmidt, and D.T. Shindell, Forced annular variations in the 20th century Intergovernmental Panel on Climate Change Fourth Assessment Report models, *J. Geophys. Res.*, *111*, D18101, doi: 10.1029/2005JD006323, 2006.

Min, S.-K., and S.-W. Son, Multi-model attribution of the Southern Hemisphere Hadley Cell widening: Major role of ozone depletion, *J. Geophys. Res*., *118*, 3007-3015, doi: 10.1002/jgrd.50232, 2013.

Mitchell, D.M., P.A. Stott, L.J. Gray, M.R. Allen, F.C. Lott, N. Butchart, S.C. Hardiman, and S.M. Osprey, The impact of stratospheric resolution on the detectability of climate change signals in the free atmosphere, *Geophys. Res. Lett.*, *40*, 937-942, doi: 10.1002/grl.50177, 2013.

Monge-Sanz, B.M., M.P. Chipperfield, D.P. Dee, A.J. Simmons, and S.M. Uppala, Improvements in the stratospheric transport achieved by a CTM with ECMWF (re)analyses: Identifying effects and remaining challenges, *Qurt. J. Roy. Meteorol. Soc.*, *139*, 654-673, doi:_10.1002/qj.1996, 2012.

Monge-Sanz, B.M., M.P. Chipperfield, A. Untch, J.-J. Morcrette, A. Rap, and A.J. Simmons, On the uses of a new linear scheme for stratospheric methane in global models: Water source, transport tracer and radiative forcing, *Atmos. Chem. Phys.*, *13*, 9641-9660, doi:_10.5194/acp-13-9641-2013, 2013.

Morgenstern, O., P. Braesicke, M.M. Hurwitz, F.M. O'Connor, A.C. Bushell, C.E. Johnson, and J.A. Pyle, The world avoided by the Montreal Protocol, *Geophys. Res. Lett.*, *35*, L16811, doi: 10.1029/2008GL034590, 2008.

Morgenstern, O., H. Akiyoshi, S. Bekki, P. Braesicke, N. Butchart, M.P. Chipperfield, D. Cugnet, M. Deushi, S.S. Dhomse, R.R. Garcia, A. Gettelman, N.P. Gillett, S.C. Hardiman, J. Jumelet, D.E. Kinnison, J.-F. Lamarque, F. Lott, M. Marchand, M. Michou, T. Nakamura, D. Olivié, T. Peter, D. Plummer, J.A. Pyle, E. Rozanov, D. Saint-Martin, J.F. Scinocca, K. Shibata, M. Sigmond, D. Smale, H. Teyssèdre, W. Tian, A. Voldoire, and Y. Yamashita, Anthropogenic forcing of the Northern Annular Mode in CCMVal-2 models, *J. Geophys. Res.*, *115* (D00M03), doi: 10.1029/2009JD013347, 2010.

Morgenstern, O., G. Zeng, N.L. Abraham, P.J. Telford, P. Braesicke, J.A. Pyle, S.C. Hardiman, F.M. O'Connor, and C.E. Johnson, Impacts of climate change, ozone recovery, and increasing methane on the tropospheric oxidizing capacity, *J. Geophys. Res.*, *118*, 1028-1041, doi: 10.1029/2012JD018382, 2013.

Morgenstern, O., G. Zeng, N.L. Abraham, P.J. Telford, P. Braesicke, J.A. Pyle, S.C. Hardiman, F.M. O'Connor, and C.E. Johnson, Correction to "Impacts of climate change, ozone recovery, and increasing methane on surface ozone and the tropospheric oxidizing capacity," *J. Geophys. Res.*, *119* (8), 5028-5036, doi: 10.1002/2014JD021515, 2014.

Morrison, A.K., and A.M. Hogg, On the relationship between Southern Ocean overturning and ACC transport, *J. Phys. Oceanogr*., *43* (1), 140-148, doi: 10.1175/JPO-D-12-057.1, 2013.

Myhre, G., and D. Shindell (Coordinating Lead Authors), F.-M. Bréon, W. Collins, J. Fuglestvedt, J. Huang, D. Koch, J.-F. Lamarque, D. Lee, B. Mendoza, T. Nakajima, A. Robock, G. Stephens, T. Takemura, and H. Zhang, Anthropogenic and natural radiative forcing, Chapter 8 in *Climate Change 2013: The Physical Science Basis. Contribution of Working Group I to the Fifth Assessment Report of the Intergovernmental Panel on Climate Change*, edited by T.F. Stocker, D. Qin, G.-K. Plattner, M. Tignor, S.K. Allen, J. Boschung, A. Nauels, Y. Xia, V. Bex, and P.M. Midgley, Cambridge University Press, Cambridge, UK, and New York, NY, USA, 2013.

Naik, V., L.W. Horowitz, A.M. Fiore, P. Ginoux, J. Mao, A.M. Aghedo, and H. Levy II, Impact of preindustrial to present day changes in short-lived pollutant emissions on atmospheric composition and climate forcing, *J. Geophys. Res.*, *118*, 8086-8110, doi: 10.1002/jgrd.50608, 2013.

Nash, J., Extension of explicit radiance observations by the Stratospheric Sounding Unit into the lower stratosphere and lower mesosphere, *Quart. J. Roy. Meteorol. Soc*., *114*, 1153-1171, 1988.

Nash, J., and G.F. Forrester, Long-term monitoring of stratospheric temperature trends using radiance measurements obtained by the TIROS-N series of NOAA spacecraft, *Adv. Space Res.*, *6* (10), 37-44, doi: 10.1016/0273-1177(86)90455-2, 1986.

Nash, J., and R. Saunders, A review of Stratospheric Sounding Unit radiance observations in support of climate trends investigations and reanalysis, *Forecasting Research Technical Report No. 586*, Met Office, 2013.

Ndarana, T., D.W. Waugh, L.M. Polvani, G.J.P. Correa, and E.P. Gerber, Antarctic ozone depletion and trends in tropopause Rossby wave breaking, *Atmos. Sci. Lett*., *13*, 164-168, doi: 10.1002/asl.384, 2012.

Newman, P.A., L.D. Oman, A.R. Douglass, E.L. Fleming, S.M. Frith, M.M. Hurwitz, S.R. Kawa, C.H. Jackman, N.A. Krotkov, E.R. Nash, J.E. Nielsen, S. Pawson, R.S. Stolarski, and G.J.M. Velders, What would have happened to the ozone layer if chlorofluorocarbons (CFCs) had not been regulated?, *Atmos. Chem. Phys*., *9* (6),

2113-2128, doi: 10.5194/acp-9-2113-2009, 2009.
Oberländer, S., U. Langematz, and S. Meul, Unravelling impact factors for future changes in the Brewer-Dobson circulation, *J. Geophys. Res.*, *118*, 10296-10312, doi: 10.1002/jgrd50775, 2013.
Okamoto, K., K. Sato, and H. Akiyoshi, A study on the formation and trends of the Brewer-Dobson circulation, *J. Geophys. Res*., *116*, D10117, doi: 10.1029/2010JD014953, 2011.
Oman, L., D.W. Waugh, S. Pawson, R.S. Stolarski, and P.A. Newman, On the influence of anthropogenic forcings on changes in the stratospheric mean age, *J. Geophys. Res*., *114*, doi: 10.1029/2008JD010378, 2009.
Oman, L.D., D.W. Waugh, S.R. Kawa, R.S. Stolarski, A.R. Douglass, and P.A. Newman, Mechanisms and feedbacks causing changes in upper stratospheric ozone in the 21st century, *J. Geophys. Res.*, *115*, D05303, doi: 10.1029/2009JD012397, 2010.
Orr, A., T.J. Bracegirdle, J.S. Hosking, T. Jung, J.D. Haigh, T. Phillips, and W. Feng, Possible Dynamical Mechanisms for Southern Hemisphere Climate Change due to the Ozone Hole, *J. Atmos. Sci.*, *69*, 2917-2932, doi: 10.1175/JAS-D-11-0210.1, 2012.
Orr, A., T.J. Bracegirdle, J.S. Hosking, W. Feng, H.K. Roscoe, and J.D. Haigh, Strong dynamical modulation of the cooling of the polar stratosphere associated with the Antarctic ozone hole, *J. Clim.*, *26*, 662-668, doi: 10.1175/JCLI-D-12-00480.1, 2013.
Palmeiro, F., N. Calvo, and R.R. Garcia, Future changes in the Brewer-Dobson circulation under different GHG concentrations, *J. Atmos. Sci.*, *71*, 2962-2975, doi: 10.1175/JAS-D-13-0289.1, 2014.
Parkinson, C.L., and D.J. Cavalieri, Antarctic sea ice variability and trends, 1979-2010, *Cryosphere*, *6* (4), 871-880, doi: 10.5194/tc-6-871-2012, 2012.
Perlwitz, J., S. Pawson, R.L. Fogt, J.E. Nielsen, and W.D. Neff, Impact of stratospheric ozone hole recovery on Antarctic climate, *Geophys. Res. Lett.*, *35*, L08714, doi: 10.1029/2008GL033317, 2008.
Plumb, R.A., Stratospheric transport, *J. Meteor. Soc. Japan*, *80*,793-809, 2002.
Polvani, L.M., and P.J. Kushner, Tropospheric response to stratospheric perturbations in a relatively simple general circulation model, *Geophys. Res. Lett.*, *29*, doi: 10.1029/2001GL014284, 2002.
Polvani, L.M., and K.L. Smith, Can natural variability explain observed Antarctic sea ice trends? New modeling evidence from CMIP5, *Geophys. Res. Lett*., *40*, 3195-3199, doi: 10.1002/grl.50578, 2013.
Polvani, L.M., and S. Solomon, The signature of ozone depletion on tropical temperature trends, as revealed by their seasonal cycle in model integrations with single forcings, *J. Geophys. Res*., *117*, D17102, doi: 10.1029/2012 JD017719, 2012.
Polvani, L.M., M. Previdi, and C. Deser, Large cancellation, due to ozone recovery, of future Southern Hemisphere atmospheric circulation trends, *Geophys. Res. Lett.*, *38*, L04707, doi: 10.1029/2011GL046712, 2011a.
Polvani, L.M., D.W. Waugh, G.J.P. Correa, and S.-W. Son, Stratospheric ozone depletion: The main driver of 20th Century atmospheric circulation changes in the Southern Hemisphere, *J. Clim.*, *24*, 795-812, doi: 10.1175/2010 JCLI3772.1, 2011b.
Portmann, R.W., J.S. Daniel, and A.R. Ravishankara, Stratospheric ozone depletion due to nitrous oxide: Influences of other gases, *Phil. Trans. R. Soc. B. Bio. Sci.*, *367*, 1256-1264, doi: 10.1098/rstb.2011.0377, 2012.
Previdi, M., and L.M. Polvani, Comment on "Tropospheric temperature response to stratospheric ozone recovery in the 21st century" by Hu et al. (2011), *Atmos. Chem. Phys.*, *12*, 4893-4896, doi: 10.5194/acp-12-4893-2012, 2012.
Previdi, M., and L.M. Polvani, Climate system response to stratospheric ozone depletion and recovery, *Quart. J. Roy. Meteorol. Soc.*, in press, doi: 10.1002/qj.2330, 2014.
Purich, A., and S.-W. Son, Impact of Antarctic ozone depletion and recovery on Southern Hemisphere precipitation, evaporation, and extreme changes, *J. Clim.*, *25* (9), 3145-3154, doi: 10.1175/JCLI-D-11-00383.1, 2012.
Quan, X.-W., M.P. Hoerling, J. Perlwitz, H.F. Diaz, and T. Xu, How fast are the tropics expanding?, *J. Clim.*, *27* (5), 1999-2013, doi: 10.1175/JCLI-D-13-00287.1, 2013.
Ramaswamy, V., M.D. Schwarzkopf, W.J. Randel, B.D. Santer, B.J. Soden, and G.L. Stenchikov, Anthropogenic and natural influences in the evolution of lower stratospheric cooling, *Science*, *311* (5764), 1138-1141, 2006.
Randel, W.J., and I.M. Held, Phase speed spectra of transient eddy fluxes and critical layer absorption, *J. Atmos. Sci.*, *48* (5), 688-697, doi: 10.1175/1520-0469(1991)048<0688:PSSOTE>2.0.CO;2, 1991.
Randel, W.J., and E.J. Jensen, Physical processes in the tropical tropopause layer and their roles in a changing climate, *Nature Geoscience*, *6*, 169-176, doi: 10.1038/ngeo1733, 2013.
Randel, W.J., and A.M. Thompson, Interannual variability and trends in tropical ozone derived from SAGE II satellite data and SHADOZ ozonesondes, *J. Geophys. Res.*, *116* (D7), D07303, doi: 10.1029/2010JD015195, 2011.
Randel, W.J., K.P. Shine, J. Austin, J. Barnett, C. Claud, N.P. Gillett, P. Keckhut, U. Langematz, R. Lin, C. Long,

C. Mears, A. Miller, J. Nash, D.J. Seidel, D.W.J. Thompson, F. Wu, and S. Yoden, An update of observed stratospheric temperature trends, *J. Geophys. Res.*, *114,* D02107, doi: 10.1029/2008JD010421, 2009.

Ray, E.A., F.L. Moore, K.H. Rosenlof, S.M. Davis, H. Boenisch, O. Morgenstern, D. Smale, E. Rozanov, M. Hegglin, G. Pitari, E. Mancini, P. Braesicke, N. Butchart, S. Hardiman, F. Li, K. Shibata, and D.A. Plummer, Evidence for changes in stratospheric transport and mixing over the past three decades based on multiple data sets and tropical leaky pipe analysis. *J. Geophys. Res.*, *115* (D21), D21304, doi: 10.1029/2010JD014206, 2010.

Reader, M.C., D.A. Plummer, J.F. Scinocca, and T.G. Shepherd, Contributions to twentieth century total column ozone change from halocarbons, tropospheric ozone precursors, and climate change, *Geophys. Res. Lett.*, *40* (23), 6276-6281, doi: 10.1002/2013GL057776, 2013.

Rivière, G., A dynamical interpretation of the poleward shift of the jet streams in global warming scenarios, *J. Atmos. Sci.*, *68* (6), 1253-1272, doi: 10.1175/2011JAS3641.1, 2011.

Roemmich D., J. Gilson, R. Davis, P. Sutton, S. Wijffels, and S. Riser, Decadal spinup of the South Pacific subtropical gyre., *J. Phys. Oceanogr.*, *37*, 162-173, doi: 10.1175/JPO3004.1, 2007.

Sallée, J.-B., R.J. Matear, S.R. Rintoul, and A. Lenton, Localized subduction of anthropogenic carbon dioxide in the Southern Hemisphere oceans, *Nature Geoscience*, *5*, 579-584, doi: 10.1038/ngeo1523, 2012.

Santer, B.D., J.F. Painter, C.A. Mears, C. Doutriaux, P. Caldwell, J.M. Arblaster, P.J. Cameron-Smith, N.P. Gillett, P.J. Gleckler, J. Lanzante, J. Perlwitz, S. Solomon, P.A. Stott, K.E. Taylor, L. Terray, P.W. Thorne, M.F. Wehner, F.J. Wentz, T.M.L. Wigley, L.J. Wilcox, and C.-Z. Zou, Identifying human influences on atmospheric temperature, *Proc. Natl. Acad. Sci. USA*, *110* (1), 26-33, doi: 10.1073/pnas.1210514109, 2013.

Schoeberl, M.R., A.E. Dessler, and T. Wang, Simulation of stratospheric water vapor and trends using three reanalyses, *Atmos. Chem. Phys*., *12* (14), 6475-6487, doi: 10.5194/acp-12-6475-2012, 2012.

Screen, J.A., N.P. Gillett, D.P. Stevens, G.J. Marshall, and H.K. Roscoe, The role of eddies in the Southern Ocean temperature response to the Southern Annular Mode, *J. Clim.*, *22* (3), 806-818, doi: 10.1175/2008JCLI2416.1, 2009.

Seidel, D.J., N.P. Gillet, J.R. Lanzante, K.P. Shine, and P.W. Thorne, Stratospheric temperature trends: Our evolving understanding, *WIREs Clim. Change*, *2* (4), 592-616, doi: 10.1002/wcc.125, 2011.

Seviour, W.J.M., N. Butchart, and S. Hardiman, The Brewer-Dobson circulation inferred from ERA-Interim, *Q.J.R. Meteorol. Soc.*, *138* (665), 878-888. doi: 10.1002/qj.966, 2012.

Shaw, T.A., J. Perlwitz, N. Harnik, P.A. Newman, and S. Pawson, The impact of stratospheric ozone changes on downward wave coupling in the southern hemisphere, *J. Clim., 24* (16), 4210-4229, doi: 10.1175/2011JCLI 4170.1, 2011.

Shepherd, T.G., and C. McLandress, A robust mechanism for strengthening of the Brewer-Dobson circulation in response to climate change: Critical-layer control of subtropical wave breaking, *J. Atmos. Sci*., *68* (4), 784-797, doi: 10.1175/2010JAS3608.1, 2011.

Sheshadri, A., R.A. Plumb, and D.I.V. Domeisen, Can the delay in Antarctic polar vortex breakup explain recent trends in surface westerlies?, *J. Atmos. Sci.*, *71* (2), 566-573, doi: 10.1175/JAS-D-12-0343.1, 2014.

Shindell, D., and G.A. Schmidt, Southern Hemisphere climate response to ozone changes and greenhouse gas increases, *Geophys. Res. Lett.*, *31*, L18209, doi: 10.1029/2004GL020724, 2004.

Shindell, D., G. Faluvegi, L. Nazarenko, K. Bowman, J.-F. Lamarque, A. Voulgarakis, G.A. Schmidt, O. Pechony, and R. Rudy, Attribution of historical ozone forcing to anthropogenic emissions, *Nature Clim. Change*, *3*, 567-570, doi: 10.1038/nclimate1835, 2013a.

Shindell, D.T., J.-F. Lamarque, M. Schulz, M. Flanner, C. Jiao, M. Chin, P.J. Young, Y.H. Lee, L. Rotstayn, N. Mahowald, G. Milly, G. Faluvegi, Y. Balkanski, W.J. Collins, A.J. Conley, S. Dalsoren, R. Easter, S. Ghan, L. Horowitz, X. Liu, G. Myhre, T. Nagashima, V. Naik, S.T. Rumbold, R. Skeie, K. Sudo, S. Szopa, T. Takemura, A. Voulgarakis, J.-H. Yoon, and F. Lo, Radiative forcing in the ACCMIP historical and future climate simulations, *Atmos. Chem. Phys*., *13* (6), 2939-2974, doi: 10.5194/acp-13-2939-2013, 2013b.

Shindell, D.T., O. Pechony, A. Voulgarakis, G. Faluvegi, L. Nazarenko, J.-F. Lamarque, K. Bowman, G. Milly, B. Kovari, R. Ruedy, and G.A. Schmidt, Interactive ozone and methane chemistry in GISS-E2 historical and future climate simulations, *Atmos. Chem. Phys*., *13* (5), 2653-2689, doi: 10.5194/acp-13-2653-2013, 2013c.

Shine, K.P., J.J. Barnett, and W.J. Randel, Temperature trends derived from Stratospheric Sounding Unit radiances: The effect of increasing CO_2 on the weighting function, *Geophys. Res. Lett.*, *35*, L02710, doi: 10.1029/ 2007GL032218, 2008.

Sigmond, M., and J.C. Fyfe, Has the ozone hole contributed to increased Antarctic sea ice extent?, *Geophys. Res. Lett*., *37* (18), L18502, doi: 10.1029/2010GL044301, 2010.

Sigmond, M., and J.C. Fyfe, The Antarctic sea ice response to the ozone hole in climate models, *J. Clim.*, *27* (3), 1336-1342, doi: 10.1175/JCLI-D-13-00590.1, 2014.

Sigmond, M., and T.G. Shepherd, Compensation between resolved wave driving and parameterized orographic gravity wave driving of the Brewer-Dobson circulation and its response to climate change, *J. Clim.*, *27* (14), 5601-5610, doi: 10.1775/JCLI-D-13-00644.1, 2014.

Sigmond, M., M.C. Reader, J.C. Fyfe, and N.P. Gillett, Drivers of past and future Southern Ocean change: Stratospheric ozone versus greenhouse gas impacts, *Geophys. Res. Lett.*, *38* (12), L12601, doi: 10.1029/2011GL047120, 2011.

Simpkins, G.R., and A.Y. Karpechko, Sensitivity of the southern annular mode to greenhouse gas emission scenarios, *Clim. Dyn.*, *38* (3-4), 563-572, doi: 10.1007/s00382-011-1121-2, 2012.

Simpkins, G.R., L.M. Ciasto, D.W.J. Thompson, and M.H. England, Seasonal relationships between large-scale climate variability and Antarctic sea ice concentration, *J. Clim.*, *25* (16), 5451-5469, doi: 10.1175/JCLI-D-11-00367.1, 2012.

Simpson, I.R., M. Blackburn, and J.D. Haigh, The role of eddies in driving the tropospheric response to stratospheric heating perturbations, *J. Atmos. Sci.*, *66* (5), 1347-1365, doi: 10.1175/2008JAS2758.1, 2009.

Simpson, I.R., M. Blackburn, and J.D. Haigh, A mechanism for the effect of tropospheric jet structure on the annular mode-like response to stratospheric forcing, *J. Atmos. Sci.*, *69* (7), 2152-2170, doi: 10.1175/JAS-D-11-0188.1, 2012.

Simpson, I.R., T.G. Shepherd, P. Hitchcock, and J.F. Scinocca, Southern annular mode dynamics in observations and models. Part II: Eddy feedbacks, *J. Clim.*, *26* (14), 5220-5241, doi: 10.1175/JCLI-D-12-00495.1, 2013.

Sioris, C.E., C.A. McLinden, V.E. Fioletov, C. Adams, J.M. Zawodny, A.E. Bourassa, C.Z. Roth, and D.A. Degenstein, Trend and variability in ozone in the tropical lower stratosphere over 2.5 solar cycles observed by SAGE II and OSIRIS, *Atmos. Chem. Phys.*, *14* (7), 3479-3496, doi: 10.5194/acp-14-3479-2014, 2014.

Smith, K.L., C.G. Fletcher, and P.J. Kushner, The role of linear interference in the annular mode response to extratropical surface forcing, *J. Clim.*, *23*, 6036-6050, doi: 10.1175/2010JCLI3606.1, 2010.

Smith, K.L., L.M. Polvani, and D.R. Marsh, Mitigation of 21st century Antarctic sea ice loss by stratospheric ozone recovery, *Geophys. Res. Lett*., *39* (20), L20701, doi: 10.1029/2012GL053325, 2012.

Solomon, S, J.S. Daniel, R.R. Neely III, J.-P. Vernier, E.G. Dutton, and L.W. Thomason, The persistently variable "background" stratospheric aerosol layer and global climate change, *Science*, *333* (6044), 866-870, doi: 10.1126/science.1206027, 2011.

Solomon, S., P.J. Young, and B. Hassler, Uncertainties in the evolution of stratospheric ozone and implications for recent temperature changes in the tropical lower stratosphere, *Geophys. Res. Lett*., *39* (17), L17706, doi: 10.1029/2012GL052723, 2012.

Son, S.-W., L.M. Polvani, D.W. Waugh, T. Birner, H. Akiyoshi, R.R. Garcia, A. Gettelman, D.A. Plummer, and E. Rozanov, The impact of stratospheric ozone recovery on tropopause height trends, *J. Clim*., *22* (2), 429-445, doi: 10.1175/2008JCLI2215.1, 2009.

Son, S.-W., E.P. Gerber, J. Perlwitz, L.M. Polvani, N.P. Gillett, K.-H. Seo, V. Eyring, T.G. Shepherd, D. Waugh, H. Akiyoshi, J. Austin, A. Baumgaertner, S. Bekki, P. Braesicke, C. Brühl, N. Butchart, M.P. Chipperfield, D. Cugnet, M. Dameris, S. Dhomse, S. Frith, H, Garny, R. Garcia, S.C. Hardiman, P. Jöckel, J.F. Lamarque, E. Mancini, M. Marchand, M. Michou, T. Nakamura, O. Morgenstern, G. Pitari, D.A. Plummer, J. Pyle, E. Rozanov, J.F. Scinocca, K. Shibata, D. Smale, H. Teyssèdre, W. Tian, and Y. Yamashita, Impact of stratospheric ozone on Southern Hemisphere circulation change: A multimodel assessment, *J. Geophys. Res*., *115*, D00M07, doi: 10.1029/2010JD014271, 2010.

Son, S.-W., A. Purich, H.H. Hendon, B.-M. Kim, and L.M. Polvani, Improved seasonal forecast using ozone hole variability?, *Geophy. Res. Lett.*, *40* (23), 6231-6235, doi: 10.1002/2013GL057731, 2013.

Song, Y., and W.A. Robinson, Dynamical mechanisms for stratospheric influences on the troposphere, *J. Atmos. Sci*., *61* (14), 1711-1725, 2004.

Søvde, O.A., C.R. Hoyle, G. Myhre, and I.S.A. Isaksen, The HNO_3 forming branch of the HO_2 + NO reaction: Pre-industrial-to-present trends in atmospheric species and radiative forcings, *Atmos. Chem. Phys*., *11*, 8929-8943, doi: 10.5194/acp-11-8929-2011, 2011.

SPARC CCMVal (Stratosphere-troposphere Processes And their Role in Climate), *SPARC Report on the Evaluation of Chemistry-Climate Models*, edited by V. Eyring, T.G. Shepherd, and D.W. Waugh, SPARC Report No. 5, WCRP-132, WMO/TD-No. 1526, 478 pp., available: http://www.atmosp.physics.utoronto.ca/SPARC/ccmval_final/index.php, 2010.

Staten, P.W., J.J. Rutz, T. Reichler, and J. Lu, Breaking down the tropospheric circulation response by forcing, *Clim, Dyn*., *39* (9-10), 2361-2375, doi: 10.1007/s00382-011-1267-y, 2012.

Stevenson, D.S., F.J. Dentener, M.G. Schultz, K. Ellingsen, T.P.C. vanNoije, O. Wild, G. Zeng, M. Anann, C.S. Atherton, N. Bell, D.J. Bergmann, I. Bey, T. Butler, J. Cofala, W.J. Collins, R.G. Derwent, R.M. Doherty, J.

Drevet, H.J. Eskes, A.F. Fiore, M. Gauss, D.A. Hauglustaine, L.W. Horowitz, I.S.A. Isaksen, M.C. Krol, J.-F. Lamarque, M.G. Lawrence, V. Montanaro, J.-F. Müller, G. Pitari, M.J. Prather, S.A. Pyle, S. Rast, J.M. Rodriguez, M.G. Sanderson, H.H. Savage, D.T. Shindell, S.E. Strahan, K. Sudo, and S. Szopa, Multi-model ensemble of present-day and near-future tropospheric ozone, *J. Geophys. Res.*, *111*, D8301, doi: 10.1029/2005JD006338, 2006.

Stevenson, D.S., P.J. Young, V. Naik, J.-F. Lamarque, D.T. Shindell, A. Voulgarakis, R.B. Skeie, S.B. Dalsoren, G. Myhre, T.K. Berntsen, G.A. Folberth, S.T. Rumbold, W.J. Collins, I.A. MacKenzie, R.M. Doherty, G. Zeng, T.P.C. van Noije, A. Strunk, D. Bergmann, P. Cameron-Smith, D.A. Plummer, S.A. Strode, L. Horowitz, Y.H. Lee, S. Szopa, K. Sudo, T. Nagashima, B. Josse, I. Cionni, M. Righi, V. Eyring, A. Conley, K.W. Bowman, O. Wild, and A. Archibald, Tropospheric ozone changes, radiative forcing and attribution to emissions in the Atmospheric Chemistry and Climate Model Intercomparison Project (ACCMIP), *Atmos. Chem. Phys*., *13* (6), 3063-3085, doi: 10.5194/acp-13-3063-2013, 2013.

Stiller, G.P., T. von Clarmann, F. Haenel, B. Funke, N. Glatthor, U. Grabowski, S. Kellmann, M. Kiefer, A. Linden, S. Lossow, and M. López-Puertas, Observed temporal evolution of global mean age of stratospheric air for the 2002 to 2010 period, *Atmos. Chem. Phys*., *12* (7), 3311-3331, doi: 10.5194/acp-12-3311-2012, 2012.

Struthers H., A.M.L. Ekman, P. Glantz, T. Iversen, A. Kirkevåg, Ø. Seland, E.M. Mårtensson, K. Noone, and E.D. Nilsson, Climate-induced changes in sea salt aerosol number emissions: 1870 to 2100, *J. Geophys. Res.*, *118* (2), 670-682, doi: 10.1002/jgrd.50129, 2013.

Swart, N.C., and J.C. Fyfe, Observed and simulated changes in the Southern Hemisphere surface westerly wind-stress, *Geophys. Res. Lett*., *39* (16), L16711, doi: 10.1029/2012GL052810, 2012.

Swart, N.C., and J.C. Fyfe, The influence of recent Antarctic ice sheet retreat on simulated sea ice area trends, *Geophys. Res. Lett.*, *40* (16), 4328-4332, doi: 10.1002/grl.50820, 2013.

Tang, Q., and M.J. Prather, Five blind men and the elephant: What can the NASA Aura ozone measurements tell us about stratosphere-troposphere exchange?, *Atmos. Chem. Phys.*, *12* (5), 2357-2380, doi: 10.5194/acp-12-2357-2012, 2012.

Tang, X., S.R. Wilson, K.R. Solomon, M. Shao, and S. Madronich, Changes in air quality and tropospheric composition due to depletion of stratospheric ozone and interactions with climate, *Photochem. Photobiol. Sci.*, *10* (2), 280-291, doi: 10.1039/c0pp90039g, 2011.

Thompson, D.W.J., and T. Birner, On the linkages between the tropospheric isentropic slope and eddy fluxes of heat during Northern Hemisphere winter, *J. Atmos. Sci*., *69* (6), 1811-1823, doi: 10.1175/JAS-D-11-0187.1, 2012.

Thompson, D.W.J., and S. Solomon, Interpretation of recent Southern Hemisphere climate change, *Science*, *296* (5569), 895-899, 2002.

Thompson, D.W.J., and S. Solomon, Understanding recent stratospheric climate change, *J. Clim.*, *22* (8), 1934-1943, doi: 10.1175/2008JCLI2482.1, 2009.

Thompson, D.W.J., J.C. Furtado, and T.G. Shepherd, On the tropospheric response to anomalous stratospheric wave drag and radiative heating, *J. Atmos. Sci.*, *63* (10), 2616-2629, 2006.

Thompson, D.W.J., S. Solomon, P.J. Kushner, M.H. England, K.M. Grise, and D.J. Karoly, Signatures of the Antarctic ozone hole in Southern Hemisphere surface climate change, *Nature Geoscience*, *4*, 741-749. doi: 10.1038/ngeo1296, 2011.

Thompson, D.W.J., D.J. Seidel, W.J. Randel, C.-Z. Zou, A.H. Butler, C. Mears, A. Osso, C. Long, and R. Lin, The mystery of recent stratospheric temperature trends, *Nature*, *491*, 692-697, doi: 10.1038/Nature11579, 2012.

Turner, J., J.C. Comiso, G.J. Marshall, T.A. Lachlan-Cope, T. Bracegirdle, T. Maksym, M.P. Meredith, Z. Wang, and A. Orr, Non-annular atmospheric circulation change induced by stratospheric ozone depletion and its role in the recent increase of Antarctic sea ice extent, *Geophys. Res. Lett.*, *36*, L08502, doi: 10.1029/2009GL037524, 2009.

Turner, J., T.J. Bracegirdle, T. Phillips, G.J. Marshall, and J.S. Hosking, An initial assessment of Antarctic sea ice extent in the CMIP5 models, *J. Clim*., *26* (5), 1473-1484, doi: 10.1175/JCLI-D-12-00068.1, 2013.

van Vuuren, D.P., J. Edmonds, M. Kainuma, K. Riahi, A. Thomson, K. Hibbard, G.C. Hurtt, T. Kram, V. Krey, J.-F. Lamarque, T. Masui, M. Meinshausen, N. Nakicenovic, S.J. Smith, and S.K. Rose, The representative concentration pathways: An overview, *Clim. Change*, *109*, 5-31, doi: 10.1007/s10584-011-0148-z, 2011.

Vaughan, D.G., and J.C. Comiso (Coordinating Lead Authors), I. Allison, J. Carrasco, G. Kaser, R. Kwok, P. Mote, T. Murray, F. Paul, J. Ren, E. Rignot, O. Solomina, K. Steffen, and T. Zhang (Lead Authors), Observations: Cryosphere, Chapter 4 in *Climate Change 2013: The Physical Science Basis. Contribution of Working Group I to the Fifth Assessment Report of the Intergovernmental Panel on Climate Change*, T.F. Stocker, D. Qin, G.-K. Plattner, M. Tignor, S.K. Allen, J. Boschung, A. Nauels, Y. Xia, V. Bex and P.M. Midgley, Cambridge University Press, Cambridge, UK, and New York, NY, USA, 2013.

Velders, G.J.M., S.O. Andersen, J.S. Daniel, D.W. Fahey, and M. McFarland, The importance of the Montreal Protocol in protecting climate, *Proc. Natl. Acad. Sci.*, *104* (12), 4814-4819, doi: 10.1073/pnas.0610328104, 2007.

Voulgarakis, A., V. Naik, J.-F. Lamarque, D.T. Shindell, P.J. Young, M.J. Prather, O. Wild, R.D. Field, D. Bergman, P. Cameron-Smith, I. Cionni, W.J. Collins, S.B. Dalsøren, R.M. Doherty, V. Eyring, G. Faluvegi, G.A. Folberth, L.W. Horowitz, B. Josse, I.A. McKenzie, T. Nagashima, D.A. Plummer, M. Righi, S.T. Rumbold, D.S. Stevenson, S.A. Strode, K. Sudo, S. Szopa, and G. Zeng., Analysis of present day and future OH and methane lifetime in the ACCMIP simulations, *Atmos. Chem. Phys*., *13* (5), 2563-2587, doi: 10.5194/acp-13-2563-2013, 2013.

Wang, L., and D.W. Waugh, Chemistry-climate model simulations of recent trends in lower stratospheric temperature and stratospheric residual circulation, *J. Geophys. Res*., *117* (D9), D09109, doi: 10.1029/2011 JD017130, 2012.

Wang, L., C-Z. Zou, and H. Qian, Constructions of stratospheric temperature data records from stratospheric sounding units, *J. Clim.*, *25* (8), 2931-2946, doi: 10.1175/JCLI-D-11-00350.1, 2012.

Watson, P.A.G., D.J. Karoly, M.R. Allen, N. Faull, and D.S. Lee, Quantifying uncertainty in future Southern Hemisphere circulation trends, *Geophys. Res. Lett*., *39* (23), L23708, doi: 10.1029/2012GL054158, 2012.

Waugh, D.W., Changes in the ventilation of the southern oceans, *Phil. Trans. R. Soc. A*, *372* (2019), doi: 10.1098/ rsta.2013.0269, 2014.

Waugh, D.W., L. Oman, S.R. Kawa, R.S. Stolarski, S. Pawson, A.R. Douglass, P.A. Newman, and J.E. Nielsen, Impacts of climate change on stratospheric ozone recovery, *Geophys. Res. Lett.*, *36*, L03805, doi: 10.1029/ 2008GL036223, 2009.

Waugh, D.W., F. Primeau, T. DeVries, and M. Holzer, Recent changes in the ventilation of the southern oceans, *Science*, *339* (6119), 568-570, doi: 10.1126/science.1225411, 2013.

Wilcox, L.J., A.J. Charlton-Perez, and L.J. Gray, Trends in Austral jet position in ensembles of high- and low-top CMIP5 models, *J. Geophys. Res*., *117*, D13115, doi: 10.1029/2012JD017597, 2012.

Wilcox, L.J., and A.J. Charlton-Perez, Final warming of the Southern Hemisphere polar vortex in high- and low-top CMIP5 models, *J. Geophys. Res.*, *118* (6), 2535-2546, doi: 10.1002/jgrd.50254, 2013.

Wild, O., Modelling the global tropospheric ozone budget: Exploring the variability in current models, *Atmos. Chem. Phys.*, *7* (10), 2643-2660, doi: 10.5194/acp-7-2643-2007, 2007.

Wittman, M.A.H., L.M. Polvani, R.K. Scott, and A.J. Charlton, Stratospheric influence on baroclinic lifecycles and its connection to the Arctic Oscillation, *Geophys. Res. Lett.*, *31*, L16113, doi: 10.1029/2004GL020503, 2004.

WMO (World Meteorological Organization), *Scientific Assessment of Ozone Depletion: 2002*, Global Ozone Research and Monitoring Project–Report No. 47, Geneva, Switzerland, 2003.

WMO (World Meteorological Organization), *Scientific Assessment of Ozone Depletion: 2010,* Global Ozone Research and Monitoring Project - Report No. 52, Geneva, Switzerland, 2011.

Wu, Y., L.M. Polvani, and R. Seager, The importance of the Montreal Protocol in protecting Earth's hydroclimate, *J. Clim.*, *26* (12), 4049-4068, doi: 10.1175/JCLI-D-12-00675.1, 2013.

Xie S.-P., B. Lu, and B. Xiang, Similar spatial patterns of climate responses to aerosol and greenhouse gas changes, *Nature Geoscience*, *6*, 828-832, doi: 10.1038/ngeo1931, 2013.

Young, P.J., K.H. Rosenlof, S. Solomon, S.C. Sherwood, Q. Fu, and J.-F. Lamarque, Changes in stratospheric temperatures and their implications for changes in the Brewer-Dobson circulation, 1979-2005, *J. Clim.*, *25* (5), 1759-1772, doi: 10.1175/2011JCLI4048.1, 2012.

Young, P.J., A.T. Archibald, K.W. Bowman, J.-F. Lamarque, V. Naik, D.S. Stevenson, S. Tilmes, A. Vougarakis, O. Wild, D. Bergmann, P. Cameron-Smith, I. Cionni, W.J. Collins, S.B. Dalsøren, R.M. Doherty, V. Eyring, G. Faluvegi, L.W. Horowitz, B. Josse, Y.H. Lee, I.A. MacKenzie, T. Nagashima, D.A. Plummer, M. Righi, S.T. Rumbold, R.B. Skeie, D.T. Shindell, S.A. Strode, K. Sudo, S. Szopa, and G. Zeng, Pre-industrial to end 21st century projections of tropospheric ozone from the Atmospheric Chemistry and Climate Model Intercomparison Project (ACCMIP), *Atmos. Chem. Phys*., *13* (4), 2063-2090, doi: 10.5194/acp-13-2063-2013, 2013a.

Young, P.J., A.H. Butler, N. Calvo, L. Haimberger, P.J. Kushner, D.R. Marsh, W.J. Randel, and K.R. Rosenlof, Agreement in late twentieth century Southern Hemisphere stratospheric temperature trends in observations and CCMVal-2, CMIP3, and CMIP5 models, *J. Geophys. Res*., *118* (2), 605-613, doi: 10.1002/jgrd.50126, 2013b.

Zeng, G., O. Morgenstern, P. Braesicke, and J.A. Pyle, Impact of stratospheric ozone recovery on tropospheric ozone and its budget, *Geophys. Res. Lett*., *37* (9), L09805, doi: 10.1029/2010GL042812, 2010.

Zunz, V., H. Goosse, and F. Massonnet, How does internal variability influence the ability of CMIP5 models to reproduce the recent trend in Southern Ocean sea ice extent?, *The Cryosphere*, *7* (2), 451-468, doi: 10.5194/tc-7-451-2013, 2013.